WATER WATER WATER WATER WATER WATER WATER WATER WATER WATER

1978

PROJECT COMPLETION
REPORT NO. 527X

The Turbulent Transport and Biological Structure of Eutrophication Models

Volume II

Comparative Study of the Mathematical Formulations For Primary Productivity in Stratified Lakes

R. M. Sykes,
Associate Professor

K. W. Bedford,
Associate Professor

K. M. Smarkel,
Research Assistant

Department of Civil Engineering
The Ohio State University

United States Department
of the Interior

CONTRACT NO.
A-039-OHIO
B-063-OHIO

State of Ohio
Water Resources Center
Ohio State University

THE TURBULENT TRANSPORT AND BIOLOGICAL STRUCTURE OF EUTROPHICATION MODELS

Volume II

Comparative Study of the Mathematical Formulations For Primary Productivity in Stratified Lakes

by

R. M. Sykes, Ph.D.
Associate Professor of Civil Engineering,

K. W. Bedford, Ph.D.
Associate Professor of Civil Engineering, and

K. M. Smarkel, Ph.D.
Research Assistant

The Department of Civil Engineering
The Ohio State University

* * * *

Project Completion Report, Volume II
Office of Water Resources Research and Technology
Matching Grant B-036-OHIO

* * * *

May 31, 1978

* * * *

PREFACE

The analysis of eutrophication processes and pollutant transport has been aided by an overwhelming number of numerical models, each purporting some advantage over existing formulations. Difficulties with these models exist and their utility is often called into question, particularly with regard to verification. The following research report is a two-volume report which attempts to review, and clarify, the basic assumptions in these models and to suggest extensions or improvements in the structure which will reduce the amount of artificial empiricism. The first volume suggests improvements in the turbulent transport structure and the second volume describes the primary productivity formulation available and identifies optimal representation.

ACKNOWLEDGMENTS

This volume is the second volume of the project completion for OWRT Matching Grant contract B-036-OHIO. The principal investigators, Drs. K. W. Bedford and R. M. Sykes, were extremely fortunate to have been able to support and associate with an excellent group of graduate students. As a result, this volume is in substantial part the doctoral thesis of Kenneth Smarkel, whose precise, concise, and clear work is gratefully acknowledged. He and his fellow doctoral candidate, Christos Babajimopoulos, provided excellent examples of proper science and research to the other students on this project, Michael Trimeloni and Bipin Shah. The authors wish to thank the staff of the Water Resources Center for their help in the smooth administration of this project in the face of ever-increasing paperwork. Last, but certainly most importantly, the authors very much thank the Office of Water Resources Research and Technology for their support of this research.

TABLE OF CONTENTS

		Page
PREFACE		ii
ACKNOWLEDGMENTS		iii
LIST OF TABLES		vi
LIST OF FIGURES		viii
LIST OF SYMBOLS		xi
Chapter		
I.	INTRODUCTION	1
II.	LITERATURE REVIEW	4
	Phosphorus Uptake and Storage	4
	Oxygen Depletion Models	8
	Eutrophication Models	10
	Ecosystem Models	15
	Parameter Ranges	17
	Literature Critique and Study Objectives	18
III.	CONSTRUCTION OF EUTROPHICATION MODELS	24
	Lake Choice	24
	The Mass Balance Equation	29
	Evaluation of Diffusion Coefficients	30
	Algal Models	36
	Aerobic Ecosystem Structures	58
	Anaerobic Ecosystem Structure	76
	Minimum Necessary Model Structure	78
	Phosphorus Conservation	79
IV.	THE NUMERICAL SOLUTION TECHNIQUE	81
	Solution Algorithms	81
	Time-Step Restrictions	90
V.	CAYUGA LAKE CUMULATIONS	96
	Verification Criteria	96
	Algae Only	98

TABLE OF CONTENTS (continued)

		Page
	Algae and Detritus	108
	Algae and Zooplankton	110
	Algae, Detritus, and Zooplankton	121
	Second Bloom Verifications	125
	Minimal Biological Structures	133
VI.	CANADARAGO LAKE SIMULATIONS	137
	Algae Only	138
	Algae and Detritus	143
	Algae and Zooplankton	149
	Algae, Detritus, and Zooplankton	156
VII.	DISCUSSION AND CONCLUSIONS	162
	Cayuga Lake Verifications	162
	Canadarago Lake Verifications	167
	Conclusions	171
	Summary	177
APPENDIX		
	A Cayuga Lake Data	178
	B Canadarago Lake Data	181
	C Equations	185
	D Computer Programs	197
REFERENCES		198

LIST OF TABLES

		Page
1.	Literature Ranges for Some of the Common Biological Coefficients Used in Formulating Species Interaction	19
2.	Variability of Species Choice and Process Formulations of the Surveyed Biological Analogs	22
3.	Lake Characteristics	25
4.	Cayuga Lake Discretizations	84
5.	Canadarago Lake Discretizations	85
6.	Biological Parameter Values for the Algae-Only Comparison in Cayuga Lake	100
7.	Biological Parameter Values for the Algae Plus Detritus Comparisons in Cayuga Lake	112
8.	Biological Parameter Values for the Algae Plus Zooplankton Comparisons in Cayuga Lake	116
9.	Biological Parameter Values for the Algae, Detritus, and Zooplankton Comparisons in Cayuga Lake	123
10.	Biological Parameter Values for the Second Bloom Algae Plus Zooplankton Comparisons in Cayuga Lake	128
11.	Biological Parameter Values for the Second Bloom Algae, Detritus, and Zooplankton Comparisons in Cayuga Lake	131
12.	Biological Parameter Values for the Algae-Only Comparisons in Canadarago Lake	141
13.	Biological Parameter Values for the Algae Plus Detritus Comparisons in Canadarago Lake	146
14.	Biological Parameter Values for the Algae Plus Zooplankton Comparisons in Canadarago Lake	152

LIST OF TABLES (continued)

Page

15. Biological Parameter Values for the Algae, Detritus, and Zooplankton Comparisons in Canadarago Lake 159

LIST OF FIGURES

Page

1. Algal Phosphorus Yield Coefficients for Batch Cultures with Differing Initial Nitrogen to Phosphorus Ratios, Inoculated on Day 0 6

2. Predicted Thermal Profiles and Horizontally Averaged Field Data for Cayuga Lake 1973 33

3. Predicted Thermal Profiles and Horizontally Averaged Field Data for Canadarago Lake 1969 . . 37

4. Diagrammatic Representation of the Three Algal Structures for Nutrient Utilization 40

5. Light Function Curves for a 12-Hour Photoperiod with a = .6, and x = 0, Beginning at Sunrise . . 47

6. Light Function Curves in Depth Profile at the Vernal Equinox and the Summer Solstice 48

7. Matrix of Possible Algal and Ecosystem Combinations with the Model Authors in Their Respective Sections 59

8. Diagram of the Algae-Only Ecosystem Structure . 60

9. Diagram of the Algae Plus Detritus Ecosystem Structure 67

10. Diagram of the Algae Plus Zooplankton Ecosystem Structure 69

11. Zooplankton Growth Rates; Approximate *in situ* Growth rates (Zaika, 1973), and Growth Rates Reduced to Non-limiting Algal Concentrations (Hall, 1964) 71

12. Diagram of Algae, Zooplankton, and Detritus Ecosystem Structure 75

13. Diagram of the Anaerobic Ecosystem Structure . . 77

14. Predictions of Algal Biomass, Orthophosphate, and Oxygen Concentrations Plotted Against Field Data for All Three Types of Phosphate

Page

Uptake Kinetics. No Zooplankton and No Detrital Pool. Cayuga 1973 99

15. Predictions of Algal Biomass, Orthophosphate, and Oxygen Concentrations Plotted Against Field Data for All Three Types of Phosphate Uptake Kinetics. Detrital Pool and No Zooplankton. Cayuga 1973 111

16. Predictions of Algal Biomass, Orthophosphate, and Oxygen Concentrations Plotted Against Field Data for All Three Types of Phosphate Uptake Kinetics. Zooplankton and No Detrital Pool. Cayuga 1973 115

17. Monthly Zooplankton Data Representing the Top Ten Meters of Cayuga Lake for 1968 119

18. Predictions of Algal Biomass, Orthophosphate, and Oxygen Concentrations Plotted Against Field Data for All Three Types of Phosphate Uptake Kinetics. Zooplankton and a Detrital Pool. Cayuga 1973 122

19. Second Bloom Predictions of Algal Biomass, Orthophosphate, and Oxygen Concentrations Plotted Against Field Data for Two Types of Phosphate Uptake Kinetics. Zooplankton Predation and No Detrital Pool 127

20. Second Bloom Predictions of Algal Biomass, Orthophosphate, and Oxygen Concentrations Plotted Against Field Data for Two Types of Phosphate Uptake Kinetics. Zooplankton Predation and a Detrital Pool 130

21. Lotka-Volterra Predictions of Algal Biomass and Orthophosphate Concentrations Plotted Against Field Data. Zooplankton and No Detrital Pool. Cayuga 1973 134

22. Predictions of Algal Biomass, Orthophosphate, and Oxygen Concentrations Plotted Against Field Data for All Three Types of Phosphate Uptake Kinetics. No Zooplankton or Detrital Pool. Canadarago 1969 139

LIST OF FIGURES (continued)

Page

23. Predictions of Algal Biomass, Orthophosphate, and Oxygen Concentrations Plotted Against Field Data for All Three Types of Phosphate Uptake Kinetics. Detrital Pool but no Zooplankton. Canadarago 1969 144

24. Predictions of Algal Biomass, Orthophosphate, and Oxygen Concentrations Plotted Against Field Data for All Three Types of Phosphate Uptake Kinetics. Zooplankton but No Detrital Pool. Canadarago 1969 150

25. Predictions of Algal Biomass, Orthophosphate, and Oxygen Concentrations Plotted Against Field Data for All Three Types of Phosphate Uptake Kinetics. Zooplankton and Detritus. Canadarago 1969 157

LIST OF SYMBOLS

Symbol	Definition	Units
A	Area	km
a	Natural water light extinction coefficient	m^{-1}
B	Benthos	g dry wt./m^3
b	Algal absortivity	m^2/g
C	Non-structural, soluble internal phosphorus	gP/g dry wt.
C_m	maximum non-structural, soluble internal phosphorus	gP/g dry wt.
C_α	Empirical Stokes law sinking coefficient	m cm^2/day sec
D	Dissolved Organic Matter	g dry wt/m^3
f(I)	Light Function	unitless
$\bar{f}(I)$	Light function averaged over photoperiod	unitless
$\bar{\bar{f}}(I)$	Light function averaged over photoperiod and depth	unitless
G	Acceleration factor	unitless
g	Acceleration of gravity	m/sec^2
I_j	Light intensity at node j	watts/m^2
I_s	Light intensity at the surface	watts/m^2
I_m	Maximum surface light intensity	watts/m^2
I_{mj}	Maximum light intensity at node j	watts/m^2
I_{equ}	Maximum light intensity at vernal equinox	watts/m^2

LIST OF SYMBOLS (continued)

Symbol	Definition	Units
I_{opt}	Optimal light intensity for algal growth	watts/m^2
I_{sol}	Maximum light intensity at summer solstice	watts/m^2
K	Turbulent diffusion coefficient	m^2/day
K_c	Monod half velocity for algal growth	gP/g dry wt.
K_n	Monod half velocity for orthophosphate uptake	gP/m^3
K_o	Monod half velocity for aerobic activity	g/m^3
K_s	Monod half velocity for polyphosphate formation	gP/g dry wt.
K_v	Monod half velocity for polyphosphate degradation	gP/g dry wt.
K_x	Monod half velocity for zooplankton growth	g dry wt/m^3
K_{bd}	Specific anaerobic benthic decay rate	day^{-1}
K_{bn}	Specific aerobic benthic decay rate	day^{-1}
K_{dn}	Specific dissolved organic matter decay rate	day^{-1}
K_{pn}	Specific particulate detritus decay rate	day^{-1}
K_{xn}	Specific algal decay rate to nutrients	day^{-1}
K_{xp}	Specific algal decay rate to detritus	day^{-1}
K_{zn}	Specific zooplankton decay rate to nutrients	day^{-1}
K_{zp}	Specific zooplankton decay rate to detritus	day^{-1}

LIST OF SYMBOLS (continued)

Symbol	Definition	Units
K_{max}	Maximum surface turbulent diffusion coefficient	m^2/day
L_x	Lotka-Volterra algal growth coefficient	m^3/gP day
L_z	Lotka-Volterra zooplankton growth coefficient	m^3/g day
N	Orthophosphate	g P/m^3
N_T	Total phosphorus	g P/m^3
n	Time step increment number	unitless
O	Oxygen	g/m^3
P	Particulate detritus	g dry wt/m^3
$\hat{q}$	Maximum specific orthophosphate uptake rate	g P/g dry wt.day
r_f	Maximum specific polyphosphate formation rate	g P/g dry wt day
r_d	Maximum specific polyphosphate degradation rate	g P/g dry wt day
R_i	Richardson number	unitless
S_I	Species independent sink-source term	g/m^3day
S_s	Species self-dependent sink-source term	day^{-1}
S_x	Total algal sink-source term	g/m^3day
S_α	Total arbitrary species sink-source term	g/m^3day
S_{cx}	Internal soluble phosphorus sink-source term	g/m^3day
S_{vx}	Polyphosphate sink-source term	g/m^3day

LIST OF SYMBOLS (continued)

Symbol	Definition	Units
T	Temperature	°C
t	Time	days
t_e	Time after vernal equinox	days
V	Polyphosphate	g P/g dry wt
V_m	Maximum polyphosphate concentration	g P/g dry wt
V_p	Detrital sinking rate	m/day
V_x	Algal sinking rate	m/day
V_z	Zooplankton sinking rate	m/day
V_α	Arbitrary species (α) sinking rate	m/day
V^n	Amplitude of Fourier component	g/m^3
W	Wind friction velocity	m/day
X	Algae	g/m^3
Y_{nb}	Benthic phosphorus content	gP/g dry wt.
Y_{np}	Particulate phosphorus content	gP/g dry wt.
Y_{nx}	Algal phosphorus content	gP/g dry wt.
Y_{nz}	Zooplankton phosphorus content	gP/g dry wt.
Y_{ob}	Benthic oxygen demand	g O_2/g dry wt.
Y_{od}	Dissolved organic matter oxygen demand	g O_2/g dry wt.
Y_{op}	Detrital oxygen demand	g O_2/g dry wt.
Y_{ox}	Algal oxygen demand	g O_2/g dry wt.
Y_{oz}	Zooplankton oxygen demand	g O_2/g dry wt.
Z	Zooplankton	g dry wt./m^3
z	depth	m

LIST OF SYMBOLS (continued)

Symbol	Definition	Units
α	Arbitrary species	g/m^3
α_v	Coefficient of volumetric expansion	$°C^{-1}$
Δt	Time step	day
θ	Phase angle	rad.
λ	Length of photoperiod	hr.
λ_{sol}	Length of photoperiod at summer solstice	hr.
$\hat{\mu}_x$	Maximum specific algal growth rate	day^{-1}
$\hat{\mu}_z$	Maximum specific zooplankton growth rate	day^{-1}
μ	Viscosity of water	dyne sec/cm^2
ρ	Density of water	g/cm^2
ρ_α	Density of species α	g/cm^2
τ_s	Wind surface shear	$dynes/cm^2$

Chapter I

INTRODUCTION

The addition of nutrients to a lake will cause initially pristine waters to accumulate organic and inorganic materials, which settle to the bottom, slowly filling the basin. Natural eutrophication is sustained by precipitation and the resultant erosion and transport of inorganic and organic materials to the lake. Changing the landscape to farmland and discharging large quantities of municipal and industrial waste into surface waters has accelerated this natural accumulation process.

One result of enhanced eutrophication is the magnification of algal blooms and their associated nuisances. Algal blooms clog sand filters and cause taste and odor problems in potable water supplies. They wash onto beaches where their decomposition creates unsightly debris, noxious odor, and a temporary loss of recreational area. In lakes, high algal production can have deleterious effects on the existing ecosystem. Some algal species produce toxic byproducts, while others can mat on the surface inhibiting light penetration and planktonic photosynthesis below the surface. A major problem is that of temporary oxygen depletion in the hypolimnion of thermally stratified lakes. Algae settle out of

the euphotic zone, through the thermocline, into the cold, dark epilimnion where endogenous respiration, decomposition, and predation deplete the population quickly. Since turbulent transport of oxygen through the thermocline is very small, oxygen uptake due to algal decay can easily exceed oxygen input to the hypolimnion. If hypolimnetic organic loads are high, the hypolimnion and adjacent benthic area can become anaerobic, destroying nurseries for aquatic insect larvae and hatcheries for many fish.

The physical and biochemical interactions of eutrophication are complex enough that mere data inspection is not capable of predicting ecosystem response to changing environmental conditions. Therefore, some systematic method of "modeling" these interactions is necessary. Currently, many investigators are employing mathematical models for algal growth. These equations usually take the form of material mass balances, which may or may not include some approximation to turbulent transport. No exact solution is available for these highly non-linear partial differential equations, so numerical integration techniques are used to obtain the solutions. The current overall methodology is to develop a hypothesis of aquatic ecosystem structure and interactions, to write equations describing the hypothesis and to use the solutions, with or without comparisons to field data, to suggest management strategies.

This study compares a variety of existing eutrophication models in an attempt to identify the minimum necessary model structure. For the sake of efficiency, the models have not been compared in their published form. Rather, the published models have been analyzed into their structural components, and these isolated components have been recombined in whatever ways seemed possible to derive twelve different model structures. The abilities of these reconstructed models to simulate actual field data was then tested. In certain cases (e.g. the algal polyphosphate component), the published models incorporate defective or inadequate submodels; these were replaced with improved versions. Also, each model tested includes an accurate turbulent transport algorithm, incorporating the effects of thermal stratification and sinking. This procedure allows observation of biological model inadequacies directly, without confounding due to transport inadequacies.

A detailed listing of the study objectives can be found at the end of the Literature Review (Literature Critique and Study Objectives), which follows directly.

Chapter II

LITERATURE REVIEW

The complexity of a model, and the choice of biological and chemical species to be included in it are dependent on the intended application. Some investigators only wished to estimate hypolimnetic oxygen depletion; some wanted to predict the effects of individual algal blooms or year-long algal activity; and some had ambitions of simulating the entire ecosystem from nutrients to top predator fish species. In this chapter, most of the published water quality models concerned with eutrophication are described with especial attention to model structure and verification. Certain other data on algal physiology and plankton parameter values are also collected here for convenience. Other pertinent literature is cited where needed throughout the text.

Phosphorus Uptake and Storage

In many aquatic environments, phosphorus is found at concentrations lower than those necessary for maximum algal growth rates. Therefore, many investigators have developed algal growth models which partially depend upon ambient phosphate concentrations to determine algal production rates. All of these models necessitate knowledge of algal phosphorus

content, so that uptake of soluble phosphate can be computed and ambient phosphate levels determined.

Toerien et al. (1970) demonstrated the variability of the cellular phosphorus content of Selenastrum capricornutum as a function of initial phosphate concentrations in the growth medium. A figure from Toerien's report has been replotted as Figure 1. The original figure had a vertical axis in terms of g dry wt/g P, which is the inverse of the vertical axis used in Figure 1. The graph results from batch culture experiments run at differing initial N/P ratios, with sampling and analysis for cellular phosphorus beginning after three days of growth. An accompanying figure showed final cellular phosphorus contents, which varied from 1 to 10% by weight, depending upon initial nitrogen to phosphorus ratios.

In his review of phosphorus uptake research, Lewin (1966) commented that the influence of light upon algal uptake of inorganic phosphate was negligible in experiments of short duration. Ketchum (1939), Scott (1945), Emerson et al. (1944), and Arnoff and Calvin (1948) all found that phosphate uptake by phosphorus-deficient cells was not enhanced by light. However, experiments of longer duration (75 min) by Gest and Kamen (1948) showed significant increases in uptake rates in the presence of light. These experiments imply that while light can enhance phosphate uptake on a long-term basis, it is not obligatory.

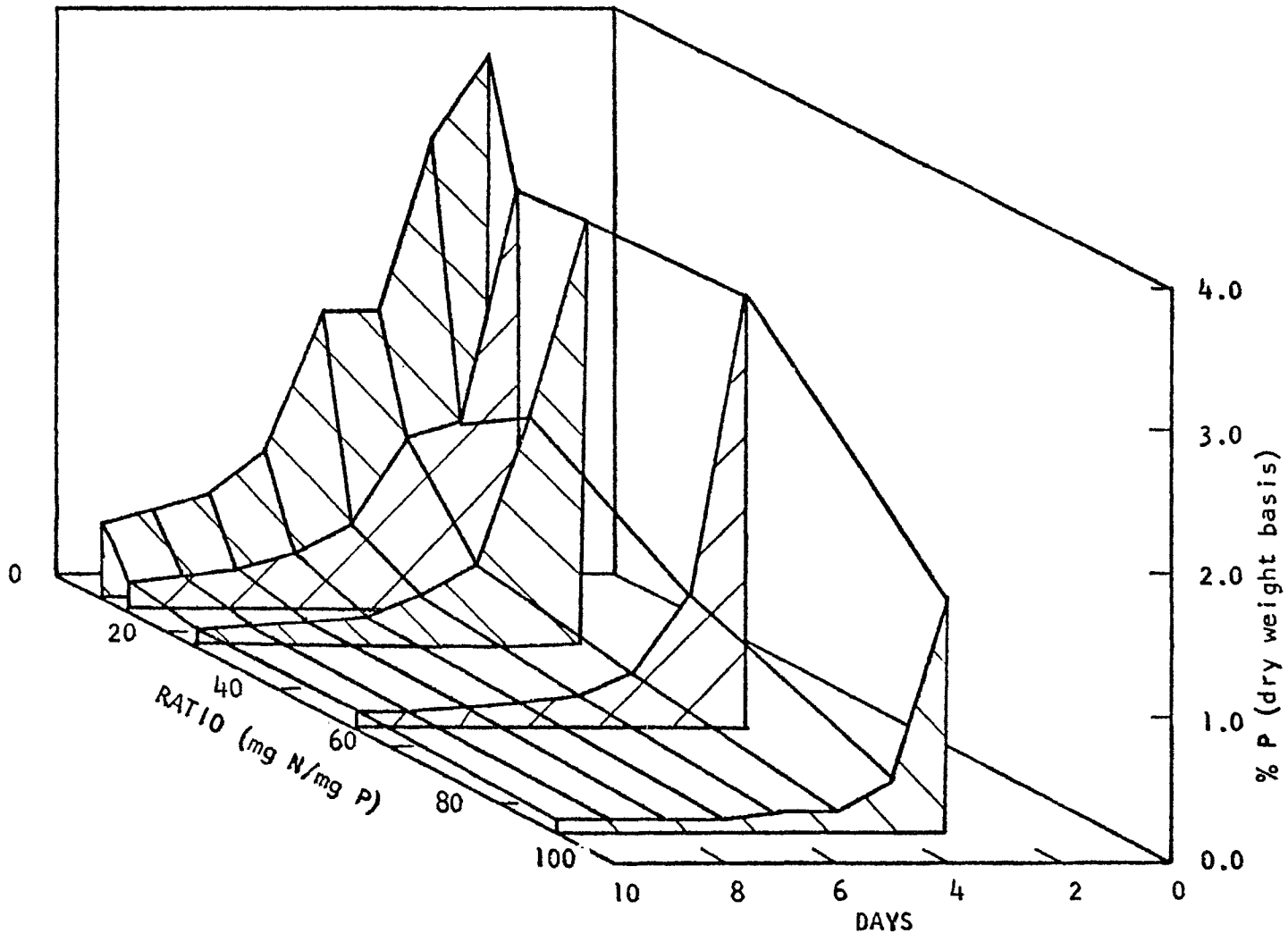

Figure 1. Algal phosphorus yield coefficients for batch cultures with differing initial nitrogen to phosphorus ratios, inoculated on day 0. (modified from Porcella 1970)

The work of Fuhs (1971) helps to clarify the dependence of phosphate uptake rates on both ambient phosphate concentrations and internal phosphorus stores. He resuspended cells, grown in chemostats at various growth rates and having different internal phosphorus contents, in media of increasing phosphate concentrations and measured uptake rates. He found that the uptake rate increased with decreasing internal phosphate levels; it increased hyperbolically with external phosphate levels. This indicates some type of feedback inhibition, the mechanism or mathematical form of which has not yet been completely identified.

Rhee (1973) showed that phosphate uptake rates can be correlated with external phosphate concentrations by a square hyperbola. He also presented evidence that the inhibition is non-competitive, using total internal phosphorus as a measure of inhibition. This is slightly in error, since polyphosphates, which are formed as a product of luxury uptake, often reside in a precipitated crystaline form (Harold, 1966) which cannot drive chemical reactions. Rhee's data, however, show a good fit to his hypothesis, since polyphosphate concentrations are approximately proportional to total internal phosphorus in the range of growth rates he employed.

An important component of intracellular phosphorus is volutin. The exact structure of the volutin crystals is unclear, but it is well established that the major constituent is polyphosphate precipitated at high ionic strength

(Lewin, 1966; Harold, 1966). The crystals have been observed to grow in the light and deteriorate in the dark, leading most investigators to postulate light as the energy source for forming the high-energy bonds found in polyphosphate. The only pathway for forming polyphosphate is a reaction catalyzed by polyphosphate kinase in which ATP donates its terminal phosphate to an existing chain. While it has been shown that a single phosphate can then be removed from volutin and added to either ADP to form ATP, glucose to form glucos-6-PO_4, or fructose to form fructose-6-PO_4, no conclusive evidence exists to prove polyphosphate is an energy storage crystal.

It is obvious from this discussion that fine resolution of algal growth and nutrient uptake kinetics requires a type of variable algal phosphorus content or polyphosphate formation or both. In the following discussion, it will be pointed out that some authors do not consider this fine resolution necessary while others put much emphasis upon their uptake components.

Oxygen Depletion Models

Varga and Falls (1972) examined several kinetic formulations for estimating oxygen depletion in the Keystone Reservoir in Oklahoma. The reservoir was taken to be two dimensional, longitudinally and vertically. They assumed the longitudinal distribution of dissolved organic matter did not vary temporally and that the transverse distribution was

uniform in space. Oxygen consumption was computed from the stoichiometries for respiration of dissolved organic matter and benthal deposits. Absorption of oxygen at the reservoir surface was calculated using arbitrary transfer coefficients; steady convective velocities and turbulent transfer coefficients then dispersed oxygen among the vertical and longitudinal compartments. Apparently implicit finite differences were used to solve the equations, but no explicit comment is made. While predictions are presented for several sets of kinetic parameters, no comparison with field data is shown.

Newbold and Liggett (1974) based their oxygen depletion model on algal growth and respiration and zooplankton predation and respiration. Periodically, during their time-marching scheme, they updated algal and zooplankton concentrations using field data; these concentrations were not calculated. They then used growth, decay, and sinking of the input species to explicitly compute dependent oxygen concentrations and the accumulation of benthic sludges, which in turn depleted oxygen. A one-dimensional, horizontally averaged, mass transport model with variable turbulent diffusion coefficients was used to impose the effects of thermal stratification on the system. Thermal data were interpolated to give daily temperature profiles that were used in conjunction with the Richardson number technique for determining vertical turbulent diffusion coefficients, but they were never verified. Predicted oxygen profiles duplicated field data very

well, suggesting that hypolimnetic oxygen depletion is closely related to algal and zooplankton kinetics. However, their choice of sinking velocity and euphotic zone depth implied a gross diel-averaged growth rate, in the steady-state epilimnion, in excess of 1.0 per day.

Eutrophication Models

In this class of models, measured concentrations of biological and chemical species are not used as input data, except as initial conditions obtained from field data. All species and species interactions are predicted by simultaneous solutions of their respective mass balance equations. Bannister (1974) proposed a chlorophyll-a based algal model, utilizing algae as the dependent specie. He proposed that algal growth should not be based upon the usual kinetic formulas, but rather upon the quantum yield, or the ratio of energy absorbed by chlorophyll-a to carbon fixation. Predation and endogenous catabolism were lumped together in one, constant loss term, and the euphotic zone was assumed to be a completely mixed reactor. The only analysis consisted of a steady-state solution, which he compared to assumed steady-state field values. No time dependent solution was shown, and no field data comparisons were presented.

Lehmann et al. (1974) presented a model of biomass prediction that has separate mechanisms for cell growth and nutrient uptake; they also assume a completely mixed

epilimnion. The phosphorus uptake rate is dependent on both extracellular and intracellular phosphorus levels, but the growth rate is dependent only on intracellular levels. Using only two algal species, a diatom and a chrysophyte, limited by silicon and phosphorus, respectively, they showed a quantitative match of Synedra and Dinobryon cell counts in Linsley pond, Connecticut, over a three-month period. Unfortunately, they did not have a set of nutrient measurements synoptic with cell counts, so it is difficult to evaluate the verification attempt. Explicit finite differences were used to solve the equations.

Di Toro et al. (1971) based their model on the trophic level hypothesis. They assumed primary producers can be represented by one "average" phytoplankter and predation upon phytoplankton could be approximated by one "average" zooplankter. This allowed them to model algal activity with only three compartments: algal chlorophyll-a, nutrients, and zooplankton. The resulting mass balance equations were solved using the two-time level method of Runge. While this technique is stable, it does overestimate some Fourier components (Roache, 1976). The first verification presented by Di Toro et al. (1971) is for a single reach of the San Joaquin River, California; advective and diffusive transport was not considered. For a two-year period, the predictions qualitatively match the phytoplankton data; for a one-year period, they qualitatively matched zooplankton data. However, the model

failed to duplicate nutrient data in form, magnitude, or timing for the full two-year verification period. Di Toro (1976) subsequently added several new species to help improve predictions. First, he considered two limiting nutrients: nitrogen, which was split into organic nitrogen, ammonia, and nitrate fractions, with only nitrate available for growth; and phosphorus, which was split into organic and inorganic fractions with only inorganic phosphorus available for algal growth. Second, while retaining the trophic level hypothesis, he added two more trophic levels, carnivorous zooplankton and upper predators. The new formulation was applied to Lake Huron. The transport analog consisted of segmenting the lake into five compartments in three dimensions, in order to simulate vertical stratification and to segregate zones affected by Saginaw Bay from the rest of the lake. Exchange coefficients were adjusted until heat transport duplicated observed temperatures in each segment. Chlorophyll-a, organic carbon, nitrogen, and total phosphorus data were compared to model predictions in three of the five segments. In all segments, qualitative matches of at least one species was obtained, but in no segment were all species matched simultaneously. Chlorophyll-a and carbon data were never matched synoptically in any segment.

Canale et al. (1973) modeled the Grand Traverse Bay with essentially the same biological system used by Di Toro et al. in the San Joaquin River, but they added silica

limitation to algal growth. The equations were solved by the predictor-corrector method of Adams, similar to that of Runge, used by Di Toro et al. The bay was divided into six completely mixed reactors with unverified mass flux terms approximating horizontal intercompartment mass transfer. Predictions were compared with field data for chlorophyll-a, zooplankton, ammonia, nitrate and nitrite, silica, and primary productivity for all segments in the analog for a twelve-month prediction period. The predictions show little or no agreement with field data, even in a qualitative sense.

Baca et al. (1976) also used the trophic level hypothesis to model Lakes Mendota and Wingra in Wisconsin and Lake Washington in Washington. Their dependent species were phytoplankton, chlorophyll-a, zooplankton, benthos, organic and inorganic phosphorus, organic nitrogen, ammonia, nitrite and nitrate. The transport algorithm was based on horizontally averaged, one-dimensional, mass transport equations with variable turbulent diffusion coefficients determined by an empirical, exponential relation obtained from stratified lake data. The system was solved with implicit finite elements using a linear interpolent. The Lake Washington verification of the model consisted of comparisons to monthly samples analyzed for chlorophyll-a, inorganic phosphorus, and nitrate between April and November. The vertical profiles presented show a good quantitative match with field data, but the use of only monthly samples and the conspicuous

absence of data for August leave questions as to verification validity. Chlorophyll-a, inorganic phosphorus and ammonia were measured monthly in Lake Mendota, between June and October. Vertical profiles in July seem to indicate an algal bloom which the model did not predict. Again, the use of monthly data leaves questions as to bloom timing and peak magnitudes. The Lake Wingra verification was done using closely spaced temporal data, for biomass and orthophosphate, for a six-month period from April to September. These comparisons show a qualitative match of the data, although an early algal bloom is completely missed by the model.

Bierman (1976) proposed a model containing four algal species, their associated limiting nutrients, and two zooplankters. The four algal species, with all kinetics based on biomass, are: (1) a diatom limited by silicon, (2) a green alga limited by either phosphate or nitrate, (3) a blue-green also limited by nitrate or phosphate, (4) and a phosphate-limited, nitrogen-fixing blue-green alga . Like Lehman et al., Bierman uncoupled nutrient uptake from algal growth, but he also introduced a steady-state polyphosphate compartment. It is steady state in that once internal phosphorus levels are known, polyphosphate levels are determined from an empirical equation derived from chemostat data in which all phosphate fractions have reached a dynamic equilibrium. The model was solved using a fourth-order Runge-Kutta method. Application to inner Saginaw Bay, Michigan,

was done assuming a completely mixed reactor. Verification was based on ten months' data for chlorophyll-a, orthophosphate, nitrogen, and silica, taken between February and November. While the silicon and nitrogen predictions qualitatively match the field data, an algal bloom that does not happen in June as predicted, and phosphate predictions are not even qualitatively like their respective field data.

Depinto et al. (1976) applied the same model to Stone Lake, Michigan, assuming it was a completely mixed reactor between the months of May and October. They showed an excellent, quantitative match of species succession during the first algal bloom in July, but they admitted that the growth rate of each algal species was set to zero when the alga reached its measured maximum biomass concentrations. The model was unable to quantitatively match the second bloom, even with the artificial constraint on computed algal biomass.

Ecosystem Models

Some investigators have attempted to simulate entire aquatic ecosystems using very large mathematical analogs. The first of these was discussed qualitatively by Chen (1970), and mathematical formulations were presented by Chen et al. (1975). They used five algae, with all kinetics based on algal biomass: diatoms, green algae, dinoflagellates (Pyrrophyta), blue-green algae, and attached Cladophora. The other species in the model are two herbivorous zooplankters,

two carnivorous zooplankters, four fish (each structured with three life stages), benthic decomposers, particulate organic matter, bacteria, the carbonate system, pH, and six nutrients (nitrogen, ammonia, nitrite, nitrate, phosphate, and silica). This entire system was linked to a one-dimensional, horizontally averaged mass transport analog which was solved by implicit finite differences. The verifications presented in Chen et al. (1972) for Lake Washington show a good qualitative match of algal biomass and oxygen profiles, but time-depth plots of nitrate isopleths showed a poor match. The model was applied next to San Francisco Bay, which was represented as a series of laterally connected, horizontally averaged, one-dimensional mass transport analogs. Good matches were obtained to August data (averaged over four years) for ammonia, nitrate, phosphate, biochemical oxygen demand (BOD), and dissolved oxygen; unfortunately, no synoptic algae data were available.

Kelly (1973) modeled the Delaware estuary with a trophic level ecosystem model. He included phosphorus, nitrate, algae, zooplankton, fish, bacteria, BOD, and oxygen. The transport analog consisted of longitudinally connected, completely mixed reactors, with dilution rates determined by using the average rate of flow and reach volume. Verification was done by comparing predicted steady-state spatial distributions of oxygen, BOD, total phosphorus, and Kjeldahl nitrogen to data observed one day in September. Oxygen and

BOD distributions match well, but phosphate and nitrogen predictions both deviate markedly from the observed data. Again no algae data are available for verification.

The most recent large-scale model is presented by Park (1974). It contains two algae, four zooplankters, two benthic invertebrates, three fish, three macrophytes, and three nutrients: phosphate, nitrate, and carbon. Scavia (1976) applied this model to each of the Great Lakes assuming each lake's transport processes could be approximated by two vertical compartments with exchange coefficients. The models were run from March to November, and verification was attempted with carbon and phosphate data separated by more than one month on a temporal scale. While carbon data and predictions were the same order of magnitude, the two seldom agreed, even qualitatively, and phosphorus variations were not matched at all.

Parameter Ranges

The random incorporation of herbivourus zooplankton predation, detrital pools, and internal algal structures in "verified" models is possible within the accepted ranges of kinetic coefficients. While all investigators claim parameter values within literature limits, these limits are wide enough to obtain a full range of system responses. This freedom will almost always allow an investigator to verify at least one species against field data, regardless of the overall model

structure. The most commonly used parameters and some of their literature values are listed in Table 1.

While some of the large variability in kinetic parameters is due to the differences between the algal species tested, values for several commonly studied algae show large variability within a species. A large portion of the variability is due to incomplete or imprecise reporting of experimental procedures. This is especially true for the light intensities used to grow the cultures, and the identification of a limiting nutrient by experimental procedures. Many investigators assumed that if a nutrient, in batch culture, is initially at a lower proportion than that necessary to support growth, it will not only terminate growth, but will also be rate limiting during the entire growth cycle. The results obtained for phosphorus uptake rates and phosphorus content are strongly dependent upon the test alga's physiological condition, which in turn is dependent upon the alga's previous environment. However, many investigators give little or no attention to this portion of the experimental procedure.

Literature Critique and Study Objectives

Few authors agree what environmental effects or species must be incorporated in a representation of an aquatic ecosystem. Some include detrital matter, while some assume instantaneous nutrient regeneration; some include zooplankton

Table 1

Literature ranges for some of the common biological coefficients used in formulating species interactions.*

Ynx; Total algal phosphorus content (gP/g dry wt.)

.004	Carpenter 1970
.004-.026	Fuhs 1969
.005-.075	Kholly 1956
.0075-.0434	Knauss & Porter 1954
.005-.028	Ketchum 1939
.013	Lund 1950
.06	Rhee 1973
.008-.017	Scott 1945
.0018-.062	Serruya & Berman 1975
.009	Jorgensen 1975
.028	Gest & Kamen 1948
.04	Fuhs 1971
.008	Gerloff & Skoog 1947
.01-.10	Porcella 1970
.011-.029	Di Toro 1971

Ynz; Total zooplankton phosphorus content (gP/g dry wt.)

.003-.038	Barlow 1965
.006-.018	Beers 1966
.006-.012	Corner 1973
.03	Culver 1973

$\hat{\mu}_x$; Maximum specific algal growth rate (day^{-1}; base e; 20°C)

.8-2.1	Bierman 1976
.4-3.9	Di Toro 1971
1.5	Fuhs 1969
1.3-2.9	Goldman & Carpenter 1974
2.1-3.6	Guillard et al. 1973
.2-8.7	Fogg 1965
2.2	Thomas & Dodson
.7-3.4	Canale 1974

$\hat{q}$ Maximum specific phosphate uptake rate (day^{-1}; base e; 20°C)

.024-.133	Bierman 1976
.75-1.07	Fuhs 1969
.053	Ketchum 1939
.02	Lehman 1975

K_n Monod half-velocity for algal growth (g/m^3)

.006-.01	Di Toro 1971
.016-.5	Lehman 1975
.018-.053	Fuhs 1971

Table 1 Continued

K_{xn};	Specific algal decay rate (day^{-1}; base e; 20°C)	
	.08-.30	Di Toro 1971
	.01-.18	Helleburst 1965
K_{zn};	Specific zooplankton decay rate (day^{-1}; base e; 20°C)	
	.04-.28	Hall 1964
	.008-.10	Di Toro 1971
Y_{zx};	Zooplankton decay rate (g dry wt. zoo./g dry wt. algae)	
	.11-.98	McCarty 1968
	.56-.73	Schindler 1968
	.6	Di Toro 1971
	.6	Bierman 1976
	.44-.997	Corner 1973
K_x;	Monod half-velocity for zooplankton predation (g dry wt./m^3)	
	.3	Di Toro 1971
	.14	Hall 1964
K_c;	Monod half-velocity for algal growth based on internal phosphate stores (gP/g dry wt. algae)	
	.004	Rhee 1973
$\hat{\mu}_z$;	Maximum specific zooplankton growth rate (day^{-1}; base e; 20°C)	
	.21-.30	Bierman 1976
	.07-.51	Hall 1964
	.31-.79	Edmondson 1962
V_x;	Algal sinking velocity (m/day)	
	.09-.49	Smayda 1974
	.15-.4	Bierman 1976
V_p;	Detrital sinking velocity (m/day)	
	.35-1.5	Smayda 1974

*Definitions in Chapter III.

as a modeled species while others assume losses to zooplankton are either constant or negligible; and some include internal algal structure. The various biological models and a tabulation of the nutrient kinetics used, and the species included, are shown in Table 2. The need for a systematic comparison of the biological analogs currently used is evident, since the disagreement shown in Table 2 must be resolved before an approximate analog to primary production can be formulated.

Any attempt to compare biological models is confounded by turbulent transport into and out of zones of net production or decomposition. Therefore, an accurate representation of turbulent transport is necessary to allow observation of the individual biological models in similar turbulent structures, unconfounded by transport inadequacies or averaging errors.

Since eutrophic and oligotrophic communities can be identified, different ecosystem models may be required in different lakes. Therefore, any comparison of biological models must take into account lake tropic status. This will necessitate comparing the models in at least two lakes on opposite ends of the trophic scale.

With these considerations in mind, the specific objectives of this report are: (1) to categorize eutrophication model structures for systematic comparison; (2) to develop verification criteria for data comparisons; (3) to

Table 2

Compartments and process formulations of the surveyed biological models.

AUTHOR	DEPENDENT ALGAL VARIABLE	PHOSPHATE UPTAKE GROWTH INDEP. ?	DETRITUS INCLUDED ?	ZOOPLANKTON INCLUDED ?
Varga	none	no	yes	no
Newbold & Liggett	biomass	no	no	yes
Bannister	chlorophyll-a	no	no	no
Lehman	biomass	yes	no	no
Di Toro	chlorophyll-a	no	yes*	yes
Canale	chlorophyll-a	no	yes*	yes
Baca	chlorophyll-a	no	yes*	yes
Bierman	biomass	yes	no	yes
Chen	biomass	no	yes	yes
Kelly	biomass	no	yes	yes
Scavia	biomass	no	yes	yes

* approximated by soluble organic unavailable nutrient pools

select two lakes with sufficient biomass and nutrient data to test the biological analogs; (4) to employ an accurate representation of turbulent transport processes to avoid confounding errors in the biological and transport models; and (5) to assess each model's ability to duplicate field data based on the verification procedure.

Chapter III

CONSTRUCTION OF EUTROPHICATION MODELS

Lake Choice

The availability of nutrient and algal data, the documentation of hydrologic phenomena and their associated nutrient loads, and trophic status were the three major criteria employed in choosing the lakes used for the biological model comparisons. Abundance or lack of data partially determines the accuracy of any comparison, since confidence in field data averages increase with increasing numbers of field samples. Also, the many solutions obtainable within the accepted range of kinetic parameters necessitate synoptic algae and nutrient data for comparison. Spatially and temporally concentrated data are needed, because no theoretical ecosystem model can claim a resolution greater than the data used to verify it. For these reasons, Cayuga Lake and Canadarago Lake were chosen as the test systems for the model comparisons.

Some of the characteristics of these lakes are listed in Table 3. Both lakes are located in the Finger Lakes region of New York at approximately 42°45' N latitude, but they are strikingly dissilimar in morphometry, hydrology,

Table 3

Lake Characteristics

Characteristic	Cayuga Lake**	Canadarago Lake*
Surface Area (km^2)	172.1	9.0
Volume (m^3)	9.4×10^9	5.75×10^7
Mean Depth (m)	54.5	7.7
Mean Hydraulic Detention Time (years)	12	0.6
Maximum Length (km)	61.4	6.4
Maximum Width (km)	5.6	1.9
Maximum Depth (m)	130	12.8
Epilimnion Thickness (m)	15	7

* Hetling, Harr, Fuhs, and Allen (1969)

** Oglesby and Allee (1974)

and trophic status. Cayuga Lake was classified as typically oligotrophic by Birge and Juday (1921) for data taken in 1910 and 1918, also by Muenschler (1931) using data taken in 1927 and finally by Burkholder (1931) using monthly data collected from 1927 to 1929. Based on the presence of blue-green algae, at a single station, Howard (1958) classified Cayuga Lake as eutrophic, but data received from Peterson (1976) for 1972 and 1973 indicated the blue-greens to be an inconspicuous contributor to total algal biomass, even during the blue-green bloom in late summer.

Peterson's data were used for the comparisons in Cayuga Lake for 1973. The data were obtained by sampling six stations, spaced along the length of Cayuga Lake. In 1973, nineteen cruises were taken during a period spanning 224 days, with a maximum temporal data separation of twenty days occurring in mid-April; the average was twelve days. During every cruise, samples were pumped from depths of 0, 2, 5, 10, 20, and 50 meters. Measurements were made for various physical, chemical, and biological parameters, including chlorophyll-a, soluble reactive phosphorus, oxygen, temperature, algal biomass, secchi disc, pH, phenolphthalein alkalinity, chloride, sulfate, calcium, magnesium, nitrate, silica, and total and volatile suspended solids. Algal cell counts were made in each sample with an inverted microscope, and volumes were estimated for over 200 species. For the purposes of this study, the cell volumes have been converted

to dry weights by assuming a specific gravity of 1 and a 90% water content. While most parameters were measured at every station, every depth, and every cruise, algal samples were collected at only three stations each cruise.

Almost half of the total hydrologic input to Cayuga Lake occurs in the first three months of the year; most of the annual nutrient load occurs then also (Oglesby et al., 1969). This impulse loading, before the beginning of the six-month prediction period (March 28 to August 29), coupled with the 12-year hydraulic detention time of the lake, allows it to be modeled as a batch reactor. Therefore, the Cayuga Lake analog needs no estimates of nutrient addition or species dilution rates; this simplifies the transport components of the model both mathematically and conceptually.

Canadarago Lake is one of several lakes intensively studied in 1969 as part of the North America Project. Based on a Vollenweider analysis, Hetling (1969) classified Canadarago Lake as typically eutrophic. The nutrient loadings to Canadarago are five times larger than the minimum required by Vollenweider's criteria, and the hypolimnion is at least partially anaerobic for much of the summer. A poorly maintained sewage treatment plant on one of the lake's tributaries accounts for much of the nutrient loading prior to 1975.

During Hetling's study, all stream flows into Canadarago Lake were recorded with staff gages. The streams were

sampled every two weeks, and the samples analyzed for sodium, potassium, magnesium, calcium, chloride, sulfate, nitrate, nitrite, ammonia, organic soluble and particulate nitrogen, reactive phosphorus, total soluble and particulate phosphorus, organic soluble and particulate carbon, and carbon dioxide. Regression analysis was used to estimate the coefficients of a second-degree polynomial relating nutrient loading to the flow rate of individual streams. These regression equations were then used in conjunction with daily flow data to obtain daily nutrient loadings to Canadarago Lake. The tabulated flows can also be used to estimate lake dilution rates.

Lake data, presented in Hetling (1969), were obtained by sampling ten different stations at three different depth zones; 0-4.5, 4.5-9.0, 9.0-12.6 meters. The nine-meter division was only nominal; it was adjusted from cruise to cruise to approximately coincide with the thermocline. The resulting uncertainty in the elevation of the top of the bottom stratum makes it difficult to determine how to average the model predictions for verification against field data. The samples were analyzed for the same constituents that were measured in the streams, with the addition of temperature at one-meter intervals, secchi disc, and dissolved oxygen. While most data are presented as horizontal averages in the three depth zones (weighted by volume), algal biomass is reported as an entire lake average ,

since the algal samples were composited before analysis. Biomass was estimated by using cell counts and average volumes, assuming water to contribute 90% of the algae's volume, and calculating weights assuming the cells had unit density.

The Mass Balance Equation

All the lake models tested incorporated one-dimensional, horizontally homogeneous discretizations: (1) because horizontal velocities and turbulent diffusion coefficients are much larger than the vertical, so the effects of thermal stratification are essentially one-dimensional; (2) because one-dimensional models can be solved inexpensively, permitting more computer time to study biological analogs.

The governing equations can be derived from the laws of mass conservation assuming that the only transport processes are species sinking and turbulent diffusive transport. Since no quantitative representation of turbulent diffusive transport exists, the usual Boussinesq analogy was employed. This states that turbulent transport (since it involves no net fluid transport) is analogous to molecular diffusion, i.e. Fick's law. Usually the turbulent diffusion coefficients, $K(z,t)$, are much larger than molecular diffusion coefficients, so in practice empirical methods are used to evaluate $K(z,t)$, which varies in time and space, and molecular diffusion is ignored. Incorporating species sinking,

turbulent diffusion, and biological interaction, the principle of mass conservation leads to Eq. 1:

$$\frac{\partial \alpha}{\partial t} = \frac{1}{A}\frac{\partial}{\partial z}\left(KA\frac{\partial \alpha}{\partial z}\right) - \frac{1}{A}\frac{\partial}{\partial z}\left(V_\alpha A\alpha\right) + S_\alpha; \qquad (1)$$

where: α = arbitrary species concentration (mass/vol.);

t = time;

A = horizontal area at depth z;

K = turbulent diffusion coefficient (area/time);

V_α = sinking rate of species α (velocity);

S_α = biological sink-source term (mass/vol./time).

The resulting mass balance equation states that the time rate of change of species α in any layer is equal to the sum of turbulent and sedimentary transport into the layer plus any additions due to biological activity.

The transport portion (K) of the equation was the same in every comparison; only the sink-source terms changed when different biological analogs were tested. The turbulent diffusion coefficients were evaluated independently from the known heat budgets of the lakes and treated as input data along with basin morphometry and daily temperature profiles. The methods employed are described in the next section and the sink-source terms are described below.

Evaluation of Diffusion Coefficients

No conservative substance exists in these lakes that can be used in a reverse solution of the transport analogs

to evaluate the turbulent diffusion coefficients. Therefore, Reynolds analogy was employed. This assumes that the eddy diffusivities, turbulent diffusion coefficients, and turbulent heat transfer coefficients are equal. The assumption is justified because the mechanisms for turbulent transfer of momentum, mass, and heat are similar. unlike viscous momentum transfer, molecular diffusion, and heat conduction.

The turbulent diffusion coefficients were determined in both lakes by using the predictive heat transport formulation of Bedford and Babajimopoulus (1977). It calculates Richardson number turbulent heat transfer coefficients defined by:

$$K(z,t) = Kmax(1 + \beta R_i)^{-n}; \qquad (2)$$

where: Kmax = maximum (surface) diffusion coefficient (area/time);

R_i = Richardson number = $-\alpha_v g z^2 (\frac{\partial T}{\partial z})/w^2$ (dimensionless);

α_v = coefficient of volumetric expansion of water (vol/°C);

g = acceleration due to gravity (velocity/time);

T = temperature (°C);

w = wind friction velocity = $(\tau_s/\rho)^{1/2}$ (velocity);

τ_s = wind surface shear (force/area);

ρ = density of water (mass/volume).

β and n = empirical coefficients.

The model uses these explicitly calculated diffusion

coefficients to simulate heat transport from the surface using the heat transport equation:

$$\frac{\partial T}{\partial z} = \frac{1}{A} \frac{\partial}{\partial z} \left(KA \frac{\partial T}{\partial z}\right). \qquad (3)$$

Having new temperature profiles, the diffusion coefficients are then recalculated, and heat transported for another day. In this way the model marches in time, calculating diffusion coefficients, and predicting daily temperature profiles. The coefficients n and β in Eq. 2 were adjusted* until the predicted thermal profiles matched the measured profiles. Calculated and field data temperatures for Cayuga Lake are shown in Figure 2. The heat added at the surface was determined by the method described in Edinger (1968). Pseudo heat-transfer coefficients and temperature gradients were calculated at the surface. They take into account (1) conduction, (2) net absorption of both long and short wave solar radiation, and (3) losses due to the latent heat of vaporization associated with evaporation.

Analysis of the field data for Canadarago Lake revealed hypolimnetic heating in excess of that possible by turbulent heat transport from the surface. The heat input method used in Cayuga Lake fails when the epilimnion is as thin as it is in Canadarago Lake. In these cases, heating of the upper hypolimnion by direct absorption of solar

---

*These adjustments were performed by Mr. Michael Trimeloni, Graduate Research Associate, Dept. Civil Engineering, The Ohio State University, Columbus, Ohio.

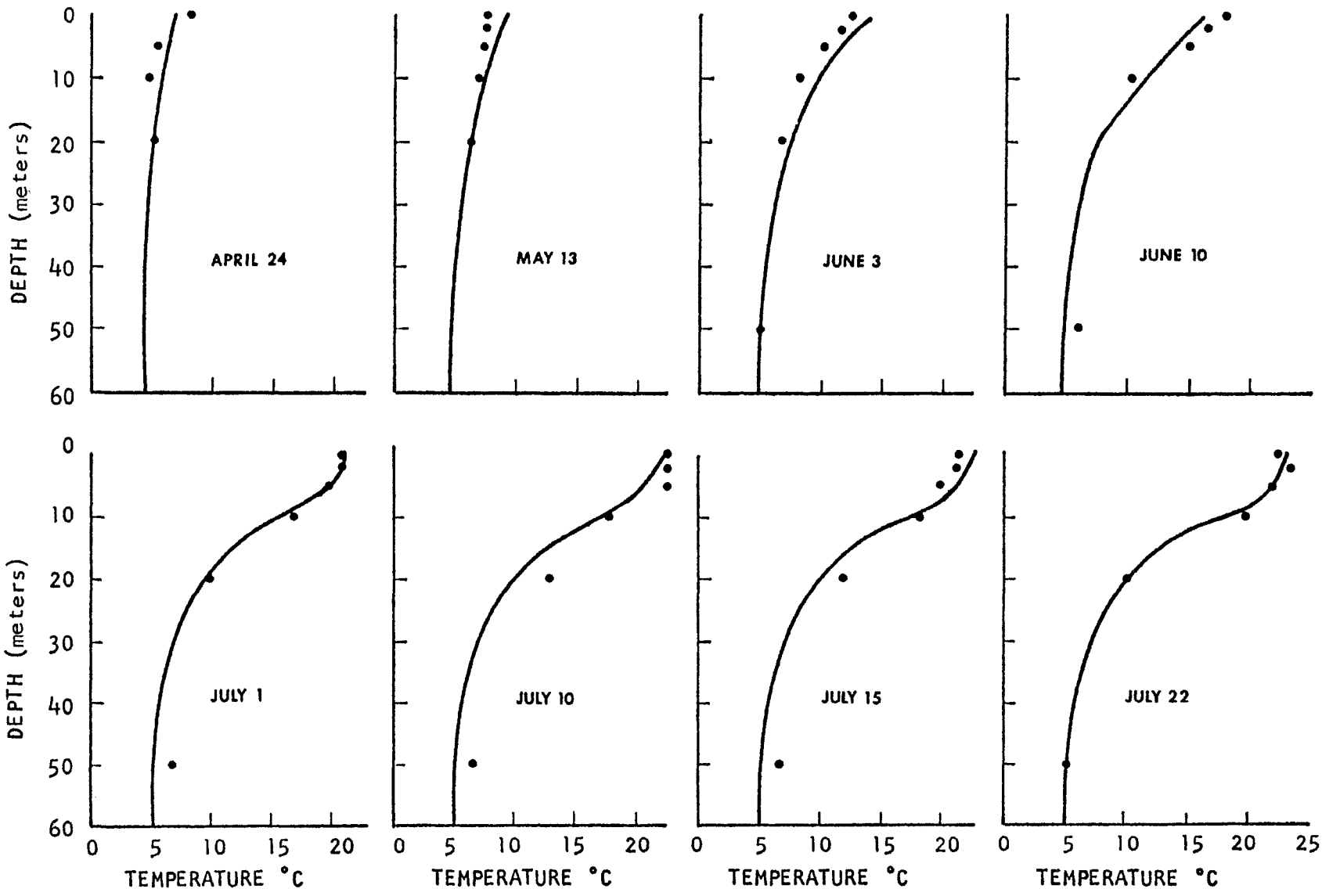

Figure 2. Predicted thermal profiles (——) and horizontally averaged field data (•) for Cayuga Lake 1973

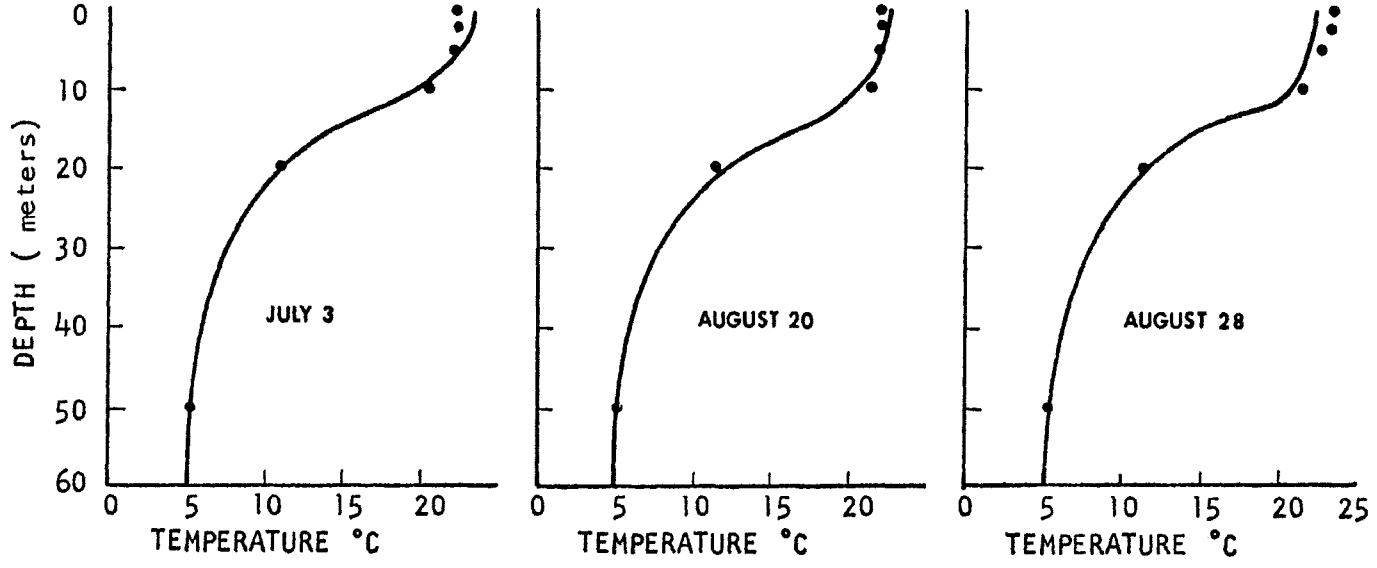

Figure 2. Continued

radiation is no longer negligible compared with turbulent transport of heat from the surface. Therefore, the heat input method was changed; the heating at the surface was assumed to be only conduction of heat from the surrounding air, and solar heating was added as a source in every layer. This approach neglected the loss of heat due to evaporation from the surface. The seasonal dependence of the high noon light intensity and length of photoperiod were described by Equations 9 and 10 (presented later in this chapter) and the Beer-Lambert law was used to define the extinction of light in the water column. The amount of heat added to the layer was equal to the solar energy absorbed by that layer. It was calculated by using a discrete approximation to the solar energy spectrum; each discrete set of wavelengths having a representative attenuation coefficient, and energy contribution. The light energy absorbed in each layer was then equal to the difference in the amount of energy incident on its upper and lower surfaces. Therefore, heat was transported from the surface by turbulent diffusion and added as a source. This more exact method of introducing heat to the lake allowed a much better fit of measured thermal profiles. The upper hypolimnion was still heated by direct absorption of solar energy after the establishment of severe stratification, as indicated by data. Computational details of the method used to transport heat are given by Bedford and Babajimopoulos (1977).

The predictions and field temperatures are shown in Figure 3.* Both in Cayuga and Canadarago Lakes, the field thermal profiles were matched to within 2° celsius by model predictions for most data points. In Canadarago Lake the match is less accurate at the bottom two nodes. This is because the bottom two nodes represent two small depressions at opposite ends of the lake with an almost negligible volume. The Richardson number approach works for "regular" basins, but begins to fail when such irregularities as those in Canadarago Lake are encountered. While the bottom turbulent diffusion coefficients are slightly in error, the small volume of the nodes makes the affect of the error minor. Whenever a horizontal segment of a lake is found in two sections, as with the two depressions in Canadarago Lake, errors will be encountered.

Algal Models

In order to test the various eutrophication models which have been proposed, a limiting nutrient or nutrients must be identified. The algae in both Cayuga Lake (Oglesby, 1969) and Canadarago Lake (Hetling, 1974) are phosphorus limited. Inspection of available field data shows that the available nitrate concentrations would allow a higher algal reproductive rate than that dictated by ambient phosphate

---

*The solar heating subroutine was programmed by William Bartlett, Graduate Research Associate, Dept. Civil Engineering, The Ohio State University, Columbus, Ohio.

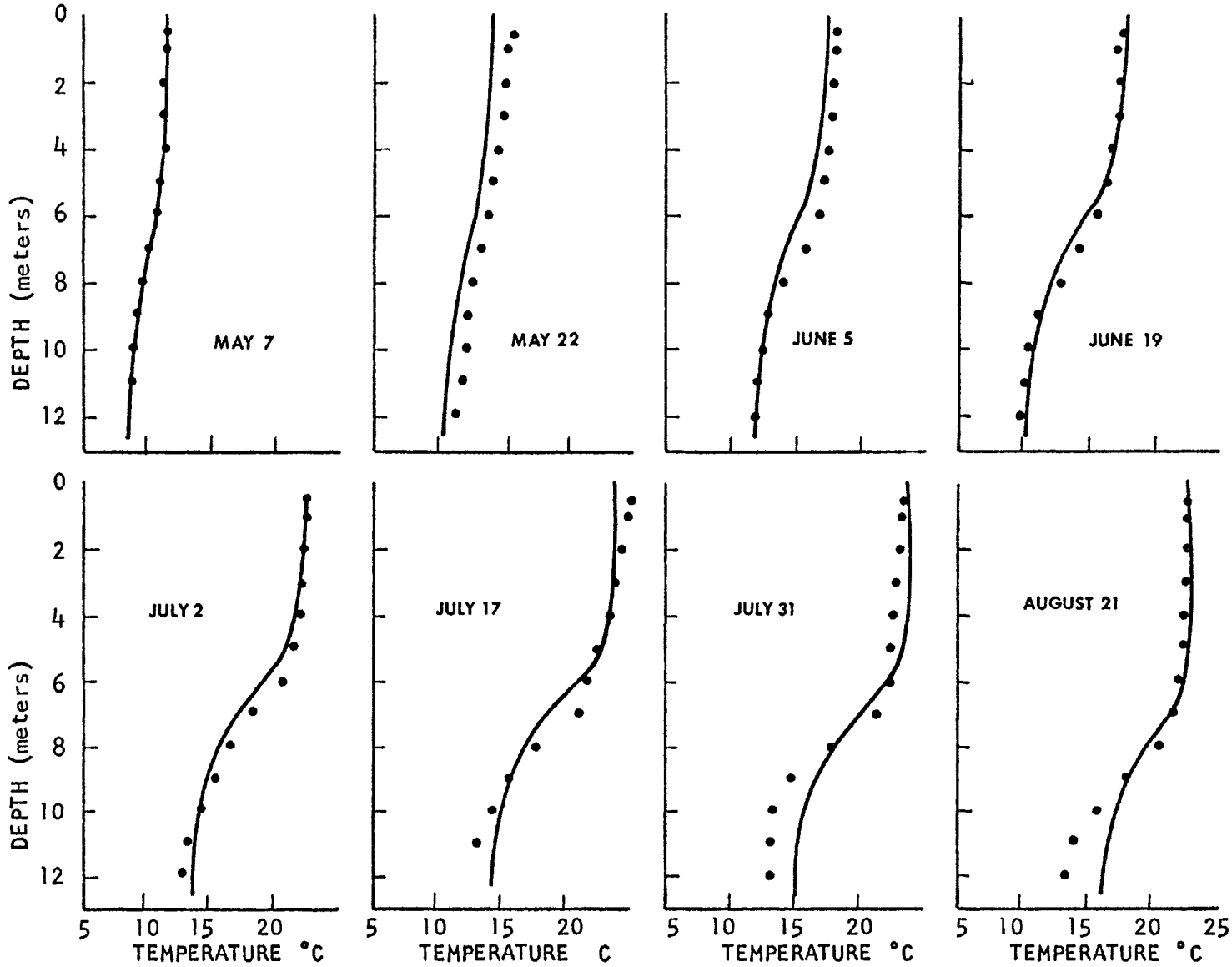

Figure 3. Predicted thermal profiles (—) and horizontally averaged field data (•) for Canadarago Lake 1969

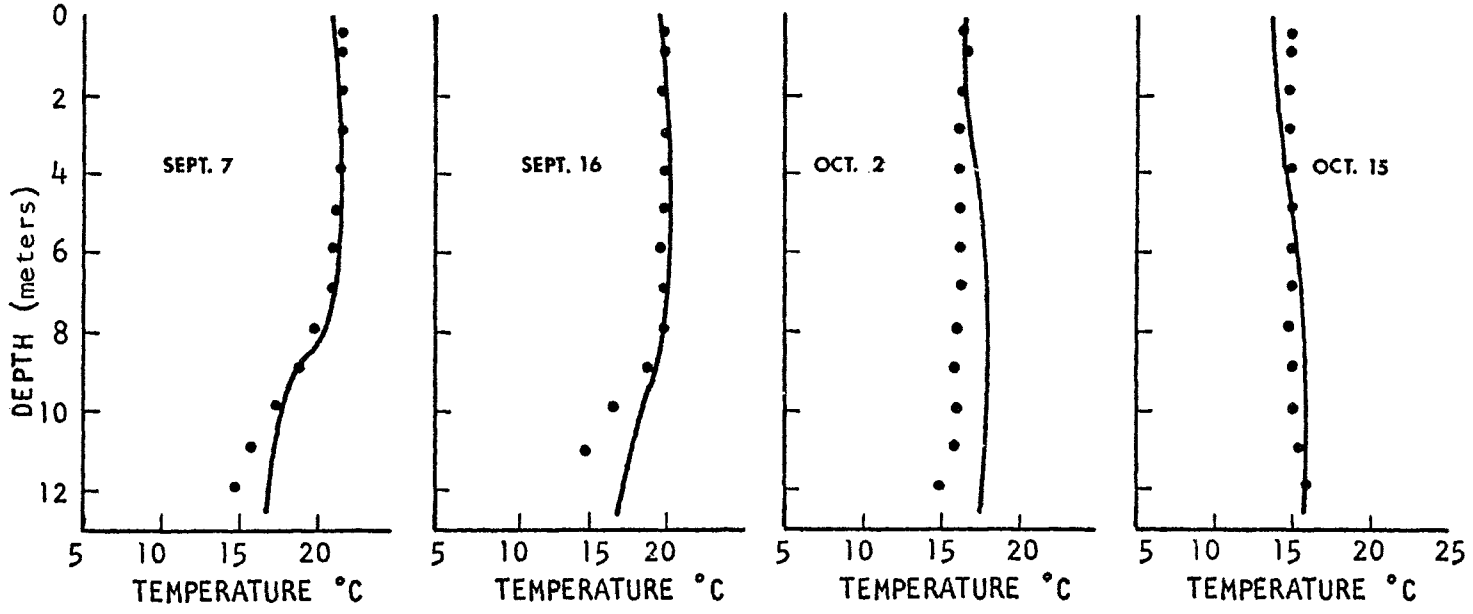

Figure 3. Continued

levels. Therefore, it was assumed that, not only is phosphorus limiting at the peak of an algal bloom, but it is the only limiting nutrient during the complete prediction period, in both lakes. This allows modeling of the ecosystem with only one limiting nutrient, phosphate.

This study did not examine algal models incorporating competition, succession, etc., among algal species; all models tested lumped all algae species together into a single compartment, total algal biomass. The general form of the algal sink-source (S_x) terms were the same regardless which level of nutrient uptake resolution was required:

$$\text{[algal reproduction]} - \text{[algal decay]} - \text{[predation]} - \text{[sinking losses to benthos]}. \quad (4)$$

The formulations of algal reproduction in the Literature Review were placed in three general categories for comparison: fixed phosphorus yield, variable phosphorus yield, and variable yield with polyphosphate formation. These categories differ in the algal reproduction term and added mass balances for internal phosphates and polyphosphates. For ease of discussion, the fixed yield model will be examined first.

Fixed Yield. In the fixed yield formulation (Figure 4a), reproductive rates are dependent upon ambient orthophosphate levels, light intensity, and temperature. The reproductive term takes the form:

$$\hat{\mu}_x \cdot \bar{f}(I) \cdot \frac{N}{N+K_n} \cdot X; \quad (5)$$

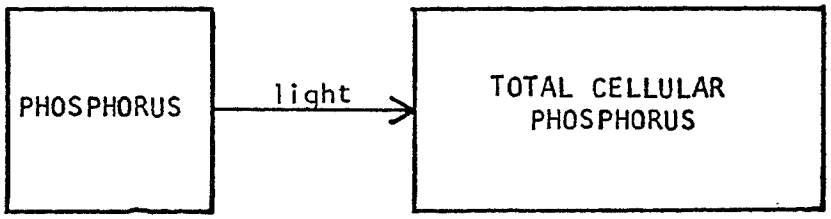

a) Fixed Yield

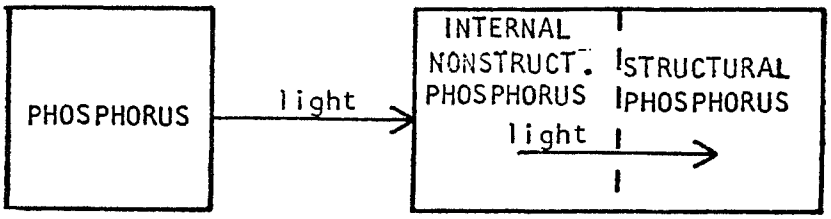

b) Variable Yield

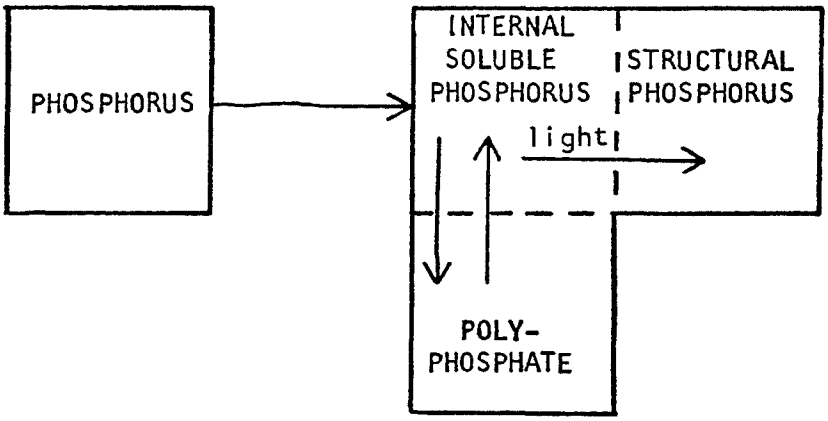

c) Polyphosphate

Figure 4. Diagramatic representation of the three algal structures for nutrient utilization.

where $\hat{\mu}_x$ = temperature dependent, maximum specific growth rate (per time);

$\bar{f}(I)$ = 24-hr averaged light function (dimensionless);

N = orthophosphate concentration (mass/volume);

X = algal dry wt. concentration (mass/volume);

K_n = Monod half velocity (mass P/volume).

Published algal growth rates were analyzed for temperature dependence by Canale and Vogel (1969). Although they had no growth rate data below 8°C, they were able to draw in two somewhat arbitrary straight lines depicting general growth rate trends for each of four taxonomic groups. These trends show growth rates for all taxa increasing linearly to at least 25°C before thermal inhibition is manifested. The growth rates then rapidly decrease to zero. Goldman and Carpenter (1974) used a chemostat to determine the maximum specific growth rates of algae grown at several temperatures ranging from 15 to 35°C. They fitted an Arrhenius exponential through the chemostate data, but the scatter in the maximum specific growth rate data would easily allow a linear fit as well. Therefore, the maximum specific growth rate and in turn the total reproductive rate was assumed to be directly proportional to temperature, with no growth at zero celsius. The high temperature inhibition indicated by Canale and Vogel was not considered in this study since the highest temperature in either lake did not exceed 25° celsius.

The dependency of algal growth on light intensity was described by the equation presented in Steele (1962). It was chosen because it describes photo-inhibition as well as light deficiency, yet it has fewer tuning parameters than the function proposed by Vollenweider (1965). Steeles' function is also used by Di Toro (1971), Lehman (1975), and Park (1974). The dimensionless function varies between 0 and 1 and has the form

$$f(I) = (I_j/I_{opt}) \text{ EXP}[1 - I_j/I_{opt}]; \qquad (6)$$

where: I_j = light intensity at any node j (energy/area);

I_{opt} = algal optimum light intensity (energy/area).

Light intensity was assumed to decline through the water column according to the Beer-Lambert law:

$$I_j = I_s \text{ EXP}[-(a + bX)z]; \qquad (7)$$

where: I_s = surface light intensity (energy/area);

a = extinct coefficient of a natural water (per length);

b = algal absortivity (mass/area);

z = depth from surface (length).

The total extinction coefficient, a+bX, is composed of light absorbed by the water, a, and the portion absorbed by the algae, bX. This self-shading effect was incorporated by Chen et al. (1975), Lehman et al. (1975), Baca and Arnett (1976), and Bierman (1976). The Beer-Lambert law was

utilized in its integrated form because the discretizations used allowed summation of the individual stratas absorption of light. Since the layers were small and algal gradients in the model were not two severe, the error in assuming uniform X there was negligible. The top ten meters of both lakes were discretized into 1-meter nodes; the light dependency of the algal growth rates and the self-shading effects were well resolved. The surface light intensity was assumed to vary during the daylight hours according to:

$$I_s = I_m \sin\left(\frac{\pi t}{\lambda}\right), \quad 0 < t < \lambda; \tag{8}$$

where: I_m = mid-day light intensity (energy/area);

λ = length of photoperiod (time).

The surface light intensity and, consequently, the reproductive rate were assumed to be zero at night.

Seasonal effects were imposed on the light function by empirical formulas describing mid-day light intensity and length of photoperiod as functions of elapsed time during the prediction period. Monthly light intensity data in Hutchinson (1957) were fitted with:

$$I_m = I_{equ} + (I_{sol} - I_{equ}) \sin\left(\frac{\pi te}{183}\right); \tag{9}$$

where I_{equ} = mid-day light intensity at the vernal equinox (energy/area);

I_{sol} = mid-day light intensity at the summer solstice (energy/area);

t_e = number of days after the equinox.

This sinusoidal function duplicated Hutchinson's data very well. Photoperiod length was similarly fitted with:

$$\lambda = 12 + (\lambda_{sol} - 12) \sin (\frac{\pi te}{183}); \qquad (10)$$

where: λ_{sol} = length of solstice photoperiod in hours.

During model solution, λ and Im were incremented daily, and Eq. 6 was averaged in time to obtain a daily average light function. When Eq. 7 and 8 are substituted into Eq. 6, the result is:

$$\bar{f}(I) = \frac{1}{24}\int_0^{\lambda} \frac{I_{mj}}{I_{opt}} \sin \frac{\pi t}{\lambda} \, EXP[1 - \frac{I_{mj}}{I_{opt}} \sin \frac{\pi t}{\lambda}] \, dt; \qquad (11)$$

where: I_{mj} = mid-day light intensity at node j.

Eq. 11 does not have an exact integral. Di Toro, et al. (1971) used the 24-hour average light intensity directly in Eq. 6 instead of integrating the fully assembled equation. Comparisons of this procedure to values obtained from a discrete numerical integration of Eq. 11 show Di Toro's method to (1) overestimate algal production at the optimal depth (i.e., where f(I) is maximum) by as much as 20% and (2) to underestimate production near the surface. Therefore, attempts to approximate Eq. 11 were initiated. The integrand can be reduced to a gamma function, but attempts to obtain solutions by this method required large amounts of computer time, since series approximations to gamma functions with fractional arguments do not converge rapidly. Attempts to expand the exponential term by a Taylor's series approximation

and integrate the resulting function also failed, since the series converged slowly (if at all) when high light intensities at the surface were used. Finally, a six-term Taylor's series approximation to the integrand was integrated, but again convergence was too slow to be useful. While the Taylor's series did not converge, it did yield some useful information. The value of the average light function, $\bar{f}(I)$, is a linear function of the photoperiod, λ. Therefore, it need only be integrated for one photoperiod length and others can be found by linear interpolation.

Since accepted engineering approaches to a solution were not fruitful, several attempts were made to fit arbitrary functions to the numerical integration of Eq. 11. A nonlinear least squares procedure explained in Babajimopoulos (1975) was used to fit several functions similar in form to Eq. 11. The empirical function finally used is:

$$f(I) = \lambda/12[.05408+(1.002I_{mj}^{1.031}-.5408)EXP(-I_{mj}^{.7853})] \quad (12)$$

Eq. 12 fits the numerical integration data well in the epilimnia, but in deeper regions where the value of the light function is approximately zero, the percent error is large. However, actual and computed reproduction rates are small in deep layers, so the light limitation function was calculated using Eq. 12. Plots showing diurnal variations of Steele's light function at several depths are shown in Figure 5, and seasonal variations of Eq. 11 in depth profile are

shown in Figure 6. The plotted diurnal variations compare very well to actual field measurements of photosynthesis presented in Ryther (1956) and Ruttner (1963).

The decay term in Eq. 4 represents a temperature dependent loss that is proportional to algal biomass. It includes all losses not already included in other terms: e.g., random cell rupture, loss of protoplasm during cellular division, endogenous respiration, etc. While it has been used by all investigators modeling algal dynamics, it has had different definitions depending what other predation and sinking terms have been explicitly included. It merely implies that, for a given temperature, some constant fraction of the algae disappear every day. Consequently, any algal loss that can be expressed as a constant decay is incorporated in this term. In this study, the term took two different meanings, although the form was always the same. If detritus was not included in the model, the decaying algae immediately regenerated their nutrients, releasing phosphate to the extracellular phosphate pool. This formulation was:

$$K_{xn} \cdot X; \qquad (13)$$

where: K_{xn} = temperature dependent specific decay rate (per time).

The specific rate of algal decay was also the specific rate of nutrient regeneration; the subscripts indicate algal decay (x) to nutrients (n). If detrital matter was included,

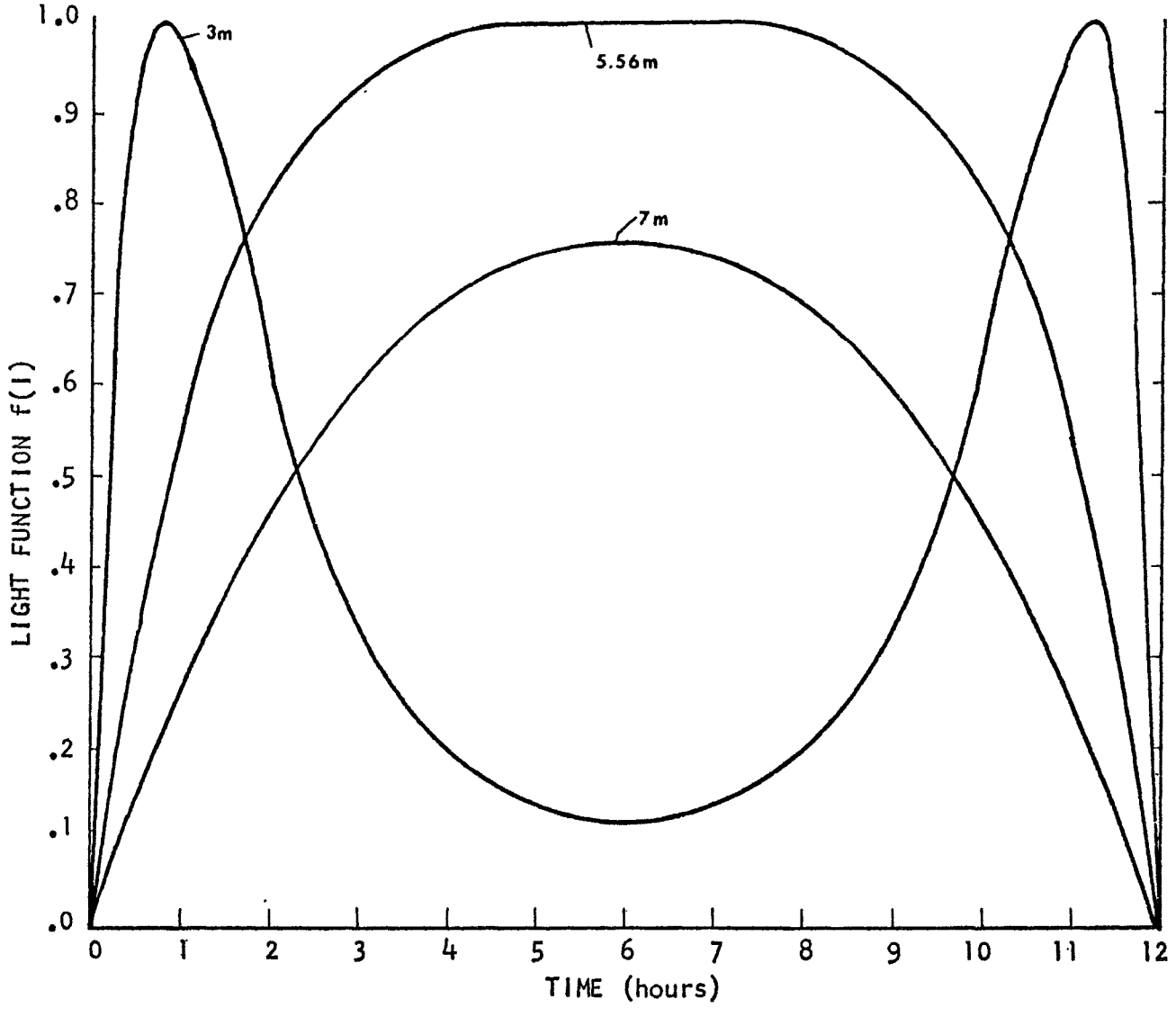

Figure 5. Light function curves for a 12 hour photoperiod with a = .6 and X = 0, beginning at sunrise.

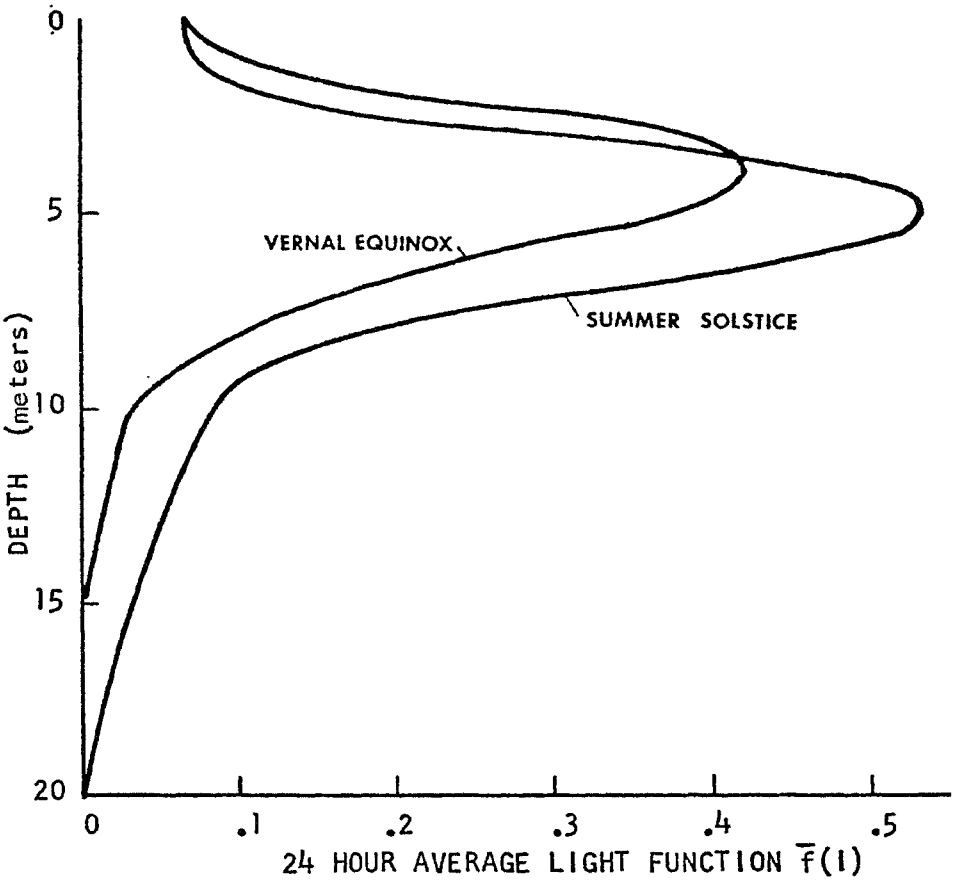

Figure 6. Light function curves in depth profile at the vernal equinox and the summer solstice.

this term still represented the same algal losses, but the nonviable biomass and nutrients were transferred to a detrital pool which in turn degraded. In this case, the term has the same form, but the subscripts on the specific decay rate change. The new decay term, $K_{xp} \cdot X$, represents the rate of algal decay (x) and the rate of biomass addition to the detrital pool (p). For lack of any definitive work on the temperature dependency of the natural losses, the same temperature dependence that is used for maximum specific growth rate is also used for the specific decay rate, regardless of the decaying alga's fate (i.e. whether to nutrients or to the detrital pool). This means that if all other parameters are held constant, the absolute difference between reproductive and decay rates increases as the water becomes warmer, but the ratio of reproduction to decay is constant.

If the sinking flux term in Eq. 1 is chain rule differentiated, the resulting three-component expression is:

$$\frac{1}{A} \frac{\partial}{\partial z}(V_\alpha A \alpha) = \alpha \frac{\partial V_\alpha}{\partial z} + \alpha \frac{V_\alpha}{A} \frac{\partial A}{\partial z} + V_\alpha \frac{\partial \alpha}{\partial z} . \qquad (14)$$

Each term has a physical interpretation. The first accounts for variable sinking velocities, the second for convergent area, and the third for variable species concentrations. In this form, the settling species is reflected off the convergent wall, but in the eutrophication models all species contacting the wall must be incorporated into benthos. The convergent area term in Eq. 14 must be cancelled in the

sink-source term and treated as a species transfer.

Therefore, the sinking term in Eq. 4 has the form:

$$X \frac{V_x}{A} \frac{\partial A}{\partial z}, \tag{15}$$

with all variables previously defined. This negates the wall reflection in Eq. 14 and isolates species interactions to the sink-source terms. The vertical thermal structure allowed computation of temperature dependent sinking velocities based on a Stokes law concept:

$$V_\alpha = C_\alpha (\rho_\alpha - \rho)/\mu; \tag{16}$$

where: C_α = empirical constant = $\frac{(V_\alpha)_{20°}(\mu)_{20°}}{(\rho_\alpha - (\rho)_{20°})}$;

ρ_α = density of species (mass/vol.);

ρ = density of water (mass/vol.);

μ = absolute viscosity of water.

Both the density and viscosity of water are functions of the ambient temperature. When these thermal dependencies are incorporated, calculated sinking velocities decrease by as much as 50% as a species sinks through the thermocline region. The constant, C_α, was calculated before the numerical solution began; this allowed input of the 20°C sinking velocity instead of a meaningless constant. The density of all sinking species was taken to be 1.025 g/cm^3 for all comparisons. While no other authors have included variable sinking velocities, one of the objectives of this dissertation was to use the best possible transport analog, allowing observation

of only biological inadequacies. Therefore, the thermal dependence of sinking velocity is incorporated in all comparisons for all sinking species.

Variable Yield. The next algal reproduction model considered is the variable yield formulation, graphically depicted in Figure 4b. In this model, nutrient uptake is still dependent on the external orthophosphate concentrations, but growth is now dependent on internal or cellular nonstructural phosphate. Phosphate must first be transported into the cell where it can then be used for biomass production and incorporated into the structure. The amount of phosphorus in structure is assumed to be a constant proportion of algal biomass. Consequently, phosphorus incorporation into structure is necessarily accompanied by biomass production. The amount of phosphorus in the nonstructural cellular pool is variable, being a dynamic component.

This new algal formulation differs only in the algal reproduction term of Eq. 4; decay, predation, and sinking are unchanged. The reproduction term becomes:

$$\hat{\mu}_x \cdot \frac{C}{C + K_C} \cdot \bar{f}(I) \cdot X; \qquad (17)$$

where: C = cellular nonstructural phosphate (mass cell. P/mass algae);

K_C = Monod half velocity for algal growth (mass cell P/mass algae).

Again a Monod function is used to describe the nutrient limitation to growth. This is the same formulation used by

Rhee (1974), but he had to subtract the structural phosphorus, since he combined structural and nonstructural cellular phosphate into one variable.

The addition of nonstructural cellular phosphate requires the addition of its mass balance equation to the system of equations constituting the eutrophication model:

$$\frac{\partial (CX)}{\partial t} = \frac{1}{A} \frac{\partial}{\partial z}\left(KA \frac{\partial (CX)}{\partial z}\right) - \frac{1}{A} \frac{\partial}{\partial z}(V_x ACX) + S_{cx}; \quad (18)$$

where CX = total nonstructural cellular phosphorus (mass cell P/vol);

S_{cx} = total cellular phosphorus sink-source (mass cell P/vol./time).

This equation can be reduced to a more tractable, more easily understood form in a manner similar to that used by Bierman (1976). By chain rule differentiation of Eq. 18 and subtraction of the algal mass balance equation (Eq. 1 applied to algae) multiplied by C, Eq. 19 is obtained:

$$X \frac{\partial C}{\partial t} = \frac{1}{A} \frac{\partial}{\partial z} (XKA \frac{\partial C}{\partial z}) + K \frac{\partial X}{\partial z} \cdot \frac{\partial C}{\partial z} - V_x \cdot X \cdot \frac{\partial C}{\partial z}$$

$$+ S_{cx} - CS_x. \quad (19)$$

Some of the components of S_{cx} (decay, sinking, and predation) are duplicated exactly in CS_x. When the two sink-source terms are combined, these terms cancel and the only processes left are those internal to the algae:

[accum. nonstructural cellular P] = [uptake from solution] - [dilution by algal growth] (20)

Therefore, the nonstructural cellular phosphate level is not directly dependent on decay, sinking, or predation of the algal crop, as expected.

Phosphate uptake from solution was assumed to be a Monod function of the ambient orthophosphate level. This assumption also was used by Fuhs (1972), Toerien (1971), and Lehman (1975). The feedback inhibition demonstrated by Fuhs (1972) and Rhee (1974) was assumed to be a linear function of nonstructural cellular phosphate, similar to that used by Lehman. The combined uptake term is:

$$\hat{q}\,\frac{N}{N+K_n}\cdot\bar{f}(I)\cdot\frac{C_m-C}{C_m}\quad X\ ; \qquad (21)$$

where: $\hat{q}$ = temperature dependent maximum specific nutrient uptake rate (mass P/mass algae/time);

C_m = maximum cellular phosphate level.

The uptake rate is a maximum when external nutrient levels are very high and the cellular phosphate level is very low. The light function is used here also since the portion of the phosphate in polyphosphate, requiring light energy for formation, has not been delineated. Therefore, all phosphate uptake is assumed light dependent. This means that algae in "dark" areas have only a minimum or structural phosphorus content. The temperature dependence of $\hat{q}$ is the same as that used for $\hat{\mu}_x$.

The phosphorus required for synthesizing new cellular components is proportional to the algal reproduction

rate described by Eq. 17:

$$Y_{nx} \cdot \hat{\mu}_x \cdot \frac{C}{C+K_c} \cdot \bar{f}(I) \cdot X; \qquad (22)$$

where: Y_{nx} = algal structural phosphate content (mass P/mass algae).

This term removes phosphate from the cellular pool and deposits it in the structural compartment of the cell. The total algal phosphorus content at any time is $Y_{nx} + C$, where C varies with time.

The last term in Eq. 20 accounts for the dilution of nonstructural cellular phosphate by increases in algal biomass. This dilution effect is formulated:

$$C \cdot \mu_x \cdot \frac{C}{C+K_c} \cdot \bar{f}(I) \cdot X. \qquad (23)$$

The loss rate, at any instant, due to dilution is merely the product of nonstructural cellular phosphate stores and the biomass production rate.

Polyphosphates. When the internal phosphorus is further subdivided to consider polyphosphate formation (Figure 4c), the algal sink-source terms are unchanged. Algal growth is still dependent on only internal orthophosphate concentrations. The cellular orthophosphate sink-source term is changed to accommodate polyphosphate formation and degradation, and the light dependency of phosphate uptake is further defined. The new cellular orthophosphate sink-source term has the form:

[uptake from solution] - [structural growth requirements] - [dilution by algal growth] - [polyphosphate formation] + [polyphosphate degradation]. (24)

The uptake term is the same as in the variable yield formulation, but uptake into the internal pool is no longer light dependent. This allows some phosphate uptake in the absence of light, with an enhancement of uptake in the presence of light, since polyphosphate formation, structural uptake, and biomass dilution quickly deplete the internal pool. The structural growth requirement and dilution terms are also unchanged by polyphosphate formation. The high-energy bonds forming the backbone of a polyphosphate chain require light energy for formation. Therefore, polyphosphate formation is assumed to be light dependent. Since only a single enzyme is known to be active in polyphosphate formation (Harold, 1966), a Monod function was used to describe the cellular orthophosphate dependence of the formation rate. Control of maximum polyphosphate levels was achieved by a linear feedback inhibition system, like the one used on the phosphate uptake rate. Even though several enzymes could simultaneously be involved in polyphosphate degradation, a Monod function was used to estimate decay rates. The polyphosphate formation and degradation terms are:

$$\hat{r}_f \cdot \frac{C}{C+K_s} \cdot f(I) \cdot \frac{V_m - V}{V_m} \cdot X; \qquad (25)$$

$$\hat{r}_d \cdot \frac{V}{V+K_v} \cdot X; \qquad (26)$$

where: $\hat{r}_f$ = temperature dependent maximum specific polyphosphate formation rate (mass P/ mass algae/time);

K_s = Monod half velocity for formation (mass P/ mass algae);

V = polyphosphate (mass P/mass algae);

$\hat{r}_d$ = temperature dependent maximum specific polyphosphate degradation rate (mass P/ mass algae/time);

K_v = Monod half velocity for degradation (mass P/mass algae).

There is no information about the temperature dependence of polyphosphate formation. Therefore, the temperature dependeicies of $\hat{r}_d$ and $\hat{r}_f$ are assumed to be the same as those for $\hat{\mu}_x$ and $\hat{q}$.

The behavior of this formulation closely resembles the experimental data cited in the Literature Review (Phosphorus Uptake and Storage). It (1) forms polyphosphate in the presence of light, (2) degrades polyphosphate in the dark, (3) maintains an approximately linear relation between polyphosphate and cellular phosphate during steady states (Rhee, 1974), and (4) allows non-growth rate determining phosphorus stores.

Bierman (1976) utilizes a different polyphosphate model in which the formation and degradation rates have been assumed to be so large that polyphosphate levels adjust almost

instantaneously to environmental changes. This allows him to determine polyphosphate levels as an algebraic formulation rather than the time varying mass balance approach used here.

The polyphosphate mass balance equation can be chain rule differentiated, like the cellular orthophosphate equation was, and the algae mass balance multiplied by V and subtracted. This reduced polyphosphate equation has the same form as Eq. 22, the cellular phosphate equation. Again, the differenced sink-source terms cancel all losses to the total polyphosphate pool caused by loss of algal biomass, and only changes on a cellular level remain. The remaining terms are:

[accum. polyphosphate] = [polyphosphate formation] - [polyphosphate degradation] - [dilution by algal growth]. (27)

The formation and degradation terms have already been defined, and dilution by biomass increase is formulated similarly to that for cellular phosphate:

$$V \cdot \hat{\mu}_X \cdot \frac{C}{C+K_c} \cdot \bar{f}(I) \cdot X. \qquad (28)$$

The addition of algal phosphate compartments adds increasing accuracy to the phosphorus uptake portion of the eutrophication model. However, two more mass balance equations and several new parameters have been added. Some of these parameter values have not been determined experimentally;

and the additional equations increase computational costs.

Aerobic Ecosystem Structures

The three algal reproduction models just described were incorporated into four ecosystem structures, as shown in Figure 7. This figure also indicates the ecosystem structures tested by other writers, for comparison. Since many biological processes are oxygen sensitive, the twelve ecosystems in Figure 7 were further modified according to whether ambient conditions were aerobic or anaerobic. This was accomplished by two Monod-like functions:

$$\frac{O}{O+K_o}\ , \tag{29}$$

and

$$\frac{K_o}{K_o+O}\ ; \tag{30}$$

where: O = dissolved oxygen concentration (mass/vol.);

K_o = Monod half velocity (mass O_2/vol.).

Eq. 29 multiplied the sink-source terms which were strictly aerobic, and Eq. 30 multiplied the anaerobic sink-source terms. This formulation allowed a rapid switchover from aerobic to anaerobic structure whenever oxygen was depleted to levels approximating K_0. For the purposes of this study, K_o was taken to be 0.1 g O_2/m^3. Therefore, when the oxygen concentration was 1.0 g O_2/m^3, the system was essentially aerobic; it was only partially aerobic when oxygen levels were 0.1 g O_2/m^3. The ecosystems described next are

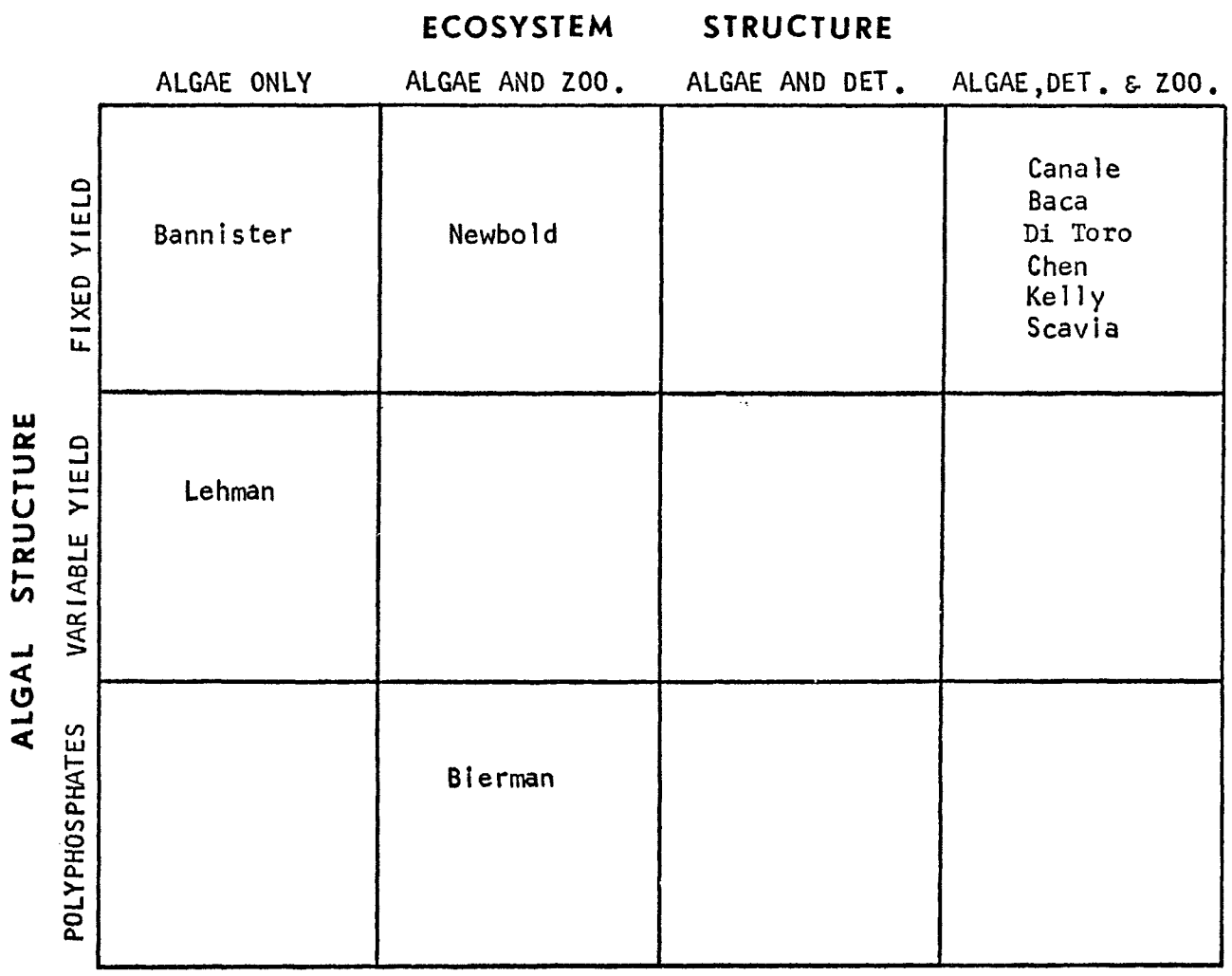

Figure 7. Matrix of possible algal and ecosystem combinations with the model authors in their respective sections.

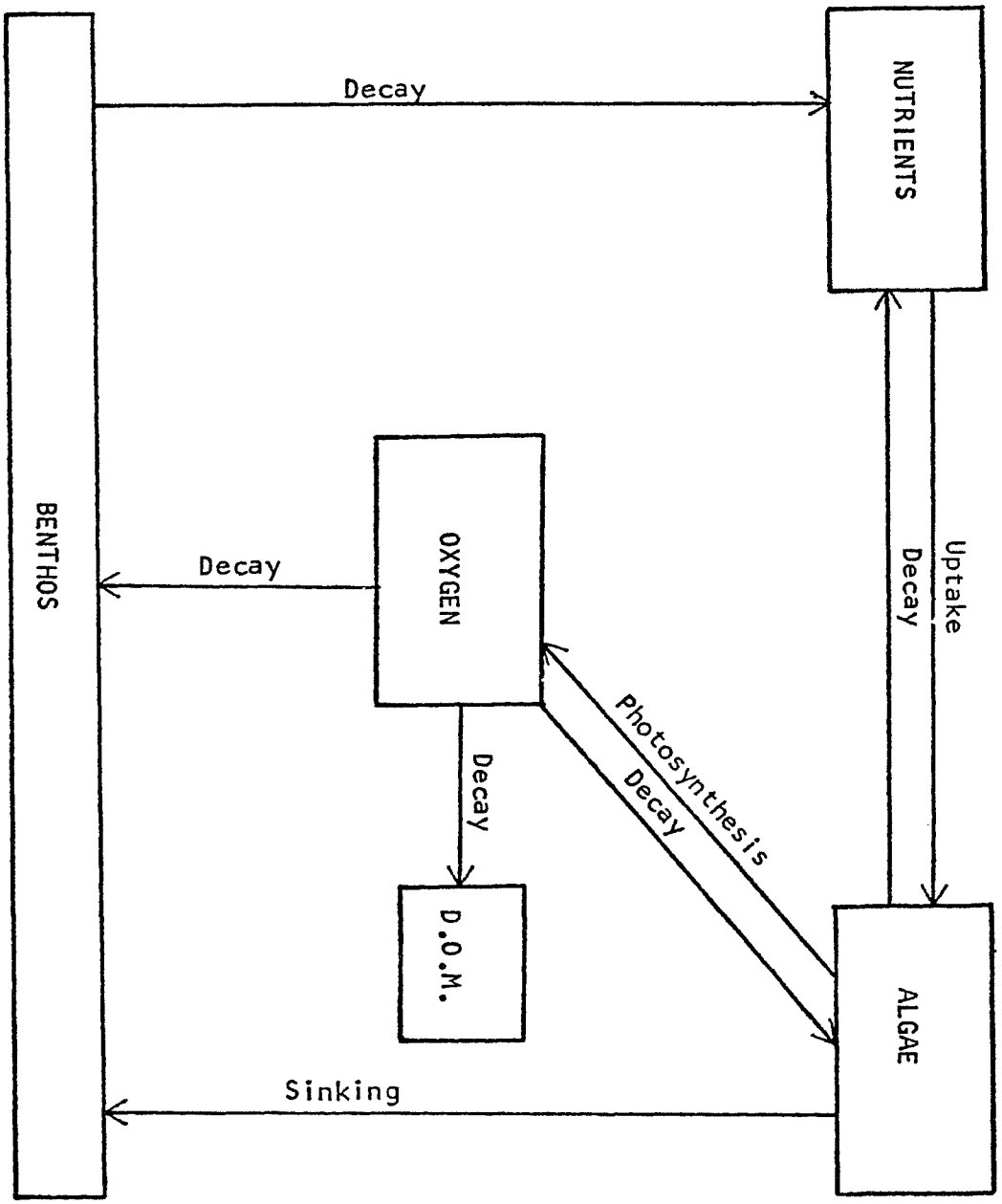

Figure 8 . Diagram of the algae only ecosystem structure

essentially aerobic; anaerobic systems are described in detail in another article.

Algae Only. The least complicated of all tested ecosystems is depicted in Figure 8. Any of the three algal reproduction models previously discussed can be fitted into the algal compartment with only minor changes in some of the nutrient sink source terms. Therefore, the system description will proceed assuming that the polyphosphate formulation was used, and the changes needed for the fixed yield, or variable yield formulations will be noted, where appropriate.

Since algal uptake rates are dependent on local orthophosphate concentrations, an equation representing orthophosphate transport and uptake was necessary. The mass balance equation for orthophosphate must be solved simultaneously with the algal mass balances:

$$[\text{accum. of } PO_4] = -[\text{algal uptake}] + [\text{algal decay}] + [\text{benthic decay}]. \quad (31)$$

The algal uptake term has three formulations, depending upon which algal model is employed. When the fixed yield model is used, phosphate uptake rates are directly proportional to algal reproduction rates. In this case the uptake term is:

$$Y_{nx} \cdot \hat{\mu}_x \cdot \frac{N}{N+K_n} \cdot \bar{f}(I) \cdot X; \quad (32)$$

where $Y_{nx} \cdot \hat{\mu}_x$ is the maximum specific phosphate uptake rate.

If the variable yield model is used, phosphate uptake rates are independent of algal growth. The uptake term for this model has already been defined in Eq. 21. No yield coefficient is necessary in this equation since the units are already compatible with those in the phosphate equation. The polyphosphate analog's uptake term is very similar to Eq. 21, but the light dependency has been deleted. The resulting term is:

$$\hat{q} \cdot \frac{N}{N+K_n} \cdot \frac{C_m - C}{C} \cdot X. \qquad (33)$$

Again the units are compatible.

In the absence of detritus or zooplankton, it is assumed that algal decay releases phosphate to solution directly. The release rate is equal to the decay rate multiplied by a yield coefficient:

$$(Y_{nx} + C + V) \cdot K_{xn} \cdot X. \qquad (34)$$

In this equation, $(Y_{nx} + C + V) \cdot K_{xn}$ is the specific rate of nutrient release by decay. The terms in parenthesis represent the total algal phosphate content as the sum of structural phosphorus, nonstructural orthophosphate, and polyphosphate fractions. When polyphosphates or nonstructural orthophosphate is not used, it is set to zero, and the total phosphorus within the cell is the sum of the remaining components.

As Figure 8 indicates, this ecosystem model

incorporates a benthos. It is assumed that the rates of benthic release of phosphate and oxygen consumption are proportional to the mass of benthal sludge present. Thus, the benthic phosphate release term is written:

$$Y_{nb} \cdot K_{bn} \cdot B; \tag{35}$$

where: Y_{nb} = benthic phosphate yield coefficient (mass P/mass sludge);

K_{bn} = temperature dependent specific benthic decay rate (per time);

B = benthos concentration (mass sludge/vol.).

As in terms of similar form, $K_{bn} \cdot B$ is the rate of benthic decay and Y_{nb} converts this rate to the units of a phosphate release rate.

The oxygen mass balance, referred to earlier, is required both as an indicator of water quality and as a switch mechanism for aerobic to anaerobic control. The oxygen sink-source terms are:

[accum. of O_2] = [production by algal photosynthesis] - [algal decay] - [benthic decay] - [dissolved organic matter decay]. (36)

All of the oxygen sink-source terms are merely the previously discussed rates of biomass formation or decay multiplied by an appropriate coefficient. The oxygen production by photosynthetic activity for the fixed yield, and variable yield and polyphosphate models are, respectively:

$$Y_{ox} \cdot \hat{\mu}_x \cdot \bar{f}(I) \cdot \frac{N}{N+K_n} \cdot X, \tag{37}$$

$$Y_{ox} \cdot \hat{\mu}_x \cdot \bar{f}(I) \cdot \frac{c}{c+K_c} \cdot X. \tag{38}$$

The coefficient, Y_{ox}, is the same regardless which nutrient uptake model is used. Similarly, the algal decay (Eq. 13) term multiplied by Y_{ox} is the rate of oxygen consumption due to that decay:

$$Y_{ox} \cdot K_{xn} \cdot X. \tag{39}$$

The same yield coefficient was used for both algal growth and decay, since decay was assumed to produce the same nutrients used in photosynthesis: namely, CO_2, NO_3, and PO_4^{-3}. Thus the overall change in oxidation state is the same in both processes. Benthic decay also had this simple form:

$$Y_{ob} \cdot K_{bn} \cdot B, \tag{40}$$

where Y_{ob} is the oxygen yield coefficient for benthos. Dissolved organic matter, formed by anaerobic activity and described in that section, was handled similarly:

$$Y_{od} \cdot K_{dn} \cdot D; \tag{41}$$

where: Y_{od} = oxygen yield coefficient;

K_{dn} = specific rate of dissolved organic matter decay;

D = concentration of dissolved organic matter.

Theoretical oxygen demands were calculated for zooplankton, algae, and benthos using gross chemical compositions for these modeled species. Literature values for their elemental compositions (Jewell, 1968; Omori, 1969; Beers, 1966; Johannes and Satomi, 1966; Ketchum, 1939; Wetzel, 1975) were used, along with free oxygen, on the reactant side of an oxidation-reduction equation. The reaction was assumed to go to completion; the products were NO_3^-, $PO_4^{\equiv}$, and CO_2. All analyses yielded oxygen demands ranging from 1.5 to 2.0 g O_2/g dry wt., regardless of species. Therefore, for simplicity and to guarantee that oxygen was conserved, all oxygen production and uptake coefficients were set at 2.0 g O_2/g dry wt. for all of the comparisons in this dissertation.

Benthic mass balances were quite different from those for other species since no transport was involved. The benthic mass balance consisted of sinking inputs to the lake bottom. The accumulated sludge then degraded releasing nutrients and consuming oxygen. The aerobic, benthic, mass balance is:

$$\frac{\partial B}{\partial t} = \frac{V_x}{A} \frac{\partial A}{\partial z} \cdot X - K_{bn} \cdot B. \qquad (42)$$

All of the completely assembled mass balance equations for each algal and ecosystem model are listed in Appendix C for clarity.

Algae and Detritus. The addition of particulate detritus to the algae-only system is depicted in Figure 9. In this structure, decaying algae go into a detrital pool before final degradation to nutrients; this final decay is accompanied by oxygen uptake. The decay rate K_{xn}, in the algal sink-source term (Eq. 13) is changed to K_{xp} to denote a new destination for the biomass. The sink-source term for detritus then has the form:

[accum. detritus] = [algal decay] - [detrital decay] - [sinking losses to benthos]. (43)

Algal decay to detritus was discussed in Algal Models (Fixed Yield, Eq. 13). Detrital decay itself is handled in the same manner as benthal and dissolved organic matter decay:

$$K_{pn} \cdot P; \tag{44}$$

where: K_{pn} = temperature dependent specific detrital decay rate (per time);

P = particulate concentration (mass/vol.).

Like all other previously discussed temperature dependencies, the specific particulate decay rate is assumed directly proportional to the local ambient temperature. As the particulates are degraded by bacteria, nutrients are released and oxygen is consumed. The phosphate sink-source term (Eq. 31) is changed so that the algal input is deleted and particulate decay is added:

$$Y_{np} \cdot K_{pn} \cdot P; \tag{45}$$

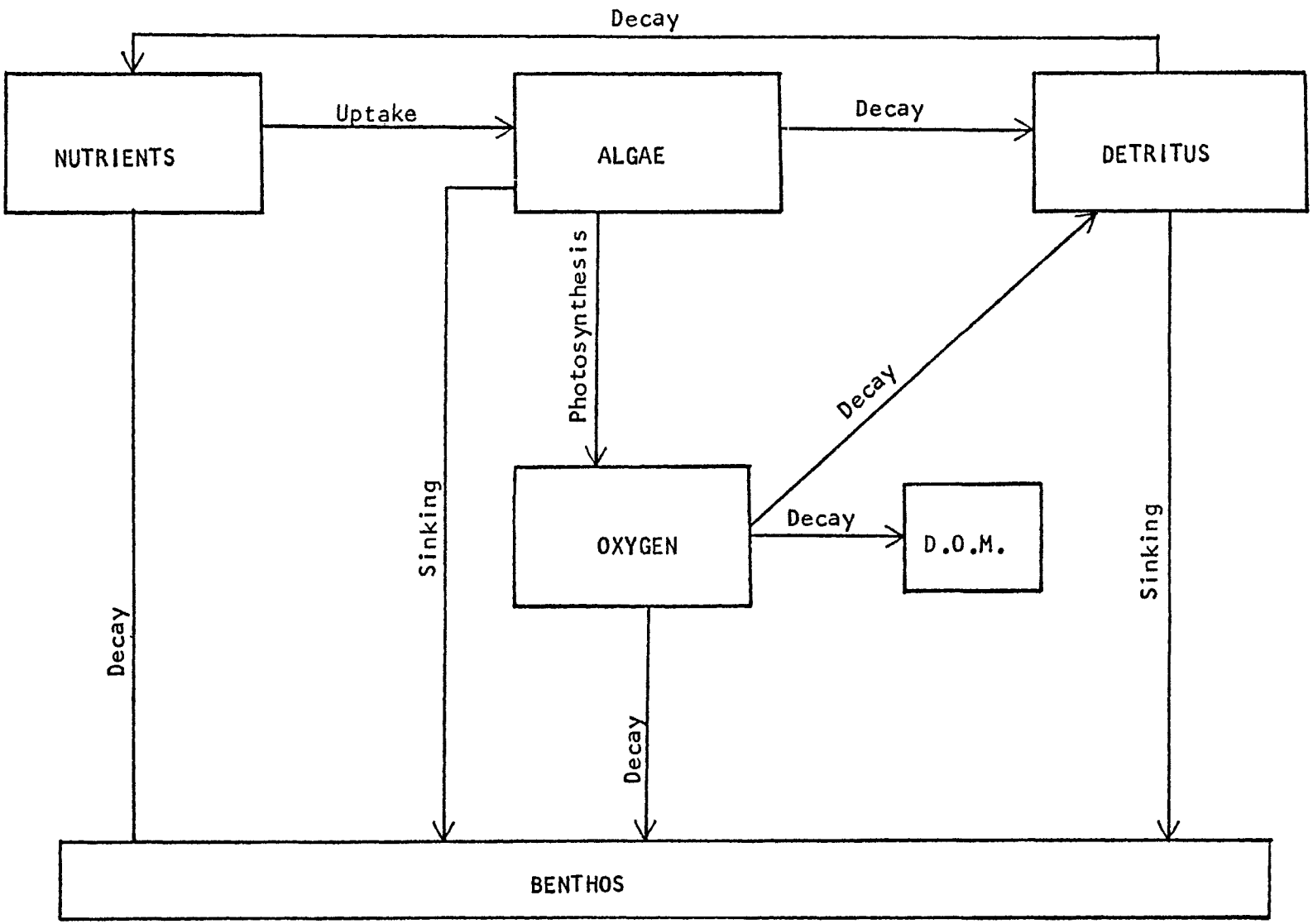

Figure 9 . Diagram of the algae plus detritus ecosystem structure

where Y_{np} is the nutrient content of particulates. The oxygen mass balance (Eq. 36) is modified also by deletion of its algal decay term and addition of a detrital decay term:

$$Y_{op} \cdot K_{pn} \cdot P; \tag{46}$$

where Y_{op} is the oxygen demand of the particulates. The sinking term in the particulate sink-source equation is the same as its associated input to benthos:

$$\frac{V_p}{A} \cdot \frac{\partial A}{\partial z} \cdot P. \tag{47}$$

Eq. 45 is then added to Eq. 42 to obtain the new benthic mass balance.

Algae and zooplankton. The interactions which occur when zooplankton predation is added to the algae-only structure are depicted in Figure 10. The zooplankton predation term in Eq. 4 (the algal mass balance) has the same form in all models incorporating predation:

$$\frac{\hat{\mu}_z}{Y_{zx}} \cdot \frac{X}{X+K_x} \cdot Z; \tag{48}$$

where:

$\hat{\mu}_z$ = temperature dependent maximum specific growth rate of the predator (per time);

Y_{zx} = mass of zooplankton formed per unit mass of algae consumed (mass zoo./mass algae);

K_x = Monod half velocity for predation (mass algae/vol.);

Z = Zooplankton dry weight concentration (mass/vol.).

This is the same predation term used by Kelly (1973), Di Toro

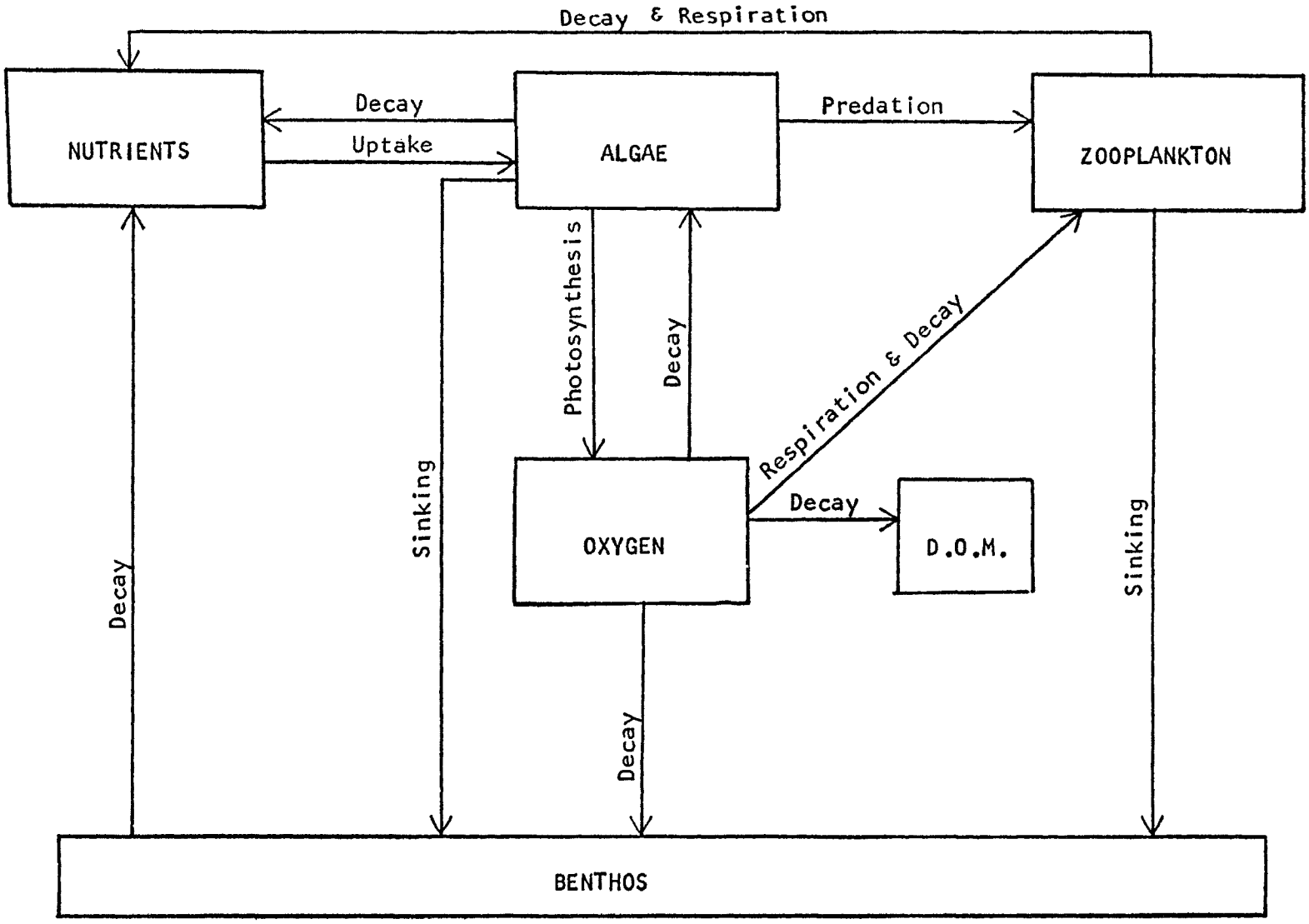

Figure 10. Diagram of the algae plus zooplankton ecosystem structure

(1971), Baca (1976), and Chen (1972). Bierman (1976) uses a similar function, but his has been modified by preference factors which allow different grazing effectiveness on different algal taxa. His eutrophication model incorporates four algal species.

Data presented by Hall (1964) for a single zooplankter grown at three temperatures (11, 20, and 25°C) and three algal concentrations (20, 1.25, and 0.31 g dry wt./m^3) were used to determine the temperature dependence of the maximum specific growth rate. The reduced data from Hall are shown in Figure 11. Also included are growth rates from Zaika (1973); most of these are <u>in situ</u> rates without indication as to whether algae are rate-limiting or not. Zaika's data have been included to show that virtually all <u>in situ</u> growth rates fall below the line on Figure 11 defined by

$$\hat{\mu}_z = (\hat{\mu}_z)_{20°} \left(\frac{T-7}{13}\right), \quad T \geq 7; \tag{49}$$

where: T = temperature (°C).

The temperature dependency of zooplankton growth rate was determined using Eq. 49. If the temperature was less than 7°C, the growth rate was set to zero. Hall's data also show a strong temperature dependency of the Monod half velocity, which was fitted with a linear function:

$$K_x = (K_x)_{20°} (1.95 - .047\ T). \tag{50}$$

Because both $\hat{\mu}_z$ and K_z depend on temperature, the zooplankters

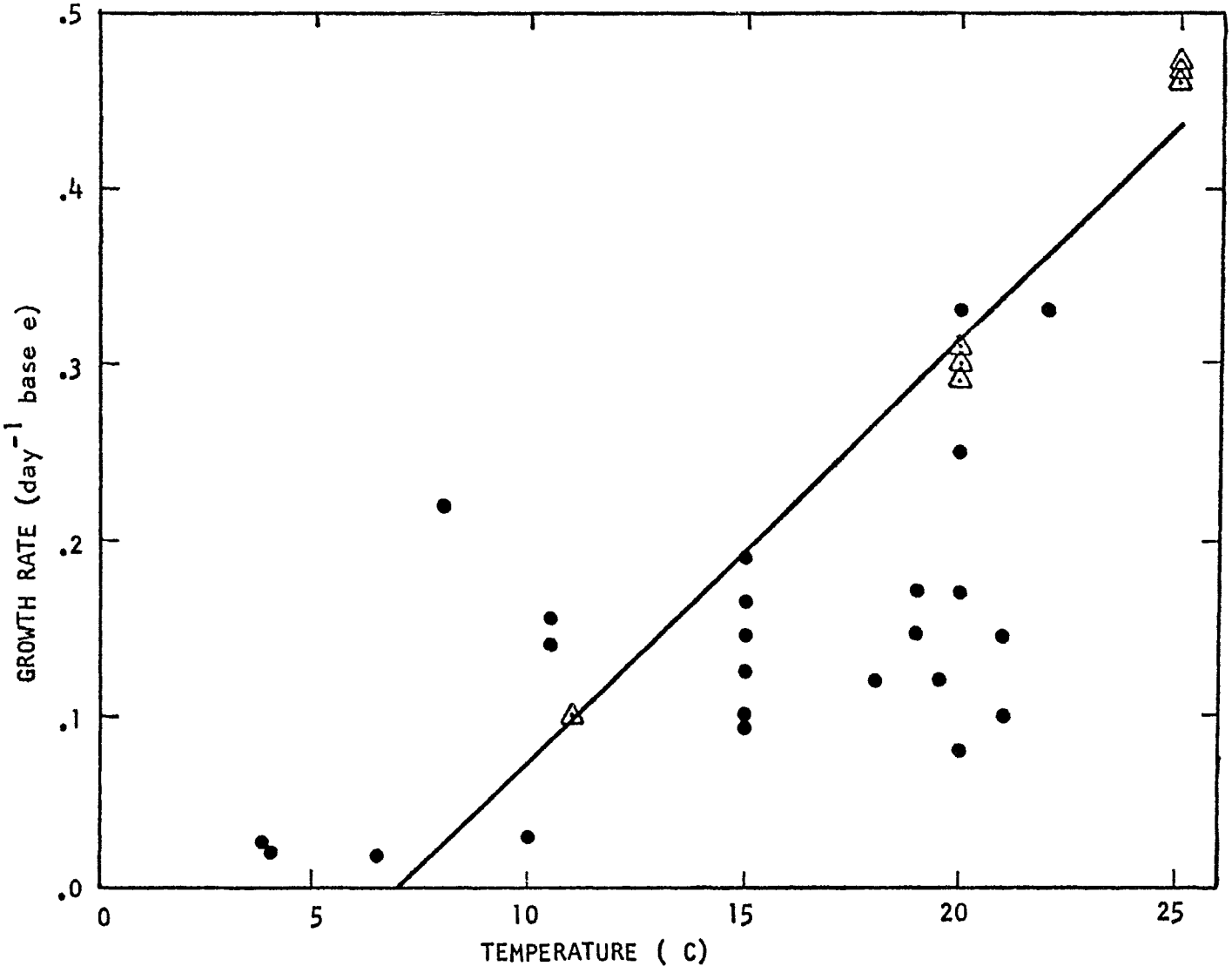

Figure 11 Zooplankton growth rates; approximate in situ growth rates (Zaika, 1973) ●, and growth rates reduced to non-limiting algal concentrations (Hall, 1964) △.

become dramatically more effective predators as the lake gets warmer. Not only do they feed faster and grow faster, they can reduce phytoplankton populations to much lower levels before their growth is limited by a lack of prey. The yield coefficient in Eq. 48, Y_{zx}, converts the rate of zooplankton production to the rate of phytoplankton loss due to grazing. While this yield coefficient is not constant, no definitive work has established what the functional form might be. In fact, the major parameters controlling the yield coefficient value have not been identified. Therefore, a somewhat arbitrary value of 0.6 gram zooplankton formed per gram dry weight algae consumed was employed in all model comparisons. This is well within the limits of literature values in Table 1.

The mass balance for zooplankton is Eq. 1 (the Mass Balance Equations) with the following sink-source terms:

[accum. zooplankton] = [zooplankton growth] - [zooplankton decay] - [zooplankton sinking loss to benthos]. (51)

Zooplankton growth is proportional to the rate of predation on algae, the proportionality coefficient being Y_{zx}:

$$\hat{\mu}_z \cdot \frac{x}{x+K_x} \cdot Z. \tag{52}$$

This term also occurs in Eq. 48. The zooplankton decay term is expressed:

$$K_{zn} \cdot Z; \tag{53}$$

where: K_{zn} = temperature dependent specific zooplankton decay rate (per time).

The thermal dependency of K_{zn} was assumed to be the same as that of $\hat{\mu}_z$. Since no higher trophic level was modeled, this constant drain on the zooplankton population includes all zooplankton mortality: endogenous respiration, death, predation by carnivorous zooplankton, etc. The sinking loss term for zooplankton is the same as its associated input to benthos:

$$\frac{V_z}{A} \frac{\partial A}{\partial z} \cdot Z. \tag{54}$$

Therefore Eq. 54 also is added to the benthic mass balance (Eq. 42) to account for zooplankton entering the sludge as well as algae.

A portion of the algae ingested by zooplankton is assumed to be assimilated into structure with no net oxidation or reduction, and a portion is oxidized for energy. Therefore, zooplankton provide two sources of nutrient release. The two terms added to the phosphate sink-source term (Eq. 31) are zooplankton decay

$$Y_{nz} \cdot K_{zn} \cdot Z, \tag{55}$$

and phosphate release by oxidation

$$(Y_{nx}+C+V)\left(\frac{1}{Y_{zx}} -1\right) \hat{\mu}_z \frac{X}{X+K_x} \cdot Z. \tag{56}$$

The sum $(Y_{nx}+C+V)$ is the total algal nutrient content (C and V can be zero depending on which algal model is used)

released to the ambient orthophosphate pool when the non-assimilated portion of ingested algae is oxidized.

This oxidation, as well as algal decay, requires oxygen. Therefore the two terms added to the oxygen sink-source term (Eq. 36) are zooplankton decay

$$Y_{oz} \cdot K_{zn} \cdot Z, \tag{57}$$

and the uptake by oxidation

$$Y_{ox} \cdot \left(\frac{1}{Y_{zx}} - 1\right) \hat{\mu}_z \frac{X}{X+K_x} \cdot Z. \tag{58}$$

This oxidation term demands that respiration and nutrient regeneration by zooplankton be proportional to zooplankton growth, and if zooplankton be constant, proportional to the specific zooplankton growth rate.

Algae, detritus, and zooplankton. The species interactions when detritus is added to the algae and zooplankton structure are shown in Figure 12. In this ecosystem model, both algal and zooplankton decay are treated as inputs to the detrital pool. As before, the mass balance equation for detritus is Eq. 1. The detrital sink-source formulation is:

$$K_{xp} \cdot X + K_{zp} \cdot Z - K_{pn} \cdot P - \frac{V_p}{A} \frac{\partial A}{\partial z} \cdot P. \tag{59}$$

The terms are respectively algal decay, zooplankton decay, particulate detritus decay, and sinking losses. Therefore, both the specific algal decay rate and the specific zooplankton decay rate must be changed to denote the destination of

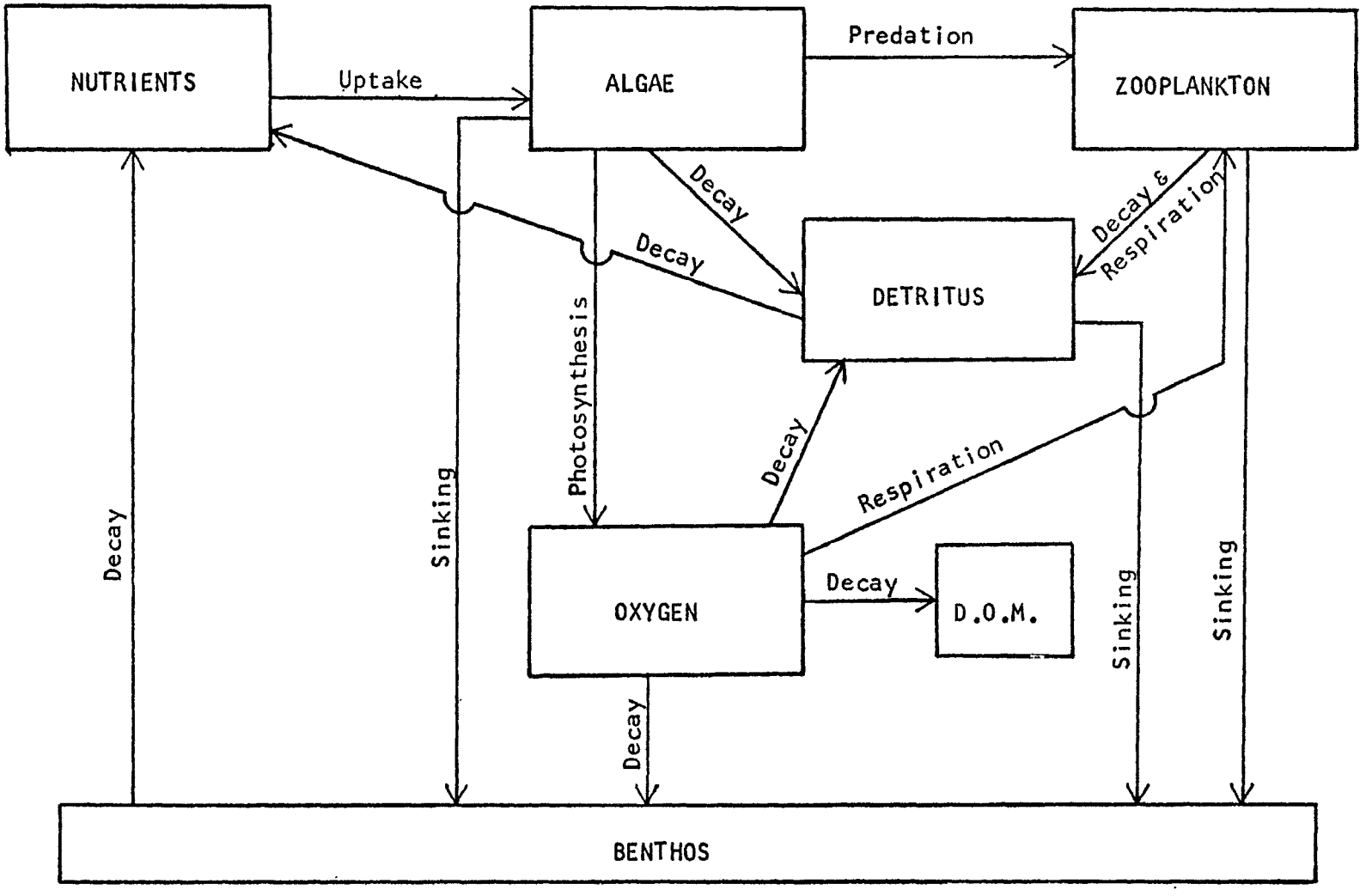

Figure 12. Diagram of the algae, zooplankton, and detritus ecosystem structure

of the lost biomass: K_{xn} to K_{xp} in Eq. 13 and K_{zn} to K_{zp} in Eq. 53. The corresponding nutrient release terms in the phosphate sink-source equation (Eq. 31) must be deleted and a detrital decay term added (Eq. 45). The oxygen sink-source (Eq. 36) also has both associated uptake terms deleted and an uptake by particulate decay added (Eq. 46). As before, particulate sinking and benthos input has the formulation of Eq. 47.

Anaerobic Ecosystem Structure

When oxygen levels are low, the anaerobic sink-source terms dominate the system interactions. The anaerobic structure is shown in Figure 13. Sinking into benthic deposits was included in both the aerobic and anaerobic systems, but all of the other sink-source terms described in the previous section approached zero as the oxygen concentration became small. However, it was assumed that the benthic deposits would putrify at low dissolved oxygen levels with no net oxidation or reduction. The products of this fermentation were assumed to be short-chain volatile fatty acids and methane. It was further assumed that all phosphorus-containing compounds are degraded anaerobically, and phosphate is released to solution during degradation. Therefore, the dissolved organic matter is composed of short-chain acids containing no phosphorus. The benthic mass balance equation is:

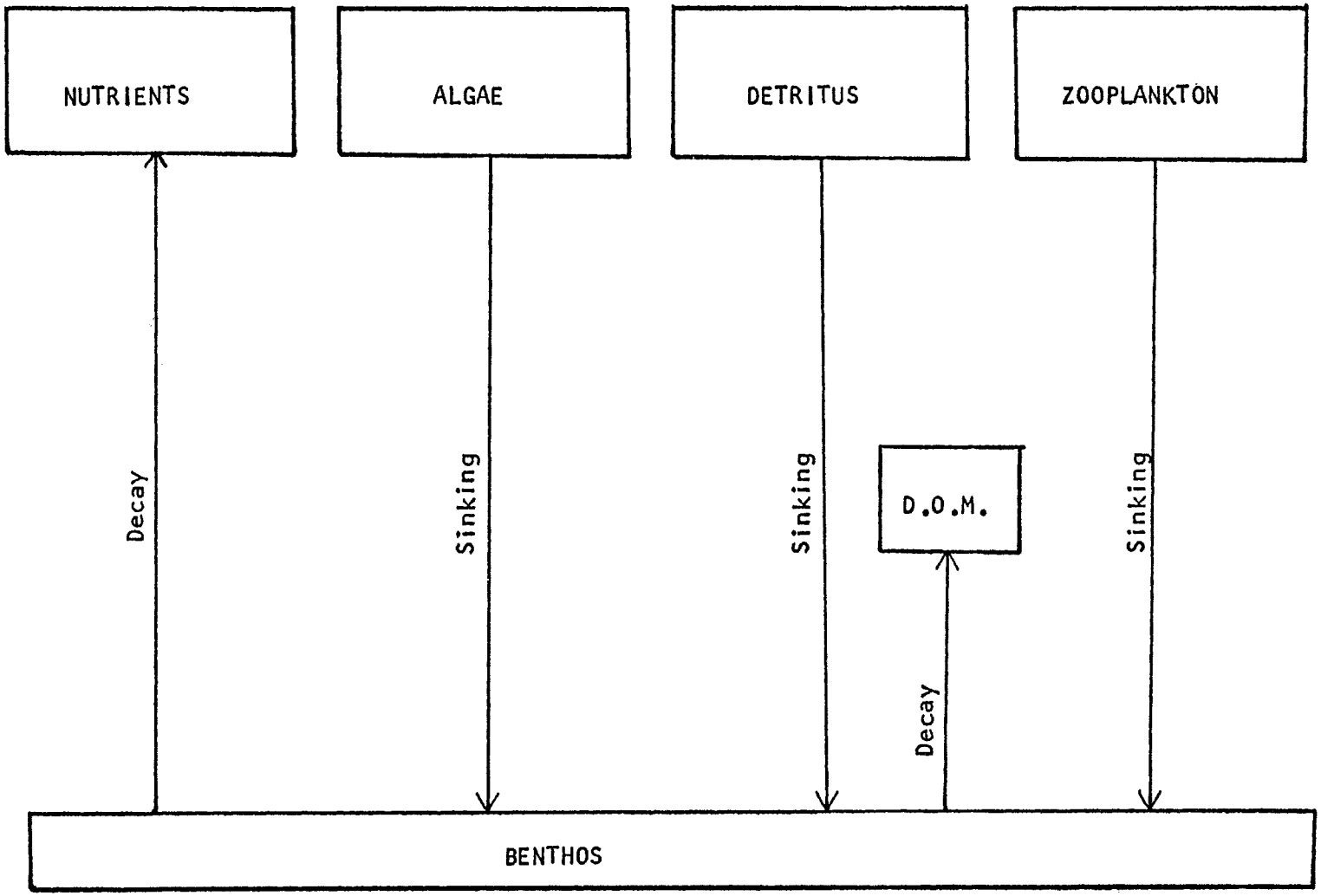

Figure 13. Diagram of the anaerobic ecosystem structure

$$\frac{V_x}{A}\frac{\partial A}{\partial z} \cdot X + \frac{V_z}{A}\frac{\partial A}{\partial z} \cdot Z + \frac{V_p}{A}\frac{\partial A}{\partial z} \cdot P - K_{bd} \cdot B; \quad (60)$$

where K_{bd} = anaerobic specific decay rate of benthos (per time).

The sink-source portion of the dissolved organic matter equation is $K_{bd} \cdot B$, since the only input is anaerobic benthic decay and oxidation does not occur. The phosphate sink-source is also only one term: $Y_{nb} \cdot K_{bd} \cdot B$.

Minimum Necessary Model Structure

In order to better estimate the minimum model complexity required to simulate field data, the fixed yield algal reproduction model was combined with the aerobic algae plus zooplankton ecosystem structure and cast into Lotka-Volterra form. This meant that the Monod functions used to represent growth rates were replaced by growth rate formulas in which the specific growth rates were proportional to food source concentration. The terms for algal and zooplankton growth, respectively, were:

$$\frac{\hat{\mu}_x}{2K_n} \cdot N \cdot X \cdot \bar{f}(I), \quad (61)$$

$$\frac{\hat{\mu}_z}{2K_x} \cdot X \cdot Z. \quad (62)$$

This formulation assured that the Lotka-Volterra growth terms (Eq. 61 and Eq. 62) and the original Monod formulations for growth (Eq. 5 and Eq. 52) predict the same value of the specific growth rates when the food concentration is equal

to its respective Monod half velocity constant. In previous models, the growth rates asymptotically approach a maximum, but in this formulation, no maximum growth rate is defined.

The linear response also allows grazing to be more severe, since the predation rate of zooplankton on algae continues to be proportional to the algal standing crop, even at high algal densities. It is important to identify the minimum algal structure, since Monod functions require extra computational time and negate any attempts of solution by implicit solution techniques.

The restructured growth rate terms (Eq. 61 and 62) require analogous restructuring of their respective phosphate sink-source terms (Eq. 32 and 56), the algal predation term (Eq. 48), and the oxygen sink-source term (Eq. 37 and 58), so that they all reflect the new linear dependence on food source.

Phosphorus Conservation

Since the total phosphorus in the system must be conserved, the summation of all of the sink-source terms multiplied by their respective phosphorus yield coefficients must be zero. In other words, the phosphorus leaving any species at any time must be received in total by the other species compartments. When the yield coefficients are the same for each species (algae, detritus, zooplankton, and benthos), the existing terms cancel exactly. When they

differ, new phosphorus conservation terms are needed for transfers between biological species. For example, if algae containing 3% phosphorus decays into the detrital pool containing 1% phosphorus, the difference must be released to the orthophosphate pool or phosphorus is lost from the system.

The terms that need to be added to the phosphate sink-source equations are:

(1) algae decay to detritus,

$$(Y_{nx} + C + V - Y_{np})\ K_{xp} \cdot X; \tag{63}$$

(2) zooplankton decay to detritus,

$$(Y_{nz} - Y_{np})\ K_{zp} \cdot Z; \tag{64}$$

(3) algae are assimilated by zooplankton,

$$(Y_{nx} + C + V - Y_{nz})\ \hat{\mu}_z \cdot \frac{x}{x+K_x} \cdot Z; \tag{65}$$

(4) algae sinks into benthos,

$$(Y_{nx} + C + V - Y_{nb})\ \frac{V_x}{A}\frac{\partial A}{\partial z} \cdot X; \tag{66}$$

(5) zooplankton sinks into benthos,

$$(Y_{nz} - Y_{nb})\ \frac{V_z}{A}\frac{\partial A}{\partial z} \cdot Z; \tag{67}$$

(6) and detritus sinks into benthos,

$$(Y_{np} - Y_{nb})\ \frac{V_p}{A}\frac{\partial A}{\partial z} \cdot P. \tag{68}$$

These conservation terms were added to the orthophosphate sink-source equations whenever the processes they represent were also included.

Chapter IV

THE NUMERICAL SOLUTION TECHNIQUE

Solution Algorithms

The mass balance equation (Eq. 1) has an infinite number of solutions. Any function which satisfies Eq. 2, is twice differentiable in space and once in time, is a solution which will yield the time rate of change of a species at any point in the solution space. To obtain a unique solution, some more information is needed; values of the species α or its derivative $\frac{\partial \alpha}{\partial z}$ at several values of z. Also, since the unique solution will provide only a time rate of change of species α, some starting value, or initial conditions are required. Equation 1 is second order in space. This means that the value of α (or $\frac{\partial \alpha}{\partial z}$) must be specified at two points in the solution space. The two points where information or equation behavior are known are at the surface and bottom of the lakes. At the surface, no flux occurs:

$$-KA \frac{\partial \alpha}{\partial z} + V_{\alpha} A \alpha = 0. \qquad (69)$$

This equation states that diffusion to the surface is equal and opposite to sinking from the surface, at z = 0. The bottom boundary condition is:

$$-KA \frac{\partial \alpha}{\partial z} + V_\alpha A\alpha = V_\alpha A\alpha \qquad (70)$$

This boundary condition states that no diffusive flux exists at the bottom of the lake but species can sink to the floor of the bottom segment.

No analytic solution to Eq. 1 is available. Therefore, finite difference analogs were used to numerically approximate the solution. This procedure requires that the lake be divided into discrete layers. Since algal production is restricted to the surface region of lakes (Ruttner, 1963), the top ten meters of each lake were divided into one-meter layers to permit resolution of the productive region. Discretizations with larger spacings near the surface are plagued with the problem of finding an average epilemnetic growth rate. This is very difficult, since the average growth rate in any layer depends not only on biological parameters, but the turbulence structure as well. The discretization used for Cayuga Lake and Canadarago Lake are shown in Tables 4 and 5, respectively.

When Eq. 1 is expressed as finite differences, averaging problems again result. Evaluation of the diffusive flux gradient($\frac{\partial}{\partial z}[KA \frac{\partial \alpha}{\partial z}]$)at any node requires evaluation of the product $KA \frac{\partial \alpha}{\partial z}$ at half node intervals. To avoid averaging this non-linear term, Eq. 1 is expanded:

$$\frac{\partial \alpha}{\partial t} = \frac{\partial \overset{*}{K}}{\partial z} \frac{\partial \alpha}{\partial z} + \frac{K}{A} \frac{\partial A}{\partial z} \cdot \frac{\partial \alpha}{\partial z} + K \frac{\partial^2 \alpha}{\partial z^2} + \alpha \cdot \frac{\partial \overset{*}{V}_\alpha}{\partial z} + \frac{V_\alpha}{A} \alpha \frac{\partial A}{\partial z}$$

$$+ V_\alpha \frac{\partial \overset{*}{\alpha}}{\partial z} + S_s \alpha + S_I; \qquad (71)$$

Table 4

Cayuga Lake Discretizations*

Nodal Number	Depth (m)	Area (km^2)	Thickness (m)	Volume ($m^3 \times 10^6$)	Benthal Area (km^2)
1	0	172.1	0.5	86.1	3.3
2	1	165.4	1.0	165.4	6.7
3	2	158.7	1.0	158.7	6.7
4	3	152.1	1.0	152.1	6.7
5	4	145.4	1.0	145.4	6.7
6	5	138.7	1.0	139.7	4.7
7	6	135.9	1.0	135.9	2.8
8	7	133.1	1.0	133.1	2.8
9	8	130.4	1.0	130.4	2.8
10	9	127.6	1.0	127.6	2.8
11	10	124.8	1.5	187.3	2.7
12	12	122.2	2.0	244.5	2.6
13	14	119.7	2.0	239.4	2.6
14	16	117.1	2.0	234.2	2.6
15	18	114.6	2.0	229.6	2.6
16	20	112.6	2.0	224.5	2.1
17	22	110.4	2.0	220.8	1.6
18	24	108.8	2.5	271.5	2.0
19	27	106.4	3.0	319.2	2.4
20	30	104.0	3.5	362.6	3.2
21	34	100.0	4.0	399.8	4.0
22	38	95.9	4.0	383.3	4.2
23	42	91.5	4.0	365.6	4.6
24	46	86.7	4.0	346.8	4.8
25	50	81.9	4.5	369.3	4.5
26	55	77.8	5.0	388.8	4.2
27	60	73.6	5.0	368.3	4.0
28	65	69.7	5.0	348.5	3.9
29	70	65.8	5.0	329.4	3.7
30	75	62.3	5.0	311.2	3.6
31	80	58.7	5.0	292.9	3.8
32	85	54.7	5.0	273.5	4.0
33	90	50.7	5.0	253.2	4.1
34	95	46.5	5.0	232.5	4.2
35	100	42.3	5.0	211.5	4.2
36	105	38.1	5.0	190.5	4.2
37	110	33.9	5.0	163.6	6.6
38	115	25.0	5.0	124.7	9.0
39	120	16.0	5.0	80.4	8.8
40	125	7.4	5.0	39.5	7.6
41	130	0.8	2.5	2.0	3.3

* Oglesby and Allee (1974)

Table 5

Canadarago Lake Discretions*

Nodal Number	Depth (m)	Area (km^2)	Thickness (m)	Volume ($m^3 \times 10^6$)	Benthal Area (km^2)
1	0	9.41	0.5	4.71	0.38
2	1	8.65	1.0	8.65	0.76
3	2	7.89	1.0	7.89	0.75
4	3	7.15	1.0	7.15	0.79
5	4	6.32	1.0	6.32	0.75
6	5	5.66	1.0	5.66	0.57
7	6	5.18	1.0	5.18	0.52
8	7	4.62	1.0	4.62	0.58
9	8	4.02	1.0	4.02	0.63
10	9	3.36	1.0	3.36	0.76
11	10	2.50	1.0	2.50	0.96
12	11	1.45	1.0	1.45	0.95
13	12	0.61	0.8	0.49	0.53
14	12.6	0.39	0.3	0.12	0.11

*Hetling, Harr, Fuhs, and Allen (1969)

where the sink-source term S_α has been decomposed into $S_s\alpha$, which is proportional to α and S_I, which is independent of α.

In Cayuga Lake, all space derivatives were approximated by central differences. However, in Canadarago Lake, severe stratification, heavy nutrient loads, and resultant algal blooms combined to produce conditions at the thermocline analogous to shock fronts in streams. Special concentrations changed by over two orders of magnitude within two nodal points near the thermocline. Consequently, in Canadarago Lake, the derivatives marked with an asterisk in Eq. 71 were approximated with up-wind differences, as suggested by Roache (1975) for stream models.

Thus in Cayuga Lake, the finite difference analog for Eq. 71 at any interior node was:

$$\frac{\alpha_i^{n+1}-\alpha_i^n}{\Delta t} = \frac{K_{i+1}-K_{i-1}}{z_{i+1}-z_{i-1}} \cdot \frac{\alpha_{i+1}^{n+1}-\alpha_{i-1}^{n+1}}{z_{i+1}-z_{i-1}} + \frac{K_i}{A_i} \cdot \frac{A_{i+1}-A_{i-1}}{z_{i+1}-z_{i-1}}$$

$$\frac{\alpha_{i+1}^{n+1}-\alpha_{i-1}^{n+1}}{z_{i+1}-z_{i-1}} + \frac{2K_i}{z_{i+1}-z_{i-1}} \left[\frac{\alpha_{i+1}^{n+1}-\alpha_i^{n+1}}{z_{i+1}-z_i} - \frac{\alpha_i^{n+1}-\alpha_{i-1}^{n+1}}{z_i-z_{i-1}} \right]$$

$$- \frac{V_{i+1}-V_{i-1}}{z_{i+1}-z_{i-1}} \cdot \alpha_i^{n+1} - \frac{V_i}{A_i} \cdot \frac{A_{i+1}-A_{i-1}}{z_{i+1}-z_{i-1}} \cdot \alpha_i^{n+1}$$

$$+ V_i \cdot \frac{\alpha_{i+1}^{n+1}-\alpha_{i-1}^{n+1}}{z_{i+1}-z_{i-1}} + S_{si} \cdot \alpha_i^{n+1} + S_{Ii}. \qquad (72)$$

where: n = number of the time step;

i = nodal number.

The boundary conditions were derived in finite difference form by using the flux method. In this method the

accumulation in a layer is assumed equal to the flux in the top minus the flux out the bottom, plus any biological sink source. Applying this procedure to the top node (node 1) yields:

$$\text{Vol}\ \frac{\partial \alpha}{\partial t} = F_1 - F_{1+1/2} + \text{Vol}[S_{s_1}\alpha_1 + S_{I1}]; \quad (73)$$

where: Vol = volume of layer 1= $A_1(z_2-z_1)/2$;

F = total flux = $-KA\ \frac{\partial \alpha}{\partial z} + VA$.

The boundary condition of no flux at the surface requires that $F_1 = 0$. The finite difference analog for Eq. 73 is:

$$\frac{\alpha_1^{n+1} - \alpha_1^n}{\Delta t} = \frac{2}{A_1(z_2-z_1)}$$

$$[-V_{1+1/2}A_{1+1/2}\alpha_{1+1/2}^{n+1} + K_{1+1/2}A_{1+1/2}(\frac{\alpha_2^{n+1}-\alpha_1^{n+1}}{z_2-z_1})]$$

$$+ S_{s_1}\alpha_1^{n+1}\ S_{I1}; \quad (74)$$

Using the same procedure for the bottom node (m), and setting $F_m = V_\alpha A\alpha_m^{n+1}$ yields the bottom boundary finite diference approximation:

$$\frac{\alpha_m^{n+1}-\alpha_m^n}{\Delta t} = \frac{2}{A_m(z_{m-1}-z_m)}\ [-K_{m-1/2}A_{m-1/2}(\frac{\alpha_m^{n+1}-\alpha_{m-1}^{n+1}}{z_m-z_{m-1}}) + V_{m-1/2}$$

$$A_{m-1/2}\ \alpha_{m-1/2}^{n+1} - V_mA_m\alpha_m^{n+1} + S_{s_m}\alpha_{m-1/2}^{n+1} + S_{Im}. \quad (75)$$

All of the finite difference equations can be rearranged into the form:

$$S_{Ii}\Delta t + \alpha_i^n = a_{i1}\alpha_{i-1}^{n+1} + a_{i2}\alpha_i^{n+1} + a_{i3}\alpha_{i+1}^{n+1}; \quad (76)$$

where a_{i1}, a_{i2}, and a_{i3} are the coefficients of the species concentration at nodes i-1, i, and i+1, respectively, in the finite difference analog at node i, these coefficients being composed of the variables K, A, V, and Z, as appropriate.

Equation 76 can be written for each node, so there are m equations involving the m unknown α_i^n. These are arranged in matrix form as follows:

$$\begin{vmatrix} a_{12} & a_{13} & 0 & 0 & \cdots & 0 \\ a_{21} & a_{22} & a_{23} & 0 & \cdots & 0 \\ 0 & a_{31} & a_{32} & a_{33} & \cdots & 0 \\ & & \vdots & & & \\ 0 & \cdots & a_{m-1} & a_{m-1,2} & a_{m-1,3} & \\ 0 & \cdots & 0 & a_{m1} & a_{m2} & \end{vmatrix} \times \begin{vmatrix} \alpha_1^{n+1} \\ \alpha_2^{n+1} \\ \alpha_3^{n+1} \\ \\ \alpha_{m-1}^{n+1} \\ \alpha_m^{n+1} \end{vmatrix} = \begin{vmatrix} L_1^n \\ L_2^n \\ L_3^n \\ \\ L_{m-1}^n \\ L_m^n \end{vmatrix} \quad (77)$$

where $L_i^m = S_{Ii}\Delta t + \alpha_i^n$.

This particular formulation is called the implicit method, because the computed values α_i^{n+1} depend upon other α_j^{n+1} as well as α_i^n; and this feature requires a simultaneous solution of m equations rather than the direct (explicit) solution of a single equation for α_i^{n+1} involving only α_i^n. The implicit procedure is usually preferred because it permits larger time steps, Δt, to be used, thereby saving computation costs (Roache, 1975). In application, all of

the mass balance equations were solved to obtain updated (n+1) values for all species; the sink-source terms were recalculated using the updated values; and the mass balances were resolved using the new source-sink terms.

The Canadarago Lake solution method was somewhat different. The equations were discretized with up-wind differences as previously indicated:

$$\frac{\alpha_i^{n+1}-\alpha_i^n}{\Delta t} = \frac{K_i-K_{i-1}}{z_i-z_{i-1}} \cdot \frac{\alpha_i^\dagger-\alpha_{i-1}^\dagger}{z_i-z_{i-1}} + \frac{K_i}{A_i}\frac{A_{i+1}-A_{i-1}}{z_{i+1}-z_{i-1}} \cdot \frac{\alpha_{i+1}^\dagger-\alpha_{i-1}^\dagger}{z_{i+1}-z_{i-1}}$$
$$+ \frac{2K_i}{z_{i+1}-z_{i-1}}\left[\frac{\alpha_{i+1}^\dagger-\alpha_i^\dagger}{z_{i+1}-z_i} - \frac{\alpha_i^\dagger-\alpha_{i-1}^\dagger}{z_i-z_{i-1}}\right] - \frac{V_i-V_{i-1}}{z_i-z_{i-1}}\alpha_i^\dagger +$$
$$+ \frac{V_i}{A_i}\frac{A_{i+1}-A_{i-1}}{z_{i+1}-z_{i-1}}\alpha_i^\dagger + V_i\frac{\alpha_i^\dagger-\alpha_{i-1}^\dagger}{z_i-z_{i-1}} + S_{s_i}\alpha_i^\dagger + S_{Ii}. \quad (78)$$

No change was made in the differencing schemes used for the boundary conditions. All of the finite difference equations can be rearranged to the form:

$$\alpha_i^{n+1} = \alpha_i^n + a_{i1}\alpha_{i-1}^\dagger + a_{i2}\alpha_i^\dagger + a_{i3}\alpha_{i+1}^\dagger S_{Ii}\Delta t; \quad (79)$$

which can be explicitly solved if $\alpha_i^\dagger$ is known.

The solution of this system of equations was obtained by using a modification of the method of Huen described in Carnahan et al. (1969). To obtain the solution for time level n+1, a first estimate is made:

$$\alpha_i^{*n+1} = \alpha_i^n + a_{i1}\alpha_{i-1}^n + a_{i2}\alpha_i^n + a_{i3}\alpha_{i+1}^n + S_{Ii}\Delta t; \quad (80)$$

where α_i^{*n+1} is the first estimated value of α_i^{n+1}.

It is then assumed that a better estimate for α_i^{n+1} is a function of the average value, $(\alpha_i^{*n+1} + \alpha_i^n)/2$, so that:

$$\alpha_i^{n+1} = \alpha_i^n + \frac{1}{2}[a_{i1}(\alpha_{i-1}^n + \alpha_{i-1}^{*n+1}) + a_{i2}(\alpha_i^n + \alpha_i^{*n+1}) + a_{i3}(\alpha_{i+1}^n + \alpha_{i+1}^{*n+1})] + S_{Ii}\Delta t. \quad (81)$$

Therefore, $\alpha_i^\dagger$ in Eq. 79 can now be defined by:

$$\alpha_i^\dagger = \frac{\alpha_i^n + \alpha_i^{*n+1}}{2}; \quad (82)$$

Equation 80 can be thought of as predicting α_i^{n+1}, and Eq. 81 can be thought of as correcting this value. If the iteration continues, each time correcting the value of α_i^{n+1} obtained in the previous iteration, this approach becomes the simplest form of a predictor-corrector method (Carnahan et al., 1969). In practice, iteration continues until the relative change between the predicted and the corrected values is less than some arbitrary number ε:

$$\left| \frac{\alpha_i^{n+1} \text{ corrected} - \alpha_i^{n+1} \text{ predicted}}{\alpha_i^{n+1} \text{ predicted}} \right| \leq \varepsilon; \quad (83)$$

where $\varepsilon = .0001$ for all solutions used in this dissertation.

Both the solutions and required computational time were observed insensitive to the choice of ε.

Time-Step Restrictions

Roache (1969) presents several methods of stability analysis for equations having the same form as Equation 1. In a discussion of the techniques, he states that the Von Neumann analysis is the most dependable, but that other techniques, like discrete perturbation analysis, may provide insight into stability not given by Von Neumann's method. He applies Von Neumann's analysis to Eq. 1, assuming no sink-source and constant coefficients. This approach can be adopted to time-varying coefficients and non-zero sink-source terms if adjustments are made in the final criteria. While this analysis will not provide exact stability criteria it will provide information useful in determining appropriate time-step size.

Equation (78) can be put into the form:

$$\alpha_i^{n+1} = (1 + S_s\Delta t)\alpha_i^n + b(\alpha_i^n - \alpha_{i-1}^n) + c(\alpha_{i+1}^n - \alpha_{i-1}^n)$$

$$+ d(\alpha_{i+1}^n - 2\alpha_i + \alpha_{i-1}^n); \qquad (84)$$

where b, c, and d are coefficients of up-wind, central, and second-order differences, respectively, occurring in Eq. 78.

The analysis proceeds by substituting for each species value one of its Fourier components:

$$\alpha_i^n = V^n e^{Ii\theta}; \qquad (85)$$

where: V^n = amplitude function at time-level n;

$I = \sqrt{-1}$;

θ = phase angle.

By substituting the respective Fourier components into Eq. 84, dividing by $V^n e^{Ii\theta}$, and substituting trigonometric identities:

$$G = 1 + S_s \Delta t + b(1+I\sin\theta-\cos\theta) + 2cI\sin\theta + 2d(\cos\theta); \quad (86)$$

where G = acceleration factor = V^{n+1}/V^n.

Roache's stability analysis depends upon the solution being bounded. However, he comments that this technique is applicable to unbounded solutions as well. Since the analysis presented here is for constant coefficients (i.e. S_s is constant), the solution must be considered as unbounded. For bounded solutions, the stability criterion is $|G| \leq 1$, but for unbounded solutions this criterion must be modified. In the case of Eq. 84, the criterion becomes $|G| \leq 1 + S_s \Delta T$. This criterion leads to the same stability condition obtained if sink-source contributions are assumed to be zero. In other words, this analysis explores only the stability of the underlying transport equations and ignores the contribution of biological activity. The resulting time-step restrictions are:

$$b + 2c > -1; \tag{86a}$$

$$2d - b < 1; \tag{86b}$$

$$(b+2c)^2 < 2d-b; \tag{86c}$$

The values of b, c, and d can then be calculated by using their definitions, which depend upon the differencing scheme (Cayuga Lake or Canadarago Lake) used. In Cayuga Lake, only central differences were used; therefore b=0. In this case, Eq. 86 reduces to the central difference restrictions shown in Roache (1969).

While this is useful for determining time-step restrictions due to the transport parameters, it provides no information concerning the restrictions, if any, imposed by biological activity. A discrete perturbation analysis does yield this information.

If Eq. 84 is perturbed by some small value, ε_i^n, at node i and time n, the remaining perturbation at time n+1 can be calculated as follows:

$$\alpha_i^{n+1} + \varepsilon_i^{n+1} = (1 + S_s\Delta t)(\alpha_i^n + \varepsilon_i^n) + b(\alpha_i^n + \varepsilon_i^n - \alpha_{i-1})$$

$$+ c(\alpha_{i+1}^n - \alpha_{i-1}^n) + d[\alpha_{i+1}^n - 2(\alpha_i^n + \varepsilon_i^n) + \alpha_{i-1}]; \tag{87}$$

By subtracting the unperturbed solution (Eq. 84) from Eq. 87 and dividing by ε_i^n, an equation for error acceleration, $G = \varepsilon_i^{n+1}/\varepsilon_i^n$, is obtained:

$$G = 1 + S_s\Delta t + b - 2d; \tag{88}$$

Using the same criteria as in the Von Neumann analysis, $|G| \leq 1 + S_s \Delta t$, and further requiring the error to die away asymptotically (Thomann and Szewczyk, 1966), the resulting criterion is:

$$0 \leq G \leq 1 + S_s \Delta t. \tag{89}$$

The non-negativity restriction is in accord with asymptotic die away, since it requires ε_i^n and ε_i^{n+1} to have the same sign. If biological loadings on the system are assumed much larger than the underlying transport processes, the criterion is:

$$S_s \alpha \Delta t \geq -\alpha. \tag{90}$$

This restriction is a statement of species non-negativity, or that the mass of any species lost to decay ($S_s < 0$) and predation in any time step must be less than the amount present at that time.

Applying this criterion to the fixed yield model, species by species, generated maximum allowable time steps for each species. Since all species were solved simultaneously, the one with the highest rate of change controlled time step choice. The nutrient equation was found to be the most restrictive species in this model. Its analysis proceeds by substituting the phosphate sink-source term into Eq. 90:

$$Y_{nx} \cdot \bar{f}(I) \cdot \mu_x \cdot \frac{N}{N+K_n} \cdot X \cdot \Delta t \leq N. \tag{91}$$

The positive contributions to the phosphate sink-source have been ignored to provide a conservative estimate. If we assume $N<<K_n$ (this will be true as nutrient concentration approaches zero), Eq. 91 can be rewritten:

$$\Delta t \leq [Y_{nx} \cdot \bar{f}(I) \cdot \hat{\mu}_x \cdot \frac{X}{K_n}]^{-1}. \qquad (92)$$

Since the parameters on the r.h.s. of Eq. 92 vary in time and space, the minimum K_n and the maximum of all of the other parameters is chosen to provide a conservative estimate of stability. This will correspond to peak algal bloom periods. Therefore, in the most restrictive case, the allowable time step (Δt_{max}) is inversely proportional to the maximum expected algal concentration. In practice, a time step of Δt_{max} ensured numerical stability no matter what parameters were chosen, since Δt_{max} is a conservative estimate based on extreme values.

A similar analysis was performed on the variable yield model equations. The phosphate sink-source term was found to restrict time step more in this formulation than in the previous model, since phosphate uptake is more rapid. In this model, uptake is independent of algal growth, where in the previous model, nutrient uptake was directly proportional to growth. Substituting the variable yield, orthophosphate sink-source term into Eq. 90 yields:

$$\Delta t \leq [\hat{q} \cdot \bar{f}(I) \cdot \frac{X}{K_n} \cdot \frac{C_m - C}{C_m}]^{-1}; \qquad (93)$$

where once more the Monod function has been simplified by assuming $N<<K_n$. The bracketed term again will attain its greatest magnitude when the algal bloom is peaking and the intercellular phosphate is depleted, i.e. C = 0. Substituting the minimum expected Monod half velocity, and the maximum of all other parameters, Δt_{max} was calculated; again stability was never a problem when this time step was used in the variable yield model.

Applying this same analysis to the polyphosphate model showed that in extreme cases, the cellular phosphate sink-source term restricted time step much more than did the orthophosphate terms. Stability criteria applied to the cellular phosphate equation yielded:

$$\Delta t \leq [\frac{\hat{\mu}_x}{K_c} \cdot Y_{nx} \cdot \bar{f}(I) + \frac{r_f}{K_s} \cdot \bar{f}(I) \cdot \frac{V_m - V}{V_m}]. \qquad (94)$$

Dilution by cellular division was ignored since when $C<<K_c$ (assumption which simplifies the Monod term), it is also true that $C<<Y_{nx}$. This will again be critical during maximum algal concentration, when cellular phosphate and polyphosphate are depleted (i.e. $V \approx 0$, $C \approx 0$). Using appropriate maximum and minimum expected values, Δt_{max} can again be calculated.

While these criteria are not to be taken as exact stability limits, they proved a useful measure of stability.

Chapter V

CAYUGA LAKE SIMULATIONS

Verification Criteria

One of the most important links in model development or in this case model comparison is verification. The models tested, all predict average values of the included compartments; none claim exact agreement with discrete or grab samples taken at arbitrary points and times. Discrete field samples are highly variable in space and time due to patchiness and the stochastic nature of biological parameters. Therefore, some form of data averaging is necessary to get a good estimate of the field conditions and to damp out some of the seemingly random perturbations observed. Since samples taken at the surface might be biased by dense air-water interface populations, the surface samples were ignored, and all samples taken at the 2 and 5 meter depths were averaged for comparison. The two-meter samples were assumed to represent a volume from 1 to 3.5 meters (half way to each next sampling depth) and the five-meter samples were assumed to represent a volume from 3.5 to 7.5 meters. Plan areas for each sampling point at each depth were found by using a Thiesen plot and planimetering the polygons. Calculated volumes for each

sample were then used to obtain a weighted average. The discrete model predictions were also averaged in the same volume weighted manner over the same depth zone (1 to 7.5 meters) to obtain a compatable prediction.

Most of the annual primary production in temperate lakes occurs during algal blooms (Wetzel, 1976). Therefore, if a mathematical model is to provide an accurate estimate of annual production, it must provide an accurate description of the algal bloom, while agreement with field data during algal minima is less important. Because agreement during blooms was deemed more important than at other times, matching the field data in a statistical sense (e.g. minimizing the sum of residual squares) over the entire prediction period was not attempted. The first algal bloom in Cayuga Lake is defined by only three temporally spaced average data points. This makes the statistical comparison of the biological analogs in Cayuga Lake impossible, since any comparison based on three points will have such a broad confidence interval that the comparisons will be meaningless. Therefore the verification process did not employ statistical hypothesis testing.

The two components of an algal bloom considered most important for model verification were the rate of algal concentration increase and the maximum algal concentration attained. It was assumed that each individual field sample had a standard deviation of ±50% of its own value. The standard deviation of the euphotic zone algal averages was

therefore estimated from $\frac{\sigma}{\sqrt{n}}$ as ±20%, since each algal average was a composite of at least six field samples. Therefore, the predicted peak algal concentration was assumed verified if it was within one standard deviation or ±20% of the maximum field data average. All verifications proceeded by first attempting to match the field data for the first algal bloom in both rate of bloom development and maximum algal concentration. After obtaining solutions for a wide range of all of the involved kinetic parameters, a narrow range of parameter values which allowed algal verification was identified. This range was then examined in an attempt to synoptically match orthophosphate field data as closely as possible. While only a single verification may be shown for any model, it is the best representation possible (within the ±20% criterion) of the observed field data and not a single attempt to match field data, as it may appear.

Algae Only

The Cayuga Lake comparisons began with the least complex of all of the ecosystem structures; it contained no zooplankton or detritus, and the algae were assumed to have a fixed phosphorus yield coefficient (see Figure 8, p.60). A plot for the euphotic zone (1 to 7.5 meters) of the model output shown in Figure 14a indicates this model eventually attains a dynamic equilibrium.

In the fixed yield model, phosphorus is either in

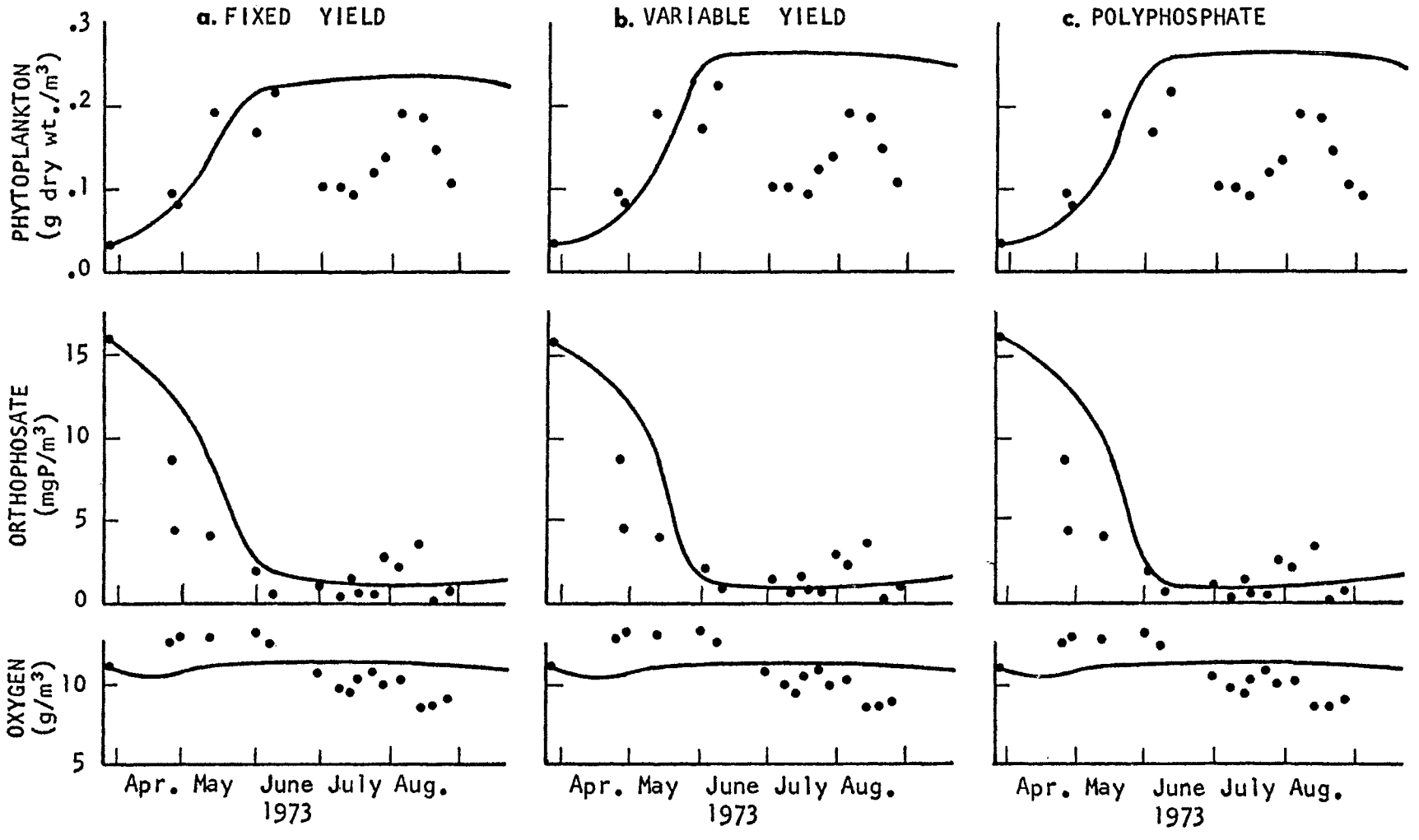

Figure 14. Predictions of algal biomass, orthophosphate, and oxygen concentrations plotted against field data for all three types of phosphate uptake kinetics. No zooplankton and no detrital pool. Cayuga 1973.

Table 6. Biological parameter values for the algae only comparisons in Cayuga Lake.

(xxx = not appropriate)

PARAMETER	FIXED YIELD	VARIABLE YIELD	POLYPHOSPHATE
V_x	0	0	0
V_p	xxx	xxx	xxx
V_z	xxx	xxx	xxx
Y_{zx}	0.6	0.6	0.6
K_{bn}	.10	.10	.10
K_{dn}	.25	.25	.25
K_{xn}	.05	.15	.10
K_{zn}	xxx	xxx	xxx
K_{pn}	xxx	xxx	xxx
K_{bd}	.03	.03	.03
$\hat{\mu}_z$	xxx	xxx	xxx
$\hat{\mu}_x$	2.0	2.0	2.0
$\hat{q}$	xxx	0.5	0.3
r_f	xxx	xxx	0.8
r_d	xxx	xxx	.003
K_x	xxx	xxx	xxx
K_c	xxx	.003	.005
K_s	xxx	xxx	.01
K_v	xxx	xxx	.001
K_n	.01	.01	.01
K_o	.10	.10	.10
C_{max}	xxx	.02	.02
V_{max}	xxx	xxx	.07

Table 6 Cont'd

PARAMETER	FIXED YIELD	VARIABLE YIELD	POLYPHOSPHATE
Y_{na}	.075	.065	.01
Y_{nz}	xxx	xxx	xxx
Y_{nb}	.01	.01	.01
Y_{np}	xxx	xxx	xxx
Y_{ox}	2.0	2.0	2.0
Y_{oz}	xxx	xxx	xxx
Y_{ob}	2.0	2.0	2.0
Y_{op}	xxx	xxx	xxx
Y_{od}	2.0	2.0	2.0

algae or in the orthophosphate pool, since benthic deposits are negligible in Cayuga Lake when compared with the suspended species. Therefore, the rate of nutrient depletion is proportional to the rate of algal growth, and the initial phosphate depletion curve would be the mirror image of the algal growth curve if the plotting scales were comparable. Since the orthophosphate depletion shown by field data is synoptic with the algal growth shown by field data, matching the algal growth rate also matches the phosphate depletion rate in this model. Testing proceeded by adjusting model rates to match the field data rates of algal growth, and adjusting algal phosphate contents to duplicate the algal peaks and orthophosphate lows at the predicted steady state.

During this steady state, the net sink-source term for each species in equilibrium must be zero. Therefore, the sink-source term formulations can be set equal to zero, one by one, to obtain algebraic relations between the kinetic parameters describing the biological interactions for each species. This analysis is useful in determining if more than one set of kinetic parameters can be used to achieve the same steady state. Ignoring the transport terms is permissible because transport into and out of the epilimnion becomes insignificant as the volume of the layer increases. Applying this procedure to the algae sink-source term:

$$\hat{\mu}_x \cdot \bar{\bar{f}}(I) \cdot \frac{N}{N+K_n} = K_{xn}; \qquad (95)$$

where $\bar{\bar{f}}(I)$ is the light function averaged over 24 hours and the euphotic zone (1 to 7.5 meters). This relation shows that during the steady state, the rate of algal reproduction is equal to the rate of algal decay. Since the nutrients equation has the same terms, no new information is obtained by applying the same analysis to it. The time pattern of algal concentrations preceding the first bloom was matched by adjusting $\hat{\mu}_x$ and K_{xn}. The steady-state phosphate levels could then be made to match field values by adjusting the Monod half velocity. This procedure allowed matching the time varying portion of the algal solution to field data, but the only method available for controlling the peak algal concentration was adjusting the algal nutrient content. Therefore, the only kinetic parameter that the steady-state analysis did not yield information for, Y_{nx}, was necessarily fixed by the verification criterion of matching the peak algal concentration. Since it appeared that the total amount of phosphorus in the euphotic zone was a constant throughout the prediction period and constant total phosphorus would allow more restraints to be placed on parameter choice, an analysis of the total phosphorus in this zone was done.

At any time, the total phosphorus in any layer of the lake is the sum of the phosphorus in the orthophosphate pool and that contained in all of the other species; in this

case the only other phosphorus containing species is algae. This is expressed by:

$$N_T = N + (Y_{nx} + C + V)\ X \tag{96}$$

where N_T = Total phosphorus. The total algal phosphorus content is the sum of all three compartments but the polyphosphate and cellular phosphate components are zero if the fixed yield algae analog is used. Differentiating Eq. 96 with respect to time and making the appropriate substitutions yields:

$$\frac{\partial N_T}{\partial t} = \frac{\partial N}{\partial t} + \frac{\partial [(Y_{nx}+C+V)X]}{\partial t} = \frac{1}{A}\frac{\partial}{\partial z}\left(KA\frac{\partial N}{\partial z}\right)$$

$$+ \frac{1}{A}\frac{\partial}{\partial z}\left(KA\frac{\partial [(Y_{nx}+C+V)X]}{\partial z}\right.$$

$$- \frac{1}{A}\frac{\partial}{\partial z}[V_x A(Y_{nx}+C+V)X]. \tag{97}$$

The sink-source terms have cancelled exactly because the biological interactions that they describe are conservative for phosphorus. By regrouping terms, and applying the definition in Eq. 96:

$$\frac{\partial N_T}{\partial t} = \frac{1}{A}\frac{\partial}{\partial z}\left(KA\frac{\partial N_T}{\partial z}\right) - \frac{1}{A}\frac{\partial}{\partial z}\left(V_x A(Y_{nx}+C+V)X\right. \tag{98}$$

Therefore, if initial conditions are such that $\frac{\partial N_T}{\partial z} \approx 0$ and algae are not allowed to sink, the change of total phosphorus with respect to time is approximately zero.

In Cayuga Lake, when algal sinking was permitted,

algae collected at, and then degraded at, the thermocline, releasing their nutrients. This resulted in a large increase in orthophosphate levels at the thermocline. While this phenomenon has been identified in some lakes, it was not apparent in the Cayuga Lake field data. Therefore, all comparisons in Cayuga Lake were done with no sinking. This reduced Eq. 98 to only a diffusive flux which also is negligible if the initial conditions include a uniform total phosphorus concentration over depth (which happens at homothermy or spring overturn).

The steady state that the algae-only model achieved was defined by Eq. 95 and 96. The orthophosphate and algal concentrations in Eq. 96 were defined by field data, and the total phosphorus, N_T, could be calculated from initial conditions. Therefore, the phosphorus yield coefficient was also fixed. To achieve the match in Figure 14a, the yield coefficient was restrained to .075 g P/g dry wt. algae. This is well within the range of values shown in Table 1. Moreover, this is approximately the phosphorus content reported for Pyrrophyta which were the dominant algal species in the Cayuga Lake spring bloom (Serruya, 1975; Godfrey, 1973).

The next algal model tested was the variable yield formulation, depicted in Figure 4b. Inspection of the comparison in Figure 14b shows the variable yield formulation had little effect on the ability of the algae-only model to match field data values. This model allows the algal growth

rate to be decoupled from the phosphate uptake rate or rate of orthophosphate depletion. While this allows an instantaneous separation of the two processes, they are so closely linked in their sink-source terms that time traces of the type shown in Figures 14a and 14b are almost indistinguishable. At most, this formulation introduces a slight lag between orthophosphate depletion and algal increase, since nonstructural, cellular phosphate must be slightly increased before growth is stimulated. In practice, using literature values for uptake and growth rates, the temporal separation between the maximum rate of orthophosphate depletion and that of algal growth is one or two days. Differences between model formulations on this scale are indistinguishable when compared with bi-weekly field data.

The same equations (Eq. 95 and 96) result when the variable yield formulation is subjected to steady-state analysis, but the total phosphorus content of an algal cell is now $Y_{nx}+C$. As in the previous verification, the specific algal growth and decay rates were adjusted to match the time varying portion to the field data values. The total phosphorus yield coefficient of algae was again restrained to .075 g P/g algal dry wt., but no restraints, by this analysis, were placed on the relative values of C and Y_{nx}. Therefore, the same steady state can be achieved by an infinite number of choices of coefficients which place different fractions of the total algal phosphorus in either structure (Y_{nx}) or

the cellular phosphate pool (C). While the steady state is amenable to this arbitrary choice, the time varying portion of the solution is not. When attempts were made to place the majority of the total algal phosphorus into the variable or cellular phosphate compartment, the algal phosphorus content became as high as .2 g P/g dry wt. before it was drained, by growth and dilution, to the steady state level. Also, the orthophosphate was depleted early in April; this is not verified by the orthophosphate data. The only parameters allowing the match shown in Figure 11b placed at least .065 g P/g dry wt. in the fixed component of the total algal phosphorus.

The polyphosphate algal model also achieved a steady state. The comparison shown in Figure 14c shows no improvement in the data match capability with the addition of a polyphosphate pool, even though the phosphate uptake and storage systems are very different than the previous two models.

The same two equations (Eq. 95 and 96) result from a steady-state analysis. In this formulation, the same restrictions were placed on $\hat{\mu}_x$, K_{xn}, and K_n, and the total phosphorus was again constrained to 7.5% of the algal dry weight. However, the total algal phosphorus has three components: structure, cellular phosphate, and volutin. Since placing a large portion of the total algal phosphorus in the cellular phosphate pool is ineffective, and it has already been demonstrated that the data can be matched with a large

portion in structure, attempts to verify the polyphosphate analog centered on placing the majority of the algal phosphorus in the polyphosphate compartment. The polyphosphate kinetic parameters (r_f, r_d, K_s, K_v) were chosen to maintain a polyphosphate content of approximately 6% of the algal dry weight when the steady state was achieved and the algal growth was equal to its decay.

Examination of Figure 14 reveals that all three phosphate uptake models are equally capable of matching the field data for the time period leading into the first bloom; they are also capable of predicting the peak algal concentration. However, early in June algal losses occurred that are not predicted by these algae-only formulations and the predictions do not even qualitatively match the algal data after the first bloom. The match of orthophosphate data is within acceptable limits, but this is of little consolation.

Algae and Detritus

The next model tested removed the necessity of assuming instantaneous nutrient regeneration by decaying algae. Instead, all algal losses became an input to the detrital pool, which then decayed at a specific decay rate, dependent only on temperature. This is the ecosystem structure shown in Figure 9. A steady-state analysis of the algal sink-source terms yielded the same algebraic relation as that shown in Eq. 95, but the algal decay rate is K_{xp} in this model

instead of K_{xn} as it was in the algae-only model:

$$\hat{\mu}_x \bar{f}(I) \frac{N}{N+K_n} = K_{xp}. \quad (99)$$

Since the phosphorus in decaying algae is no longer immediately released to solution, a steady-state analysis of the orthophosphate equation does not yield redundant information as it did in the algae-only model. The orthophosphate steady state yields:

$$(Y_{nx}+C+V) \cdot \hat{\mu}_x \bar{f}(I) \cdot \frac{N}{N+K_n} X = Y_{np} \cdot K_{pn} \cdot P. \quad (100)$$

Steady-state analysis of the detrital equation yields:

$$\frac{X}{P} = \frac{K_{pn}}{K_{xp}}. \quad (101)$$

And the addition of another phosphorus-containing species results in:

$$N_T = N + (Y_{nx}+C+V)X + Y_{np} P. \quad (102)$$

Since no field data exist for the amount of phosphorus in Cayuga Lake's algae, the concentration of phosphorus in algae and particulates is freely adjustable as long as N_T is constant. However, attempts to lower algal phosphorus content by maintaining higher detrital levels and, consequently, more total detrital phosphorus failed. While the steady state predicted by Eq. 99 through 102 was achieved, the algae initially overshot the steady-state value considerably before asymptotically returning. This is because during bloom

development, the algae are necessarily reproducing much faster than they are decaying. The transfer of phosphorus from orthophosphate to detritus, by first being incorporated into algal biomass, is not rapid enough for algae to approach its steady-state value asymptotically. Therefore, the total detrital phosphorus content was always small for asymptotic approaches to steady state, and detritus had a negligible effect on the solutions for the euphotic zone shown in Figure 15.

The solutions shown demonstrate detrital decay rates ranging from 5 to 15% per day with no appreciable change in the solutions from those shown in Figure 14. The addition of a detrital pool allowed no better match of the field data, no improvement in the large algal phosphorus content, and added another species for solution.

Algae and Zooplankton

The next ecosystem structure tested is depicted in Figure 10. A local stability analysis of a linearized form of the simultaneous mass balance equations for algae, zooplankton, and phosphate was done using a canned numerical subroutine (HSBG) of the Ohio State University computer center. The Monod terms were linearized by using a truncated Taylor series representation, centered at the steady-state values; the various parameters were assumed to be temperature independent. This analysis yielded eigenvalues

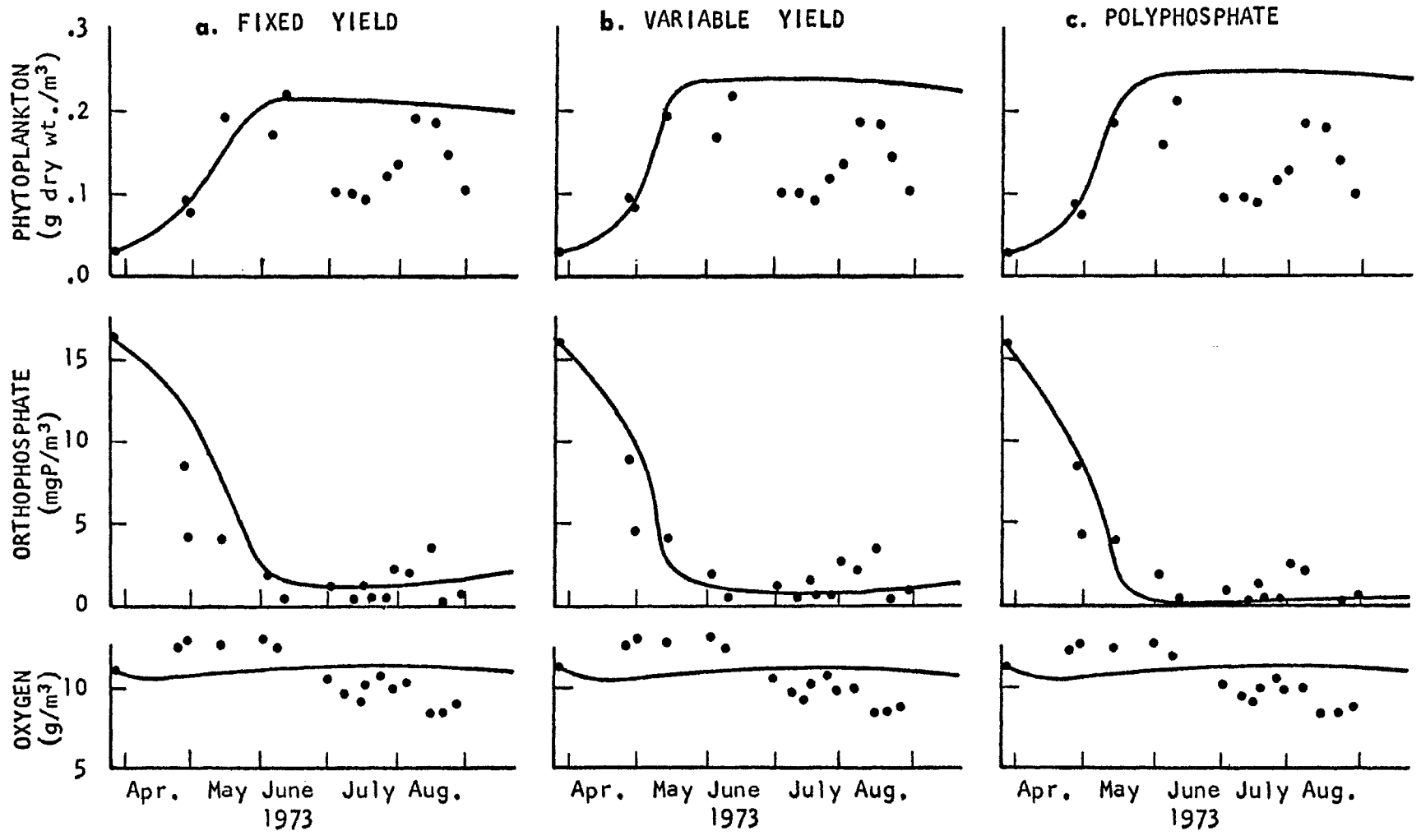

Figure 15. Predictions of algal biomass, orthophosphate, and oxygen concentrations plotted against field data for all three types of phosphate uptake kinetics. Detrital pool and no zooplankton. Cayuga 1973

Table 7. Biological parameter values for the algae plus detrirus comparisons in Cayuga Lake.

(xxx = not appropriate)

PARAMETER	FIXED YIELD	VARIABLE YIELD	POLYPHOSPHATE
V_x	0	0	0
V_p	0	0	0
V_z	xxx	xxx	xxx
Y_{zx}	0.6	0.6	0.6
K_{bn}	.10	.10	.10
K_{dn}	.25	.25	.25
K_{xp}	.05	.15	.10
K_{zp}	xxx	xxx	xxx
K_{pn}	.05	.15	.10
K_{bp}	.03	.03	.03
$\hat{\mu}_z$	xxx	xxx	xxx
$\hat{\mu}_x$	2.0	2.0	2.0
$\hat{q}$	xxx	.50	.30
r_f	xxx	xxx	0.8
r_d	xxx	xxx	.003
K_x	xxx	xxx	xxx
K_c	xxx	.003	.005
K_s	xxx	xxx	.01
K_v	xxx	xxx	.001
K_n	.01	.01	.01
K_o	.10	.10	.10
C_{max}	xxx	.07	.02
V_{max}	xxx	xxx	.07

Table 7 Cont'd

PARAMETER	FIXED YIELD	VARIABLE YIELD	POLYPHOSPHATE
Y_{nx}	.075	.065	.01
Y_{nz}	xxx	xxx	xxx
Y_{nb}	.01	.01	.01
Y_{np}	.01	.01	.01
Y_{ox}	2.0	2.0	2.0
Y_{oz}	xxx	xxx	xxx
Y_{ob}	2.0	2.0	2.0
Y_{op}	2.0	2.0	2.0
Y_{od}	2.0	2.0	2.0

which indicated that the species would return to their steady-state values by decaying oscillations around the steady-state value. However, the solutions shown in Figure 16 have oscillations which seem to grow in time. If the temperature dependencies of algal and zooplankton growth and decay rates are removed, the oscillations decay as predicted. Therefore, the amplification seen in the temperature-dependent solutions is due to the dissimilar temperature dependencies of algae and zooplankton. As the average euphotic zone temperature increases, the steady-state values of the system shift and the oscillations appear to be amplified. This effect is large since not only is the zooplankton growth rate temperature dependent, but the Monod half velocity is also. The zooplankton become much more effective grazers as the water warms.

While no zooplankton data for 1973 were available, monthly zooplankton counts were available for 1969. Converting counts to dry weights based on estimated zooplankton volumes and water contents is inaccurate, but sufficient to identify trends in zooplankton biomass. The weights were estimated for each zooplankton species by using literature values for the species' adult length and breadth and assuming either a prolate or oblate elipsoid body, depending if the species was a copepod or cladoceran, respectively (Pennak, 1955; Culver, 1977; Hall, 1964; Omori, 1969). Counts were then converted to mass for each species and totaled. The

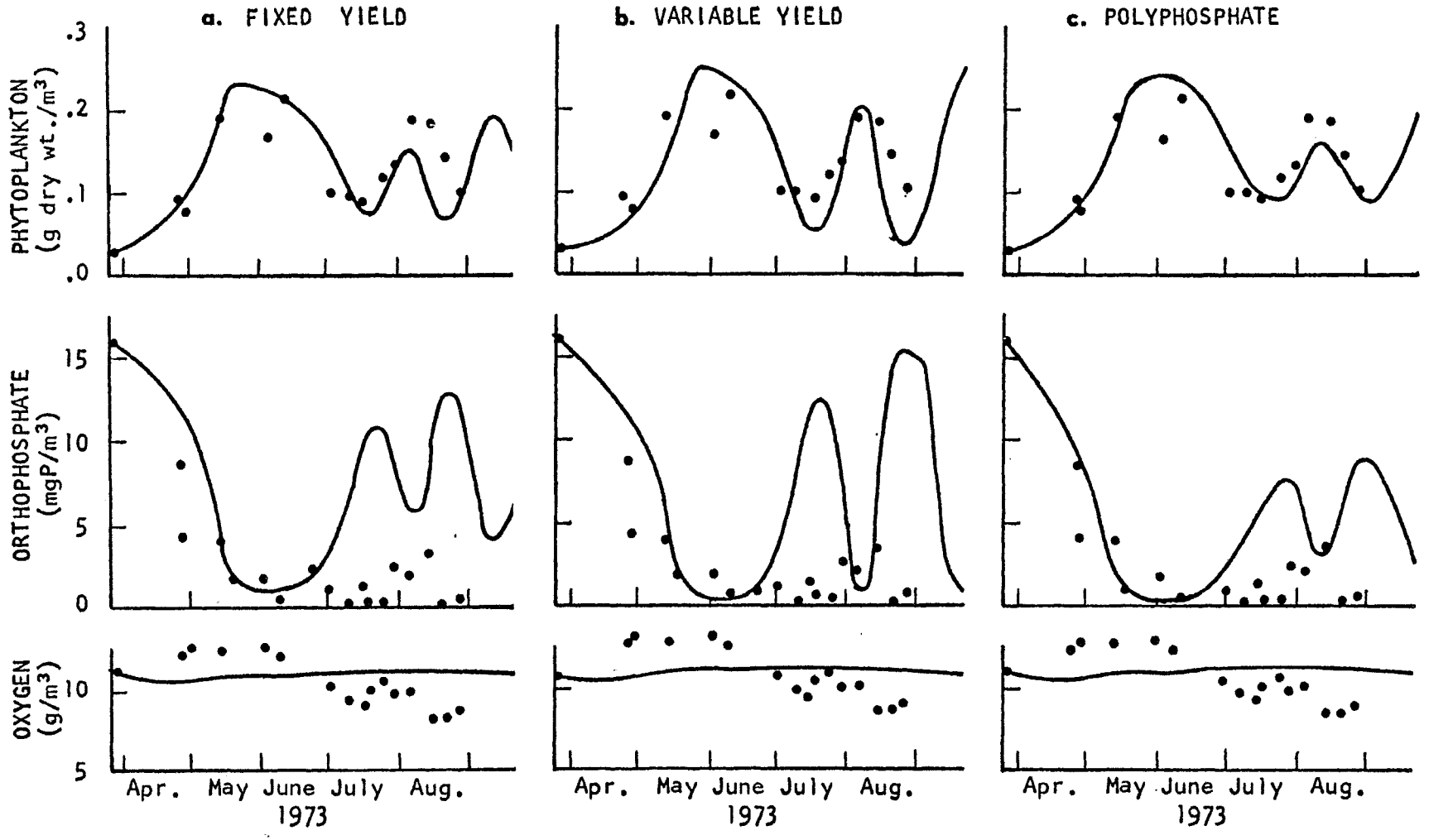

Figure 16. Predictions of algal biomass, orthophosphate, and oxygen concentrations plotted against field data for all three types of phosphate uptake kinetics. Zooplankton and no detrital pool. Cayuga 1973

Table 8. Biological parameter values for the algae plus zooplankton comparisons in Cayuga Lake.
(xxx = not appropriate)

PARAMETER	FIXED YIELD	VARIABLE YIELD	POLYPHOSPHATE
V_x	0	0	0
V_p	xxx	xxx	xxx
V_z	0	0	0
Y_{zx}	0.6	0.6	0.6
K_{bn}	.10	.10	.10
K_{dn}	.25	.25	.25
K_{xn}	.10	.15	.05
K_{zn}	.10	.10	.10
K_{pn}	xxx	xxx	xxx
K_{bd}	.03	.03	.03
$\hat{\mu}_z$	.36	.36	.36
$\hat{\mu}_x$	2.0	2.0	2.0
$\hat{q}$	xxx	.30	.30
r_f	xxx	xxx	.80
r_d	xxx	xxx	.01
K_x	.25	.25	.30
K_c	xxx	.005	.01
K_s	xxx	xxx	.01
K_v	xxx	xxx	.015
K_o	.10	.10	.10
C_{max}	xxx	.07	.02
V_{max}	xxx	xxx	.07
K_n	.01	.01	.01

Table 8 Cont'd

PARAMETER	FIXED YIELD	VARIABLE YIELD	POLYPHOSPHATE
Y_{nx}	.075	.065	.01
Y_{nz}	.03	.03	.03
Y_{nb}	.01	.01	.01
Y_{np}	xxx	xxx	xxx
Y_{ox}	2.0	2.0	2.0
Y_{oz}	2.0	2.0	2.0
Y_{ob}	2.0	2.0	2.0
Y_{op}	xxx	xxx	xxx
Y_{od}	2.0	2.0	2.0

results are plotted in Figure 17. The 1969 data showed a zooplankton peak occurring about mid-way between the two algal peaks observed in 1973. This was taken to imply that zooplankton predation was responsible for the algal minimum observed in late June of 1973. The calculated early spring concentrations of zooplankton were used as best available estimates of the initial zooplankton concentration for all comparisons.

The zooplankton temperature dependencies made them ineffective predators in the early spring. This allowed adjustment of the algal parameters to match the first bloom somewhat independently of zooplankton rates. Predation was then adjusted to match the algal minimum and to time the second bloom, which also fixed its magnitude.

The fixed yield formulation (see Fig. 16) fits the algal data through the second bloom quite well, although the second bloom's actual decay is somewhat slower than that predicted by the model. The large increase in ambient orthophosphate levels is necessary to stimulate the second bloom. None of the attempts to match the midsummer field values of orthophosphate and algae simultaneously were successful. Therefore, if the descriptive kinetics for phosphate-limited growth are correct, the algae are obtaining their phosphorus from something other than the ambient orthophosphate pool.

The variable yield formulation behaved almost identically to the fixed yield model. Therefore, the verification

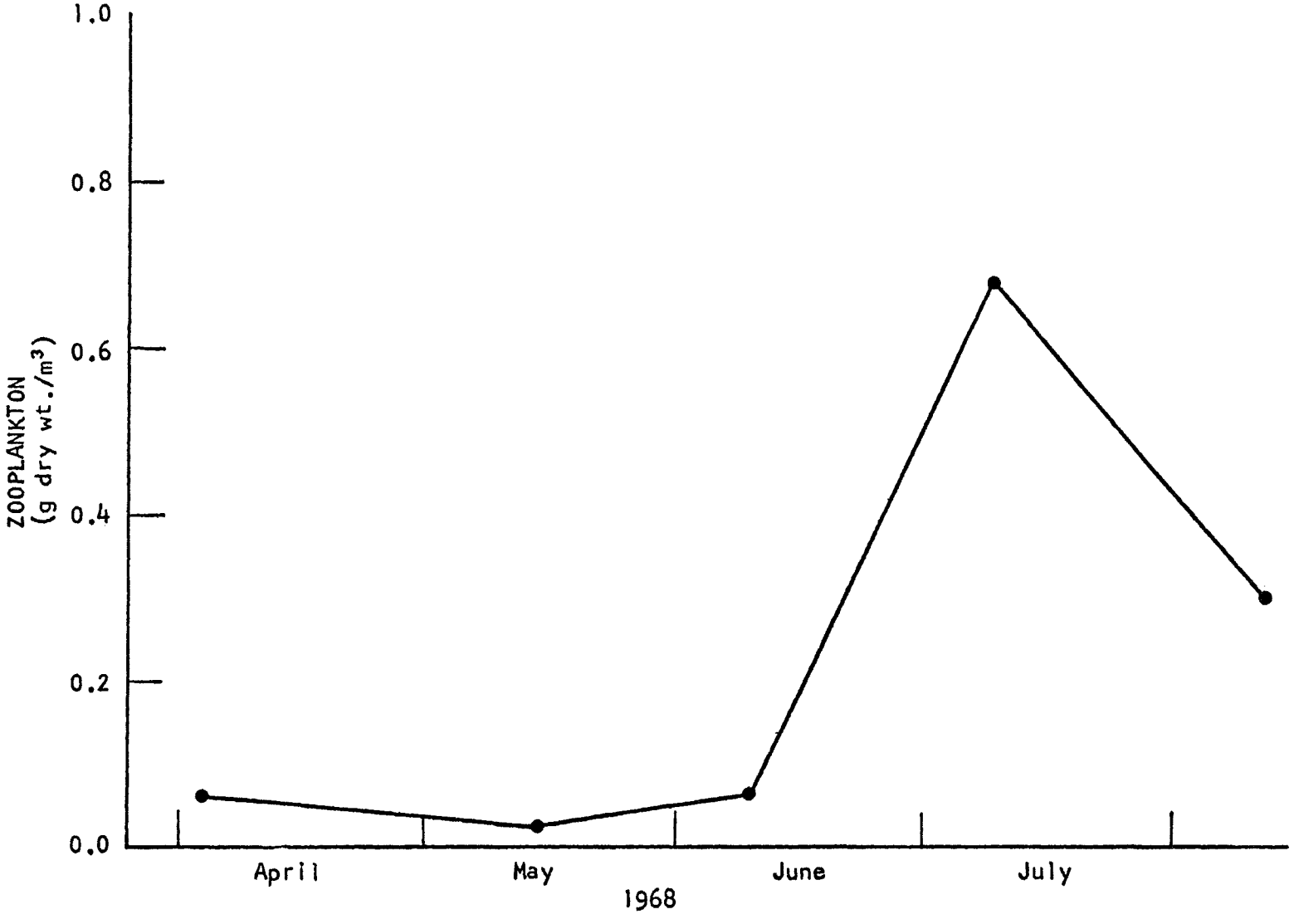

Figure 17. Monthly zooplankton data representing the top ten meters of Cayuga lake for 1968

in Figure 16b was chosen to demonstrate the different types of solutions possible within the verification limits previously described. The zooplankton parameters used are the same as those in the fixed yield verification, but the algae are growing slightly slower. This is evidenced by the slower rate of increase of the algal standing crop preceding the first bloom. Since algae are growing slower, the zooplankton deplete them to lower levels between the first and second algal bloom than they could in the fixed yield model. The farther from its equilibrium level the algae are displaced during their minimum, the higher the next algal peak will be; as can be seen comparing Figures 16a and 16b. Using the variable yield model, it was impossible to stimulate a second bloom without increasing ambient phosphate levels far in excess of field values.

The polyphosphate formulation behaved the same as the fixed and variable yield models, within the literature range of the kinetic parameters tested. This should be expected since the different uptake and growth kinetics make only minor changes internal to the algae. Algal growth and decay were adjusted to match the first bloom in each comparison. This meant that the gross behavior of the algae was the same in each analog and the zooplankton rates were approximately the same. Therefore, the algal and phosphate oscillation were the same and all three failed to match the orthophosphate data after the second bloom.

Algae, Detritus, and Zooplankton

When a detrital pool is added to the algae plus zooplankton formulations, the phosphate contained in decaying algae is no longer immediately released to the orthophosphate pool. This lag in nutrient regeneration allows less algal production during the zooplankton bloom and, consequently, allows a lower peak zooplankton concentration. When the zooplankton then decay, another lag exists, since the phosphorus in zooplankton is mediated by detritus before the algae can utilize it for growth. These lags tend to rapidly damp the oscillations obtained when detritus is excluded, or decayed very rapidly. The last case begins to approximate the assumption of instantaneous nutrient regeneration used when detritus is excluded.

The fixed yield verification in Figure 18a is the same type of solution obtained when any of the models were made to match the algal minimum after the first bloom. The oscillation that occurred in Figure 16a is damped almost to non-existence by the addition of detritus. Since no attempt could duplicate the second algal bloom, regardless of the algal formulation used, the second bloom was matched in an "average" sense by the variable yield and polyphosphate analogs. As can be seen in Figures 18b and 18c, the phosphate predictions more closely match the field data as zooplankton predation is made less severe and the algal solutions

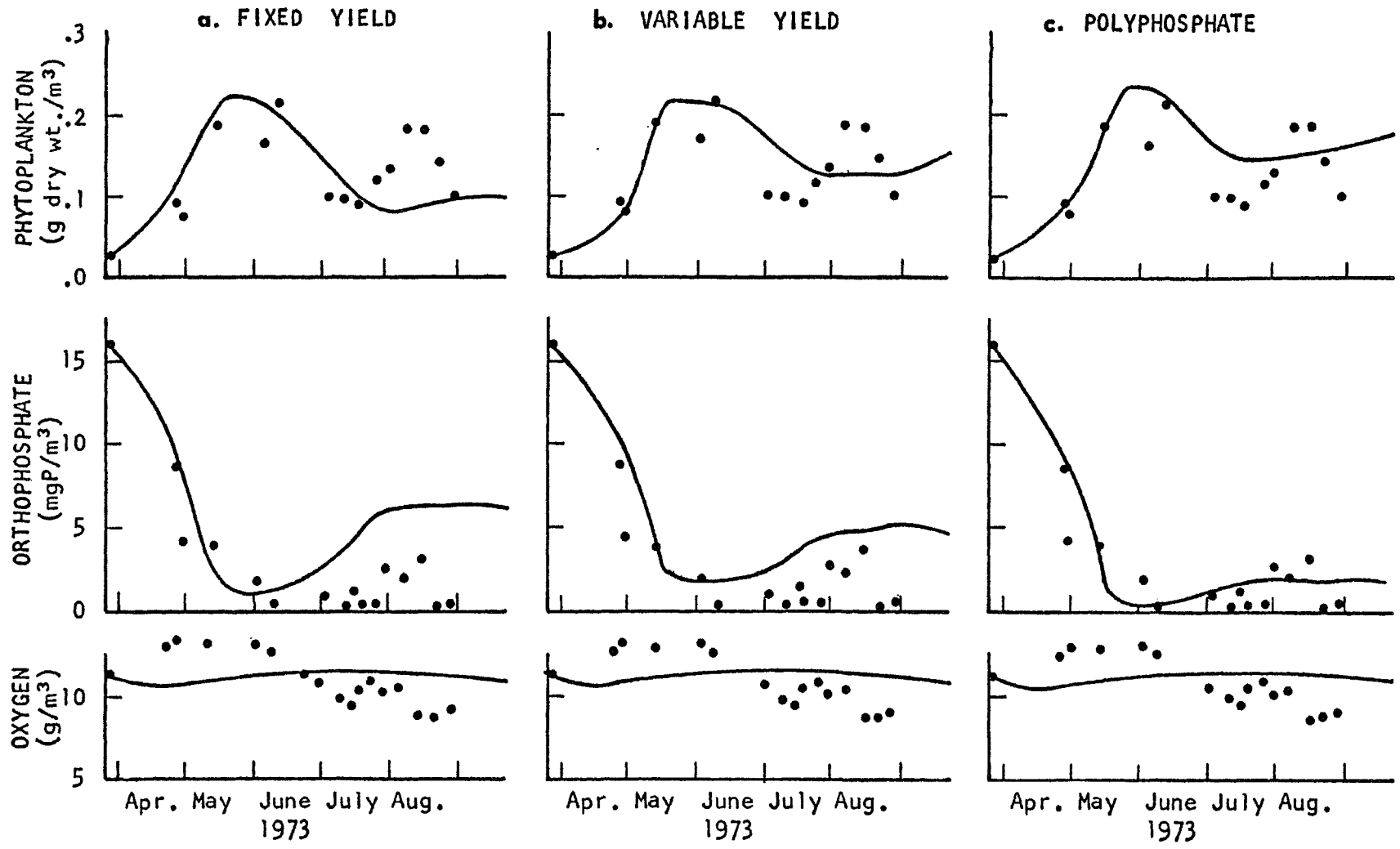

Figure 18. Predictions of algal biomass, orthophosphate, and oxygen concentrations plotted against field dat for all three types of phosphate uptake kinetics. Zooplankton and a detrital pool. Cayuga 1973

Table 9. Biological parameter values for the algae, detritus and zooplankton comparisons in Cayuga Lake.

(xxx = not appropriate)

PARAMETER	FIXED YIELD	VARIABLE YIELD	POLYPHOSPHATE
V_x	0	0	0
V_p	0	0	0
V_z	0	0	0
Y_{zx}	0.6	0.6	0.6
K_{bn}	.10	.10	.10
K_{dn}	.25	.25	.25
K_{xp}	.05	.15	.05
K_{zp}	.05	.10	.15
K_{pn}	.05	.15	.05
K_{bd}	.03	.03	.03
$\hat{\mu}_z$	.36	.36	.36
$\hat{\mu}_x$	2.0	2.0	2.0
$\hat{q}$	xxx	.50	.30
r_f	xxx	xxx	.80
r_d	xxx	xxx	.01
K_x	.50	.30	.20
K_c	xxx	.003	.01
K_s	xxx	xxx	.01
K_v	xxx	xxx	.001
K_n	.01	.01	.01
K_o	.10	.10	.10
C_{max}	xxx	.07	.02
V_{max}	xxx	xxx	.07

Table 9

PARAMETER	FIXED YIELD	VARIABLE YIELD	POLYPHOSPHATE
Y_{nx}	.075	.065	.01
Y_{nz}	.03	.03	.03
Y_{nb}	.01	.01	.01
Y_{np}	.01	.01	.01
Y_{ox}	2.0	2.0	2.0
Y_{oz}	2.0	2.0	2.0
Y_{ob}	2.0	2.0	2.0
Y_{op}	2.0	2.0	2.0
Y_{ob}	2.0	2.0	2.0

begin to approximate those in Figure 14 and 15. The orthophosphate data from mid-June to mid-August are approximated by any of algal models when the second algal bloom is ignored; the orthophosphate data are never matched when the bloom is duplicated. Therefore, orthophosphate is probably not the source of the phosphorus used in the second algal bloom. This idea will be expanded later.

Second Bloom Verifications

Inspection of the species sucession in Cayuga Lake showed the first bloom to be comprised of Pyrrophyta and Bacillariophyta, while the second bloom was mainly Chlorophyta, Chrysophyta, and Pyrrophyta. This, and the inability of any model to duplicate the second bloom algal and orthophosphate data simultaneously, indicated that attempts to match the second algal bloom separately were necessary. In previous attempts, the algal kinetic rates were adjusted to match the first bloom's development. These rates may not be the same for the second bloom since the species dominating the two blooms are different. Therefore, adjusting the algal rates to match the second bloom data, independent of any verifications of the first bloom, may allow the synoptic match of algal and orthophosphate data not otherwise achieved.

Verifications for the second bloom were done by beginning the model solution at the algal minimum in mid-July. Previous experience dictated the use of zooplankton, since

the data show oscillations are not attainable in models without predation. Using the same verification criteria as before, Figure 19 is the verification for the fixed yield and polyphosphate formulations.

The fixed yield formulation matches the algal data very well but the orthophosphate predictions are not even qualitatively like the field values. The large increase in ambient phosphorus levels needed to stimulate the bloom in the previous attempts to match both algal blooms simultaneously is not necessary in this verification, since the algae now only contain 1% phosphorus.

The polyphosphate formulation also matches the field data for algae fairly well. However, in this attempt the polyphosphates were adjusted to be depleted at the algal maximum, thus maintaining a total algal phosphorus content of about 1%. This compartmental transfer of phosphate damped the oscillations that were achievable in the fixed yield model. The polyphosphate model was also incapable of matching the orthophosphate field data simultaneously with the algal data.

Detritus was added to the system to obtain the solutions shown in Figure 20. The same damping effect seen in previous attempts was also obvious in the second bloom verification attempts. The addition of detritus to the system made the algal predictions less accurate and did not improve the match of orthophosphate field data. No model

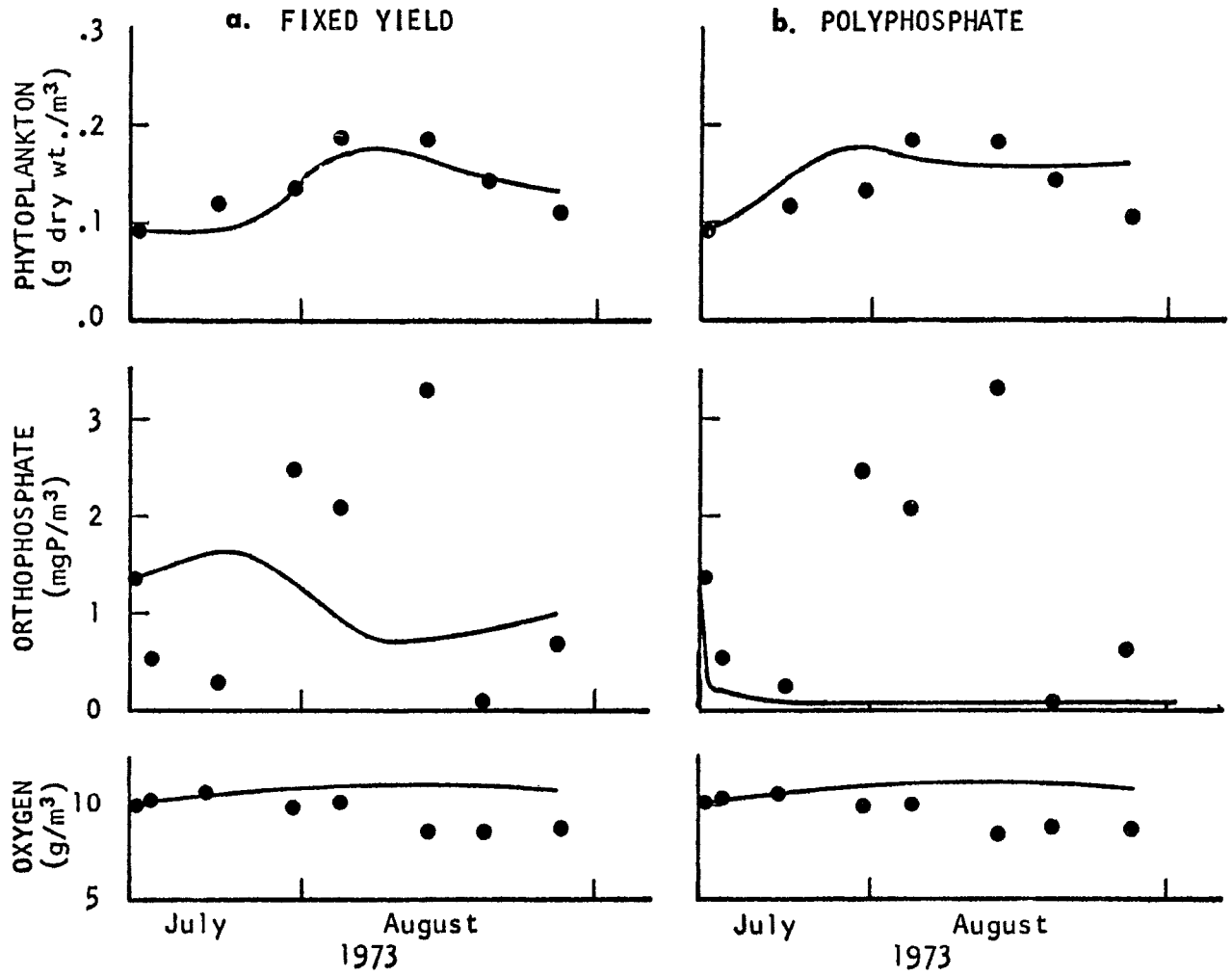

Figure 19. Second bloom predictions of algal biomass, orthophosphate, and oxygen concentrations plotted against field data for two types of phosphate uptake kinetics. Zooplankton predation and no detrital pool.

Table 10. Biological parameter values for the second bloom algae plus zooplankton comparisons in Cayuga Lake.

(xxx = not appropriate)

PARAMETER	FIXED YIELD	POLYPHOSPHATE
V_x	0	0
V_p	xxx	xxx
V_z	.10	.10
Y_{zx}	.60	.60
K_{bn}	.10	.10
K_{dn}	.10	.10
K_{xn}	.05	.05
K_{zn}	.18	.19
K_{pn}	xxx	xxx
K_{bd}	.03	.03
$\hat{\mu}_z$	.30	.30
$\hat{\mu}_x$	1.5	1.5
r_f	xxx	.40
r_d	xxx	.05
K_x	.08	.08
K_c	.01	.002
K_s	xxx	.01
K_v	xxx	.001
K_n	.001	.01
K_o	.10	.10
C_{max}	xxx	.03
V_{max}	xxx	.07
$\hat{q}$	xxx	.40

Table 10 Continued

PARAMETER	FIXED YIELD	POLYPHOSPHATE
Y_{nx}	.01	.01
Y_{nz}	.03	.03
Y_{nb}	.01	.01
Y_{np}	xxx	xxx
Y_{ox}	2.0	2.0
Y_{oz}	2.0	2.0
Y_{op}	xxx	xxx
Y_{ob}	2.0	2.0
Y_{od}	2.0	2.0

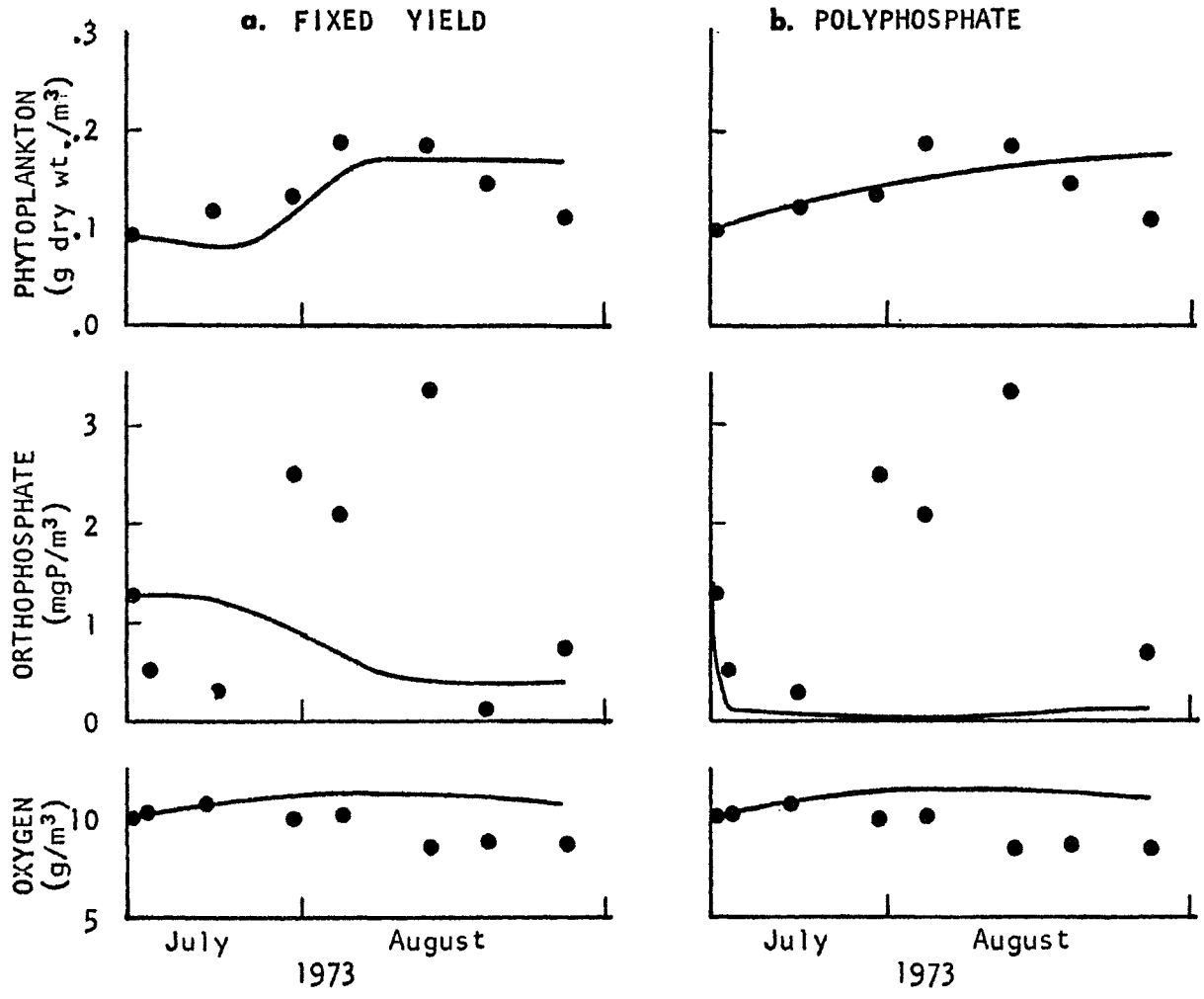

Figure 20. Second bloom predictions of algal biomass, orthophosphate, and oxygen concentrations plotted against field data for two types of phosphate uptake kinetics. Zooplankton predation and a detrital pool

Table 11. Biological parameter values for the second bloom algae, detritus, and zooplankton comparisons in Cayuga Lake. (xxx = not appropriate)

PARAMETER	FIXED YIELD	POLYPHOSPHATE
V_x	0	0
V_p	0	0
V_z	.10	.10
Y_{zx}	.60	.60
K_{bn}	.10	.10
K_{dn}	.10	.10
K_{xp}	.05	.05
K_{zp}	.20	.20
K_{pn}	.10	.10
K_{bd}	.03	.03
$\hat{\mu}_z$	.30	.30
$\hat{\mu}_x$	1.5	1.5
$\hat{q}$	xxx	.40
r_f	xxx	.40
r_d	xxx	.05
K_x	.08	.09
K_c	xxx	.002
K_s	xxx	.01
K_v	xxx	.001
K_n	.001	.01
K_o	.10	.10
C_{max}	xxx	.03
V_{max}	xxx	.07

Table 11. Continued

PARAMETER	FIXED YIELD	POLYPHOSPHATE
Y_{nx}	.01	.01
Y_{nz}	.03	.03
Y_{nb}	.01	.01
Y_{np}	.01	.01
Y_{ox}	2.0	2.0
Y_{oz}	2.0	2.0
Y_{op}	2.0	2.0
Y_{ob}	2.0	2.0
Y_{od}	2.0	2.0

tested predicts an increase of ambient orthophosphate synoptic with a bloom like that shown in the field data, regardless of analog structure or beginning of the prediction period.

Minimal Biological Structure

The Lotka-Volterra formulations (previously discussed in Minimum Necessary Model Structure) for algal and zooplankton growth rates were used in an attempt to match Cayuga Lake's field data without incorporating the non-linear Monod functions. First, all parameters were left unchanged from those given in the fixed yield column of Table 8. This resulted in the solid-line solution shown in Figure 21a. The high initial phosphorus concentration in late March allows initial growth rates eight times larger than the maximum possible in the Monod formulations. Since matching the algal bloom's magnitude and time of occurrence was deemed most important, these rapid increases in algal crops and the unrealistic algal growth rates were successively lowered until the predicted algal bloom peaked in late May, as shown by the dashed-line solution in Figure 21a. In the Lotka-Volterra formulations, the algal growth and decay rates were again dictated by the time varying portion of the solution leading into the first bloom.

A steady-state analysis of the governing sink-source terms (as in the algae-only section) led to three algebraic

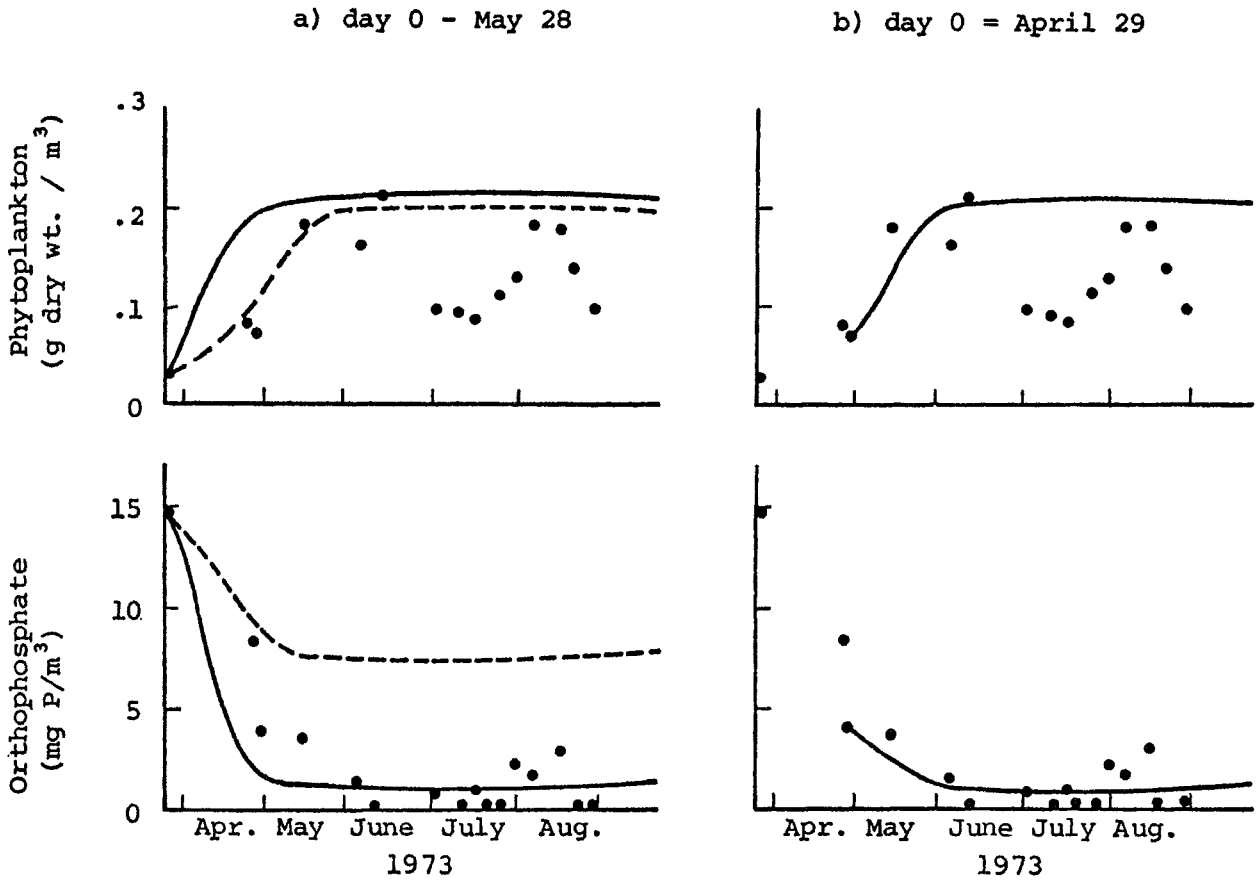

Figure 21. Lotka-Volterra predictions of algal biomass and orthophosphate concentrations plotted against field data. Zooplankton and no detrital pool. Cayuga 1973.

relations:

from the zooplankton:

$$X = K_{zn}/L_x; \tag{103}$$

where: L_x = Lotka-Volterra term for algae growth

$= \mu_x/K_n$;

from the algae:

$$Z = \frac{L_x N \bar{\bar{f}}(I) - K_{nx}}{L_z/Y_{zx}} ; \tag{104}$$

where: L_z = Lotka-Volterra term for zooplankton growth

$= \mu_z/K_x$; and

from the orthophosphate sink-source terms:

$$N = \frac{K_{xn}}{L_x f(I)} . \tag{105}$$

Since the algal growth and decay rates are fixed by the time varying portion of the solution, orthophosphate levels are also fixed according to Eq. 105. Many attempts were made to lower the steady-state orthophosphate levels while maintaining the algal peaks correlation with field data, but all failed.

The high initial orthophosphate levels required a low growth rate which raised the steady-state orthophosphate levels too high (Eq. 105). Therefore, another set of data comparisons was done beginning the model solution on April 31 and using field data from that time for initial conditions. The solutions (Figure 21b) more closely approximate those

obtained for the algae-only or algae plus detritus models (Figures 16 and 17). No solutions of the Lotka-Volterra formulations ever showed oscillations of the magnitude given by the Monod formulations (Figure 18) regardless of parameter values or the initial conditions.

Chapter VI

CANADARAGO LAKE SIMULATIONS

Hetling (1974) presents the Canadarago data in an averaged form, ready for use in model verification. The weightings for averaging were representative volumes determined by Thiesen plots. Orthophosphate and oxygen concentrations were given in three depth zones, 0-4.5, 4.5-thermocline, and thermocline-13 meters. Model predictions at one-meter nodes were averaged over zones corresponding as closely as possible to field zones: 0-4.5, 4.5-7.5, and 7.5-13 meters.

The algal field data published by Hetling are a whole lake average. Consequently, model predictions were averaged over the entire lake. Examination of the algal field data shows a single bloom. This appears to be the second bloom to occur in Canadarago Lake that year. First, it happens at a similar time and euphotic zone temperature as the second bloom in Cayuga Lake and both lakes are in the same region. Second, the initial phosphate levels are too low for this to be a first bloom. Third, interpreting the data as beginning between the first and second bloom also explains early hypolimnion anoxia, caused by decaying organic matter. Therefore, in comparing the ecosystem structures, the Canadarago verifications are treated as second bloom verifications.

Algae Only

Again, beginning with the least complex of the models (no predation, no detrital pool, and a fixed phosphorus yield), the type of solution attainable with no sinking is shown in Figure 22. The predicted algal biomass continues to increase after the initial phosphate depletion due to the continued nutrient loadings previously discussed (see page 27); predicted biomass increases are roughly proportional to net phosphorus loadings. Enough phosphate is present in late July that all three algal reproduction models are capable of matching the algal bloom peak with an algal phosphorus content of 1%. Unfortunately, the zero sinking rate necessary to match the algal peak does not simultaneously match of algal maxima, hypolimnetic oxygen depletion and orthophosphate build-up.

The orthophosphate is depleted to a steady-state level and algae shows a rapid increase during the first two weeks of model predictions. As the streams emptying into Canadarago Lake add more orthophosphate, it is immediately used by the algae to produce more biomass and the ambient orthophosphate level is essentially constant. A steady-state analysis of this system (previously done in algae-only for Cayuga Lake) assumes that at steady state, the algal growth rate is zero, but in this model it is not. While the continuous, high phosphorus loadings from allochthonous

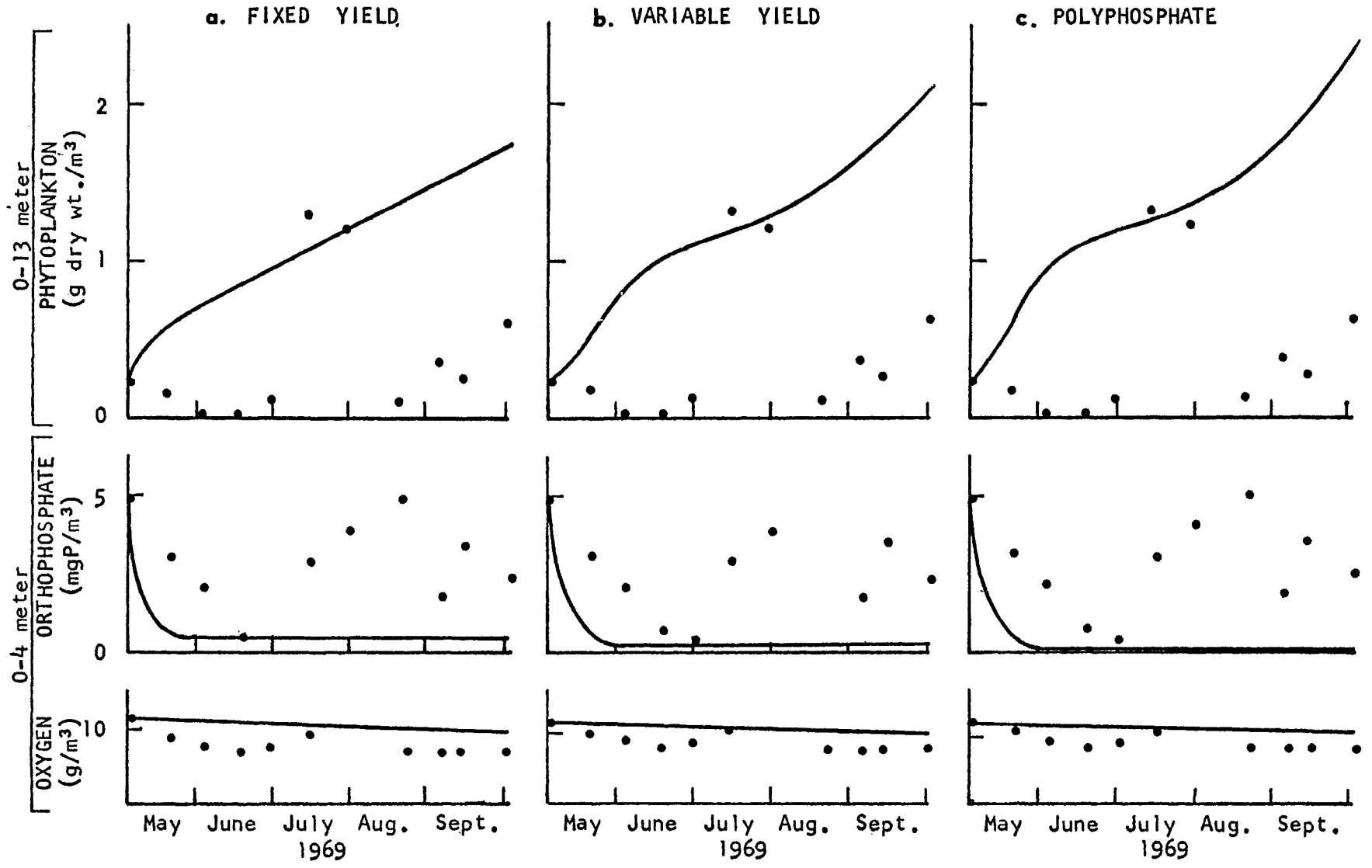

Figure 22. Predictions of algal biomass, orthophosphate, and oxygen concentrations plotted against field data for all three types of phosphate uptake kinetics. No zooplankton or detrital pool. Canadarago 1969.

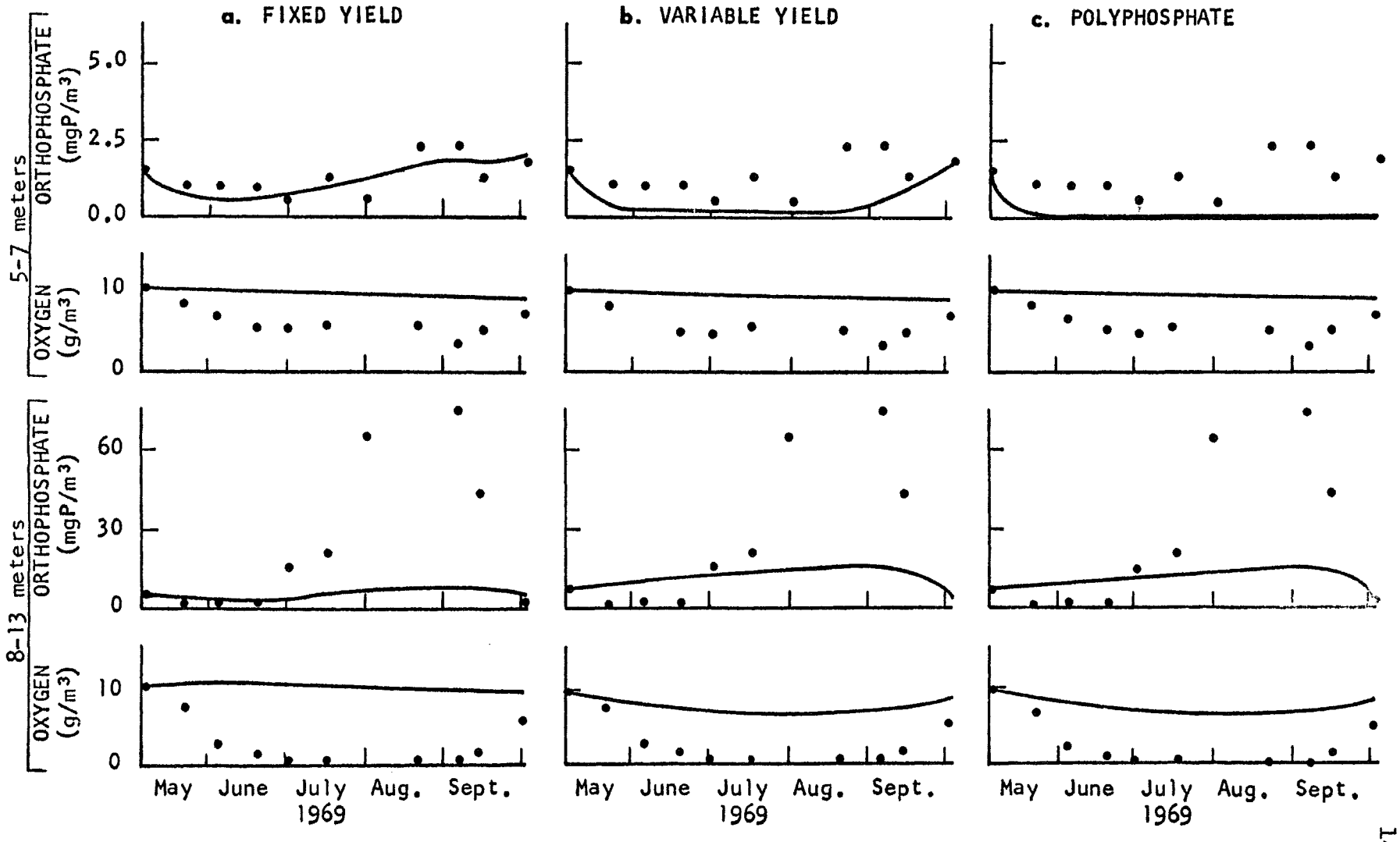

Figure 22. Continued

Table 12. Biological parameter values for the algae only comparisons in Canadarago Lake.

(xxx = not appropriate)

PARAMETER	FIXED YIELD	VARIABLE YIELD	POLYPHOSPHATE
V_x	0	0	0
V_p	xxx	xxx	xxx
V_z	xxx	xxx	xxx
Y_{zx}	0.6	0.6	0.6
K_{bn}	.10	.10	.10
K_{dn}	.25	.25	.25
K_{xn}	.05	.05	.05
K_{zn}	xxx	xxx	xxx
K_{pn}	xxx	xxx	xxx
K_{bd}	.03	.03	.03
$\hat{\mu}_z$	xxx	xxx	xxx
$\hat{\mu}_x$	2.0	1.5	1.5
$\hat{q}$	xxx	.30	.30
r_f	xxx	xxx	.40
r_d	xxx	xxx	.05
K_x	xxx	xxx	xxx
K_c	xxx	.01	.005
K_s	xxx	xxx	.01
K_v	xxx	xxx	.001
K_n	.002	.01	.01
K_o	.10	.10	.10
C_{max}	xxx	.05	.02
V_{max}	xxx	xxx	.07

Table 12 Continued

PARAMETER	FIXED YIELD	VARIABLE YIELD	POLYPHOSPHATE
Y_{nx}	.01	.01	.01
Y_{nz}	xxx	xxx	xxx
Y_{nb}	.01	.01	.01
Y_{np}	xxx	xxx	xxx
Y_{oa}	2.0	2.0	2.0
Y_{oz}	xxx	xxx	xxx
Y_{op}	xxx	xxx	xxx
Y_{ob}	2.0	2.0	2.0
Y_{od}	2.0	2.0	2.0

sources give the solutions a different form than in Cayuga Lake, they still only increase monotonically, without the algae oscillation apparent in the field data. In fact, the previous steady-state analysis still provides useful information for determining relative species concentrations at any time, since the gradual increase in total nutrients is slow compared with the rate at which the system adjusts to the new steady states. The total nutrient analysis differs from Eq. 97, since the combined sink-source terms no longer sum to zero. The remaining total phosphorus sink-source term is:

$$N^n - D^n[(Y_{nx}+C+V)X + N); \qquad (104)$$

where: N^n = time-dependent rate of phosphate addition (mass/vol/time);

D^n = time-dependent dilution rate (per time).

Therefore, the total phosphate is time dependent in this model. Phosphorus is added to and phosphorus and algae are flushed from the system, and algal orthophosphate uptake is equal to net phosphorus addition to the system.

Algae and Detritus

The addition of a detrital pool made little or no difference to model predictions, even when detrital decay rates were as low as 5% per day. The solutions presented in Figure 23 were chosen to demonstrate the effect of sinking algae and detritus on model predictions. The loss due to the

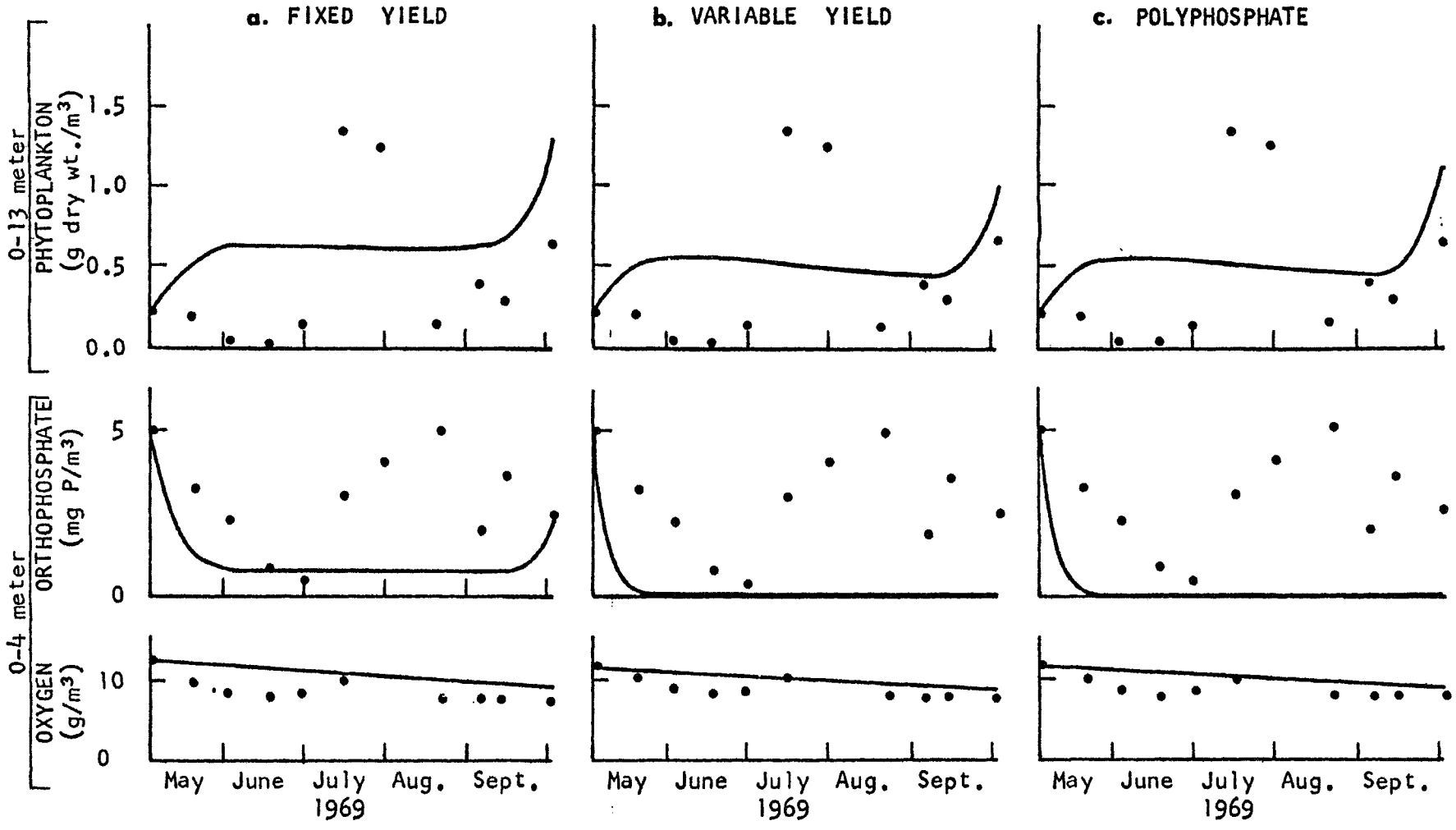

Figure 23. Predictions of algal biomass, orthophosphate, and oxygen concentrations plotted against field data for all three types of phosphate uptake kinetics. Detrital pool and no zooplankton. Canadarago 1969.

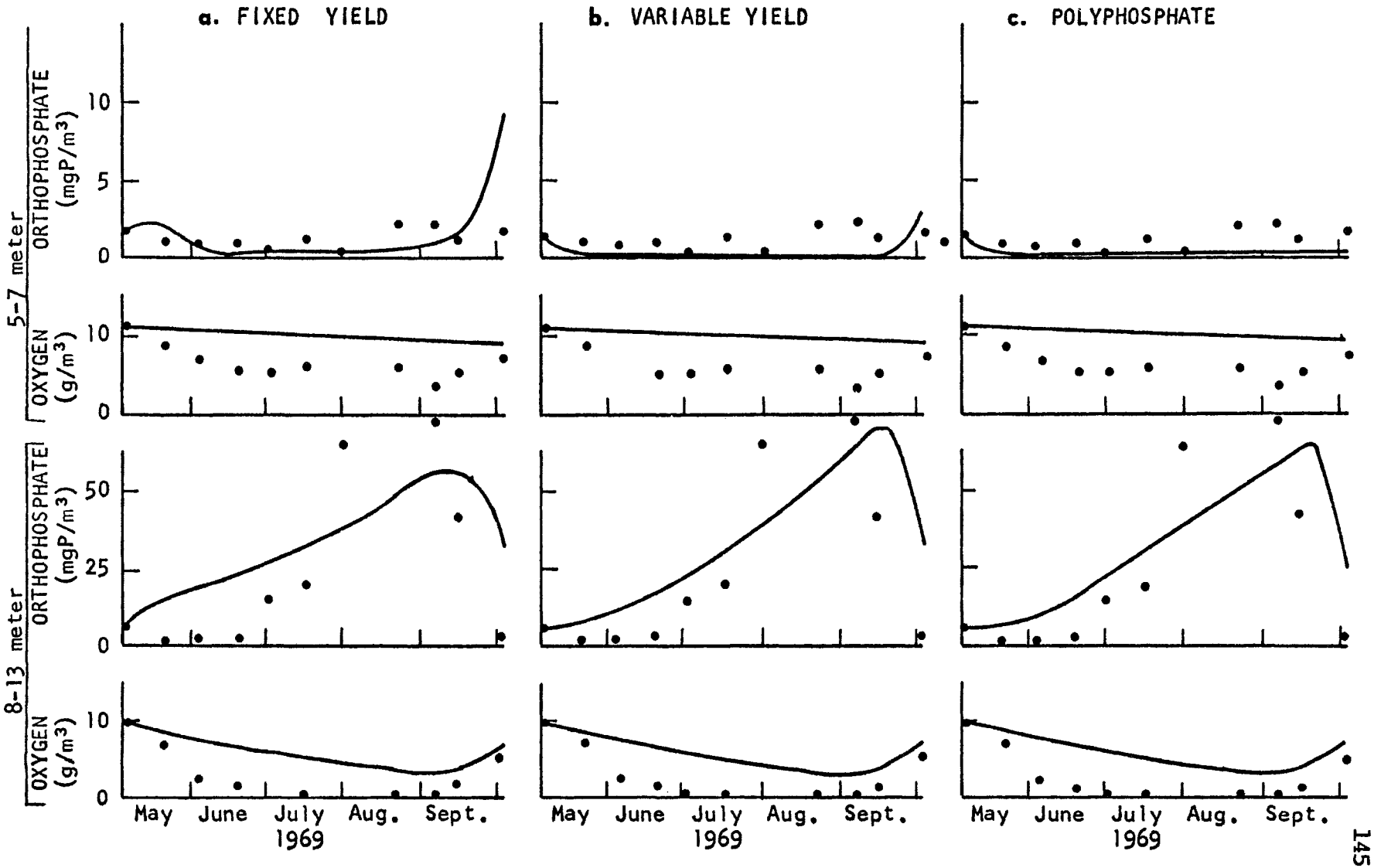

Figure 23 Continued

Table 13. Biological parameter values for the algae plus detritus comparisons in Canadarago Lake.
(xxx = not appropriate)

PARAMETER	FIXED YIELD	VARIABLE YIELD	POLYPHOSPHATE
V_x	.20	.20	.20
V_p	.20	.20	.20
V_z	xxx	xxx	xxx
Y_{zx}	.60	.60	.60
K_{bn}	.10	.10	.10
K_{dn}	.10	.10	.10
K_{xp}	.05	.05	.05
K_{zp}	xxx	xxx	xxx
K_{pn}	.05	.05	.05
K_{bd}	.03	.03	.03
$\hat{\mu}_z$	xxx	xxx	xxx
$\hat{\mu}_x$	1.5	1.5	1.5
$\hat{q}$	xxx	.80	.30
r_f	xxx	xxx	.40
r_d	xxx	xxx	.05
K_x	xxx	xxx	xxx
K_c	xxx	.005	.002
K_s	xxx	xxx	.01
K_v	xxx	xxx	.001
K_n	.002	.01	.01
K_o	.10	.10	.10
C_{max}	xxx	.05	.03
V_{max}	xxx	xxx	.07

Table 13 Continued

PARAMETER	FIXED YIELD	VARIABLE YIELD	POLYPHOSPHATE
Y_{nx}	.01	.01	.01
Y_{nz}	xxx	xxx	xxx
Y_{nb}	.01	.01	.01
Y_{np}	.01	.01	.01
Y_{ox}	2.0	2.0	2.0
Y_{oz}	2.0	2.0	2.0
Y_{ob}	2.0	2.0	2.0
Y_{od}	2.0	2.0	2.0

chosen sinking rate (.2 m/day) was approximately equal to the rate of algal increase due to allochthonous phosphate loadings, which is why the algal solutions show a steady state extending through most of the prediction period. Sinking also allows transport of large amounts of phosphate to the hypolimnion. This is evidenced by the qualitative match of hypolimnetic phosphate data and a significant zone of anoxia developing in lower layers as algae and detrital matter decay. Toward the end of the prediction period, erosion of the thermocline predicts a release of large quantities of trapped phosphate to the euphotic zone. This is why the predicted algal standing crop begins to increase rapidly in mid-September. The growth rate again exceeds losses, as during the initial phosphate depletion. While this approach yields a qualitative match of hypolimnetic activity, it fails to match orthophosphate data in the upper two layers and the algal bloom in July is missed completely.

In these comparisons the structural or fixed component of the total algal phosphorus was set at 1% of the algal dry weight. The variable yield and polyphosphate formulations consequently contained more than 1% phosphorus, even during low growth rate periods. Examination of the hypolimnetic predictions for orthophosphate show that since the variable yield and polyphosphate algae contained more phosphorus than the fixed yield algae, they carried more phosphorus into the hypolimnion, where it is trapped until

overturn begins in early September. The low orthophosphate levels in the 5 to 7 meter average compared to the large levels in the hypolimnetic zone (8 to 13 meters) show the severity of thermal stratification and the lack of turbulent transport in Canadarago Lake. Not until overturn begins in early September are the hypolimnetic nutrients available for growth and is oxygen available for reaeration.

Algae and Zooplankton

Zooplankton data were not available for Canadarago Lake during the period modeled. The only available zooplankton data were for a period after the installation of a new sewage treatment plant which eliminated most of the annual allochthonous phosphorus loading to Canadarago Lake. Estimation of initial zooplankton concentrations were therefore based on volatile suspended solids data given by Hetling et al. (1974). Zooplankton and algae were assumed to be the major constituents of the volatile-suspended solids, so the zooplankton biomass was calculated by subtracting the measured algal biomass from the measured volatile suspended solids.

The verifications for all three algal models are shown in Figure 24. Again, verification centered on attempting to match the algal bloom shown by field data, in magnitude and time of occurrence. This was accomplished by allowing the initial zooplankton to decay, releasing

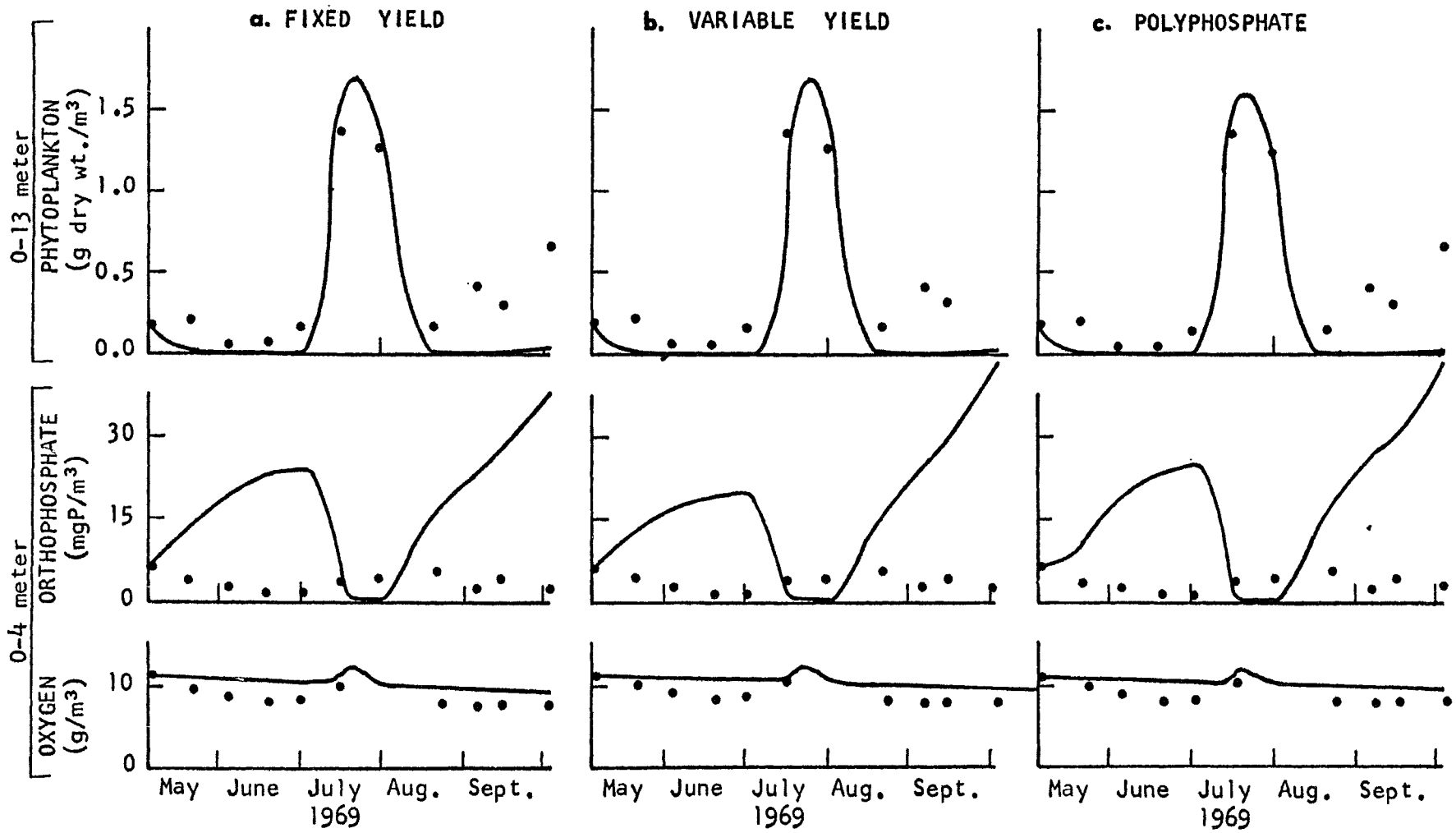

Figure 24. Predictions of algal biomass, orthophosphate, and oxygen concentrations plotted against field data for all three types of phosphate uptake kinetics. Zooplankton and no detrital pool. Canadarago 1969

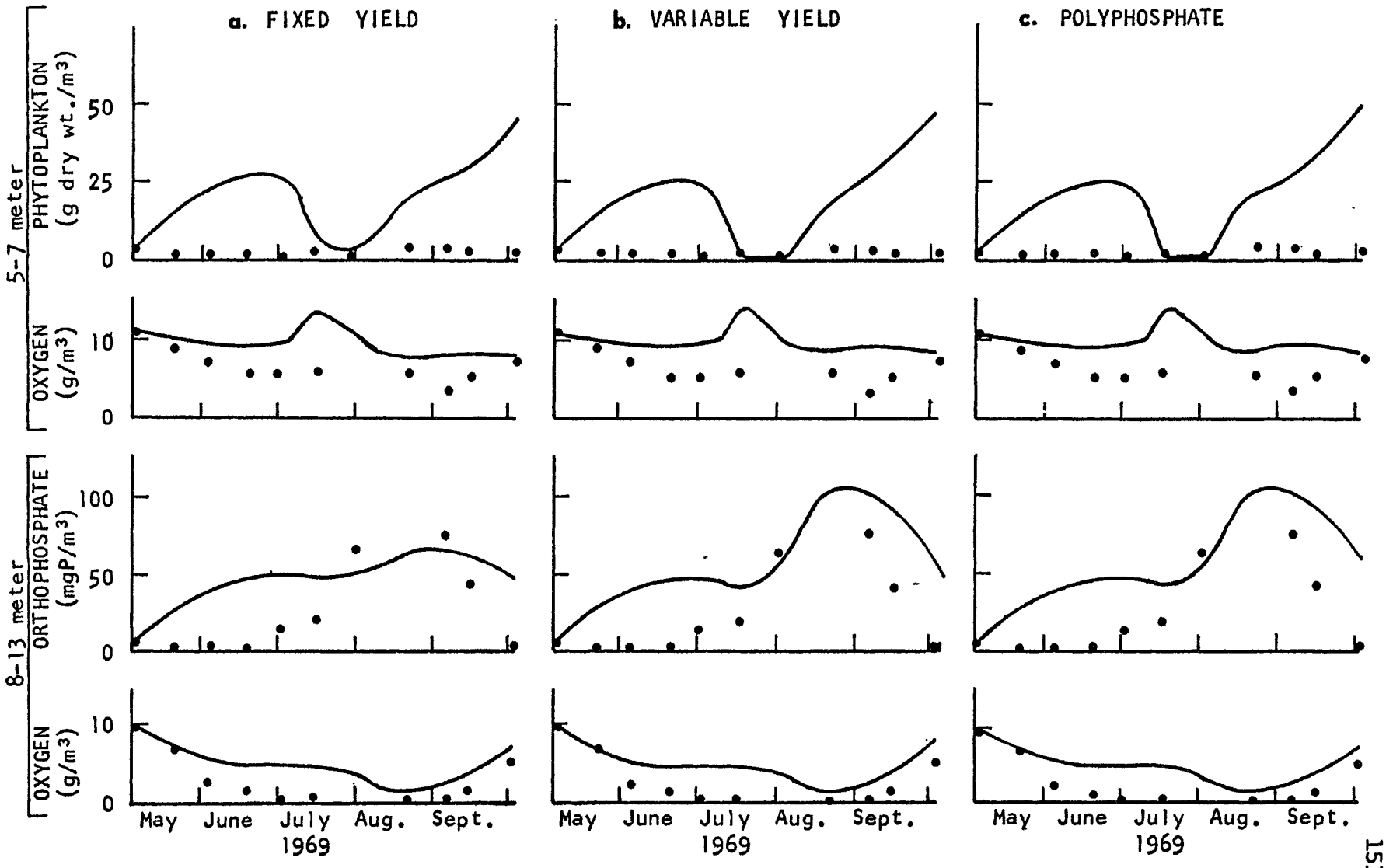

Figure 24. Continued

Table 14. Biological parameter values for the algae plus zooplankton comparisons in Canadarago Lake. (xxx = not appropriate)

PARAMETER	FIXED YIELD	VARIABLE YIELD	POLYPHOSPHATE
V_x	.20	.20	.20
V_p	xxx	xxx	xxx
V_z	.10	.10	.10
Y_{zx}	.60	.60	.60
K_{bn}	.10	.10	.10
K_{dn}	.10	.10	.10
K_{xn}	.05	.05	.05
K_{zn}	.10	.10	.10
K_{pn}	xxx	xxx	xxx
K_{bd}	.03	.03	.03
$\hat{\mu}_z$	.30	.30	.30
$\hat{\mu}_x$	1.5	1.5	1.5
$\hat{q}$	xxx	.80	.30
r_f	xxx	xxx	.40
r_d	xxx	xxx	.05
K_x	.08	.08	.08
K_c	xxx	.005	.002
K_s	xxx	xxx	.01
K_v	xxx	xxx	.001
K_n	.002	.01	.01
K_o	.10	.10	.10
C_{max}	xxx	.05	.03
V_{max}	xxx	xxx	.07

Table 14. Continued

PARAMETER	FIXED YIELD	VARIABLE YIELD	POLYPHOSPHATE
Y_{nx}	.01	.01	.01
Y_{nz}	.03	.03	.03
Y_{nb}	.01	.01	.01
Y_{ox}	2.0	2.0	2.0
Y_{oz}	2.0	2.0	2.0
Y_{op}	xxx	xxx	xxx
Y_{ob}	2.0	2.0	2.0
Y_{od}	2.0	2.0	2.0

orthophosphate. This also reduced the severity of grazing on the algae. The combination of increasing the limiting nutrient and eliminating effective predation produced an environment favorable for the algal bloom regardless which phosphate uptake model was used.

All models seemed incapable of matching both the algal bloom data and the orthophosphate data synoptically in the upper levels. The vertical scale for orthophosphate had to be reduced from previous plots so that the predictions could be presented. The predictions were so large since an orthophosphate increase to over 20 mg P/m^3 was necessary in the upper layers to simulate the bloom even with no predation. Field data show no such increase.

Oscillations of the form needed for an impulse type bloom require a rapidly oscillating system that is initially displaced far enough from equilibrium to produce an oscillation of the bloom's magnitude. Experience obtained after many attempts to match the bloom, showed that increasing zooplankton grazing effectiveness, either by decreasing its Monod half-velocity or increasing the maximum specific zooplankton growth rate, increased the frequency of algal oscillations. Also, any algal growth rate, greater than 1.5 day^{-1}, required zooplankton growth rates, in excess of their maximum literature values, whenever the algal bloom was duplicated.

When zooplankton predation was adjusted to allow the algal impulse type bloom shown in Figure 24, the model did not duplicate the September algal increase after the

large bloom in mid-July. Zooplankton predation was necessarily severe, with sudden increases in zooplankton necessary to deplete the algae as fast as indicated by the field data. The resulting large populations of zooplankton then decayed too slowly to allow an algal recovery as quickly as that shown by field data in mid-August. This might be due to the lack of an upper predator in our theoretical system which would deplete the zooplankton rapidly after their bloom.

The upper layer oxygen data seem to be matched by all three of the algal analogs' predictions, in that the predictions, while high, show an increase in oxygen concentration with the algal bloom. Unfortunately, no oxygen data were reported for the samples taken at the end of July.

Again, comparison of the different algal models shows a difference in phosphate transport to the hypolimnion, although all use the same sinking rate (.2 m/day). The fixed yield model's algae only contain 1% phosphorus as they sink through the thermocline. While the other algal analogs also predict an algal phosphorus content of approximately 1% at the peak of the algal bloom, their phosphorus content increases dramatically as the algae become predator controlled by zooplankton grazing. Consequently, as the algae sink through the thermocline after the algal bloom, the phosphorus content due to the internal pool and polyphosphates, is as high as 3% in the variable yield and polyphosphate analogs.

The hypolimnion of the lake is predicted to be anoxic for most of the summer, but the lower zone average includes some upper oxic nodes which represent comparatively large volumes. Consequently, the weighted average shows anoxia occurring for only a brief period late in August. The oxygen gradient in the hypolimnion is so severe that the field values for oxygen are strongly dependent on sample depth. Since the relationship between the boundary of the lower two averaged zones and the actual sampling depth for the lower zone is not known, the discrepancies between hypolimnetic field data and predictions might be due to the averaging techniques applied to the field data or the discrete predictions.

The predicted release of phosphate to the upper layers at overturn, common to all three of the algal analogs, is not observed in the field data. However, the predicted reaeration of the hypolimnion seems to follow rates shown in field data, at least semiquantitatively.

Algae, Detritus, and Zooplankton

The predictions shown in Figure 25 show essentially the same solutions as those presented in Figure 24, with no detrital pool. The particulates were degraded at 5% per day in all of the verifications shown in Figure 25. This low rate of decay allows an accumulation of large amounts of detrital matter and an accumulation of unavailable phosphorus.

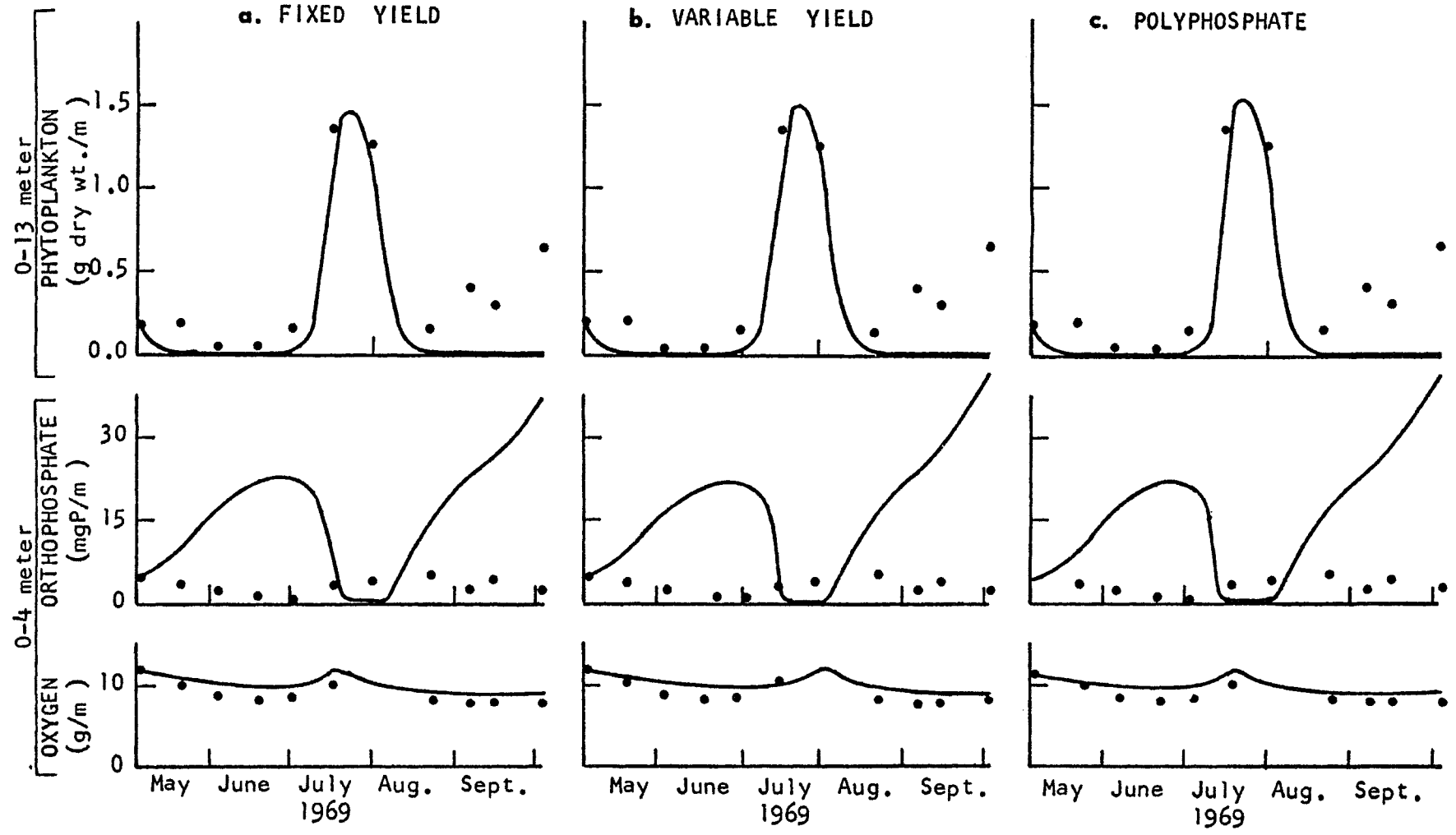

Figure 25. Predictions of algal biomass, orthophosphate, and oxygen concentrations plotted against field data for all three types of phosphate uptake kinetics. Zooplankton and detritus. Canadarago 1969.

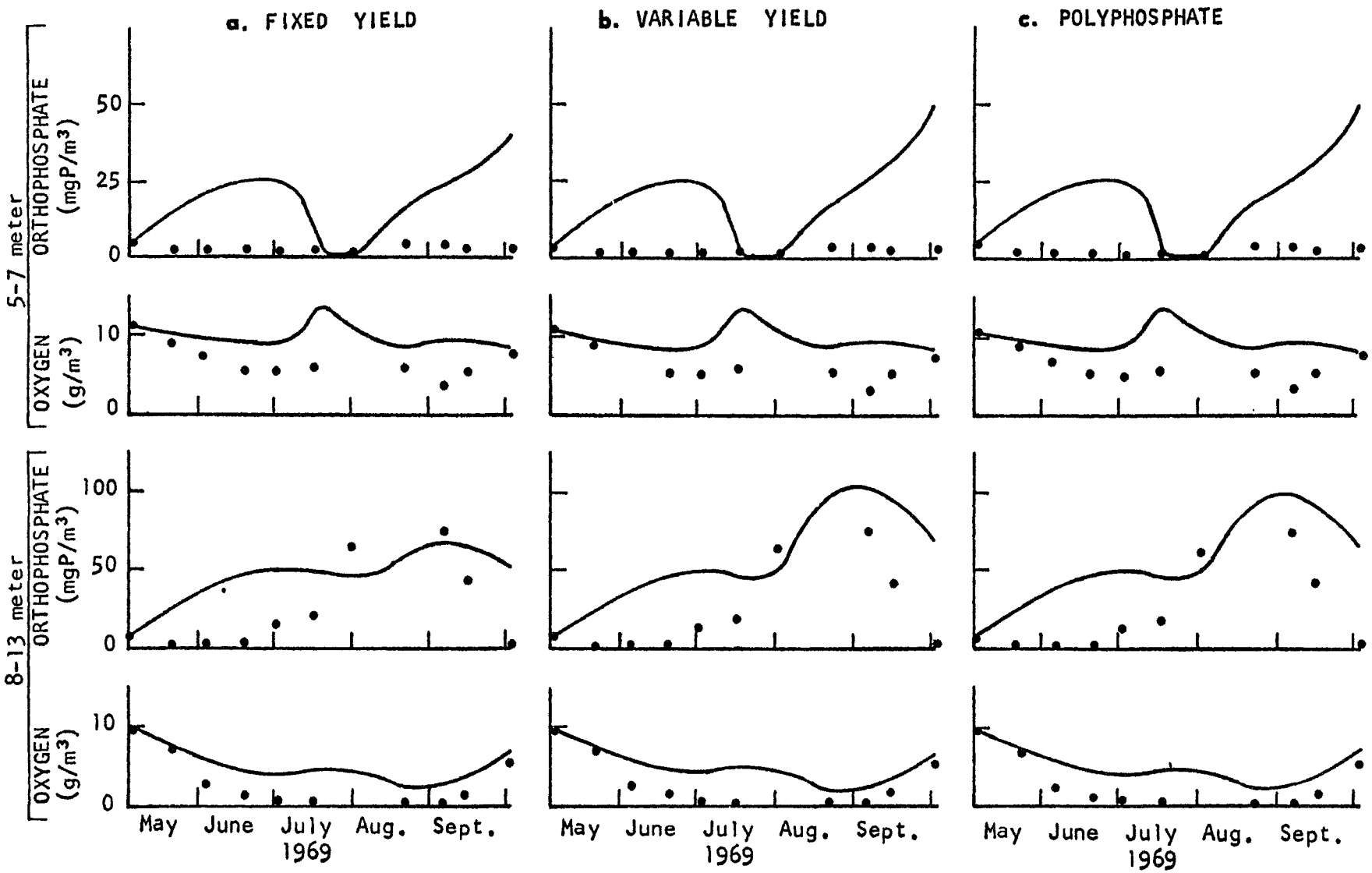

Figure 25. Continued

Table 15. Biological parameter values for the algae, detritus, and zooplankton comparisons in Canadarago Lake.
(xxx = not appropriate)

PARAMETER	FIXED YIELD	VARIABLE YIELD	POLYPHOSPHATE
V_x	.20	.20	.20
V_p	.20	.20	.20
V_z	.10	.10	.10
Y_{zx}	.60	.60	.60
K_{bn}	.10	.10	.10
K_{dn}	.10	.10	.10
K_{xp}	.05	.05	.05
K_{zp}	.10	.10	.10
K_{pn}	.05	.05	.05
K_{bd}	.03	.03	.03
$\hat{\mu}_z$	.30	.30	.30
$\hat{\mu}_x$	1.5	1.5	1.5
$\hat{q}$	xxx	.80	.30
r_f	xxx	xxx	.40
r_d	xxx	xxx	.05
K_x	.08	.08	.08
K_c	xxx	.005	.002
K_s	xxx	xxx	.01
K_v	xxx	xxx	.001
K_n	.002	.01	.01
K_o	.10	.10	.10
C_{max}	xxx	.05	.03
V_{max}	xxx	xxx	.07

Table 15. Continued

PARAMETER	FIXED YIELD	VARIABLE YIELD	POLYPHOSPHATE
Y_{nx}	.01	.01	.01
Y_{nz}	.03	.03	.03
Y_{nb}	.01	.01	.01
Y_{np}	.01	.01	.01
Y_{ox}	2.0	2.0	2.0
Y_{oz}	2.0	2.0	2.0
Y_{op}	2.0	2.0	2.0
Y_{ob}	2.0	2.0	2.0
Y_{od}	2.0	2.0	2.0

The solutions, however, show only a slight decrease in bloom magnitude even though all other parameters have the same values used in the verifications without detritus. Since no second oscillation is predicted in this lake, the damping effect of the particulates is not seen.

None of the analogs are capable of predicting the simultaneous rise in orthophosphate and algae seen in the field data. Just as in Cayuga Lake's second bloom, a large increase in ambient phosphate, not shown in the field data, is necessary to drive the algal bloom. This idea will be expanded in the next chapter.

Chapter VII

DISCUSSION AND CONCLUSIONS

For clarity of discussion, this chapter is divided into three sections: Cayuga Lake verifications, Canadarago Lake verifications including Cayuga's second bloom comparison, and conclusions.

Cayuga Lake Verifications

The transport model's predicted thermal profiles matched the horizontally averaged field temperatures quite well, generally to within 2°C. Edinger's method seems to work in lakes that establish thermoclines below the region where absorption of solar energy is an important heating mechanism. In Cayuga Lake, more than 90% of the energy in the penetrating light is converted to heat within the epilimnion. Since the top 10 meters of Cayuga Lake have relatively high turbulent diffusion coefficients, it makes little difference that in the model heat is added at the surface. The method of using the predicted diffusion coefficients to transport heat and then verifying the predicted thermal profiles against horizontal field averages yields the best available estimate of the turbulent diffusion coefficients in a horizontally averaged formulation. Furthermore, the

accuracy of the results suggests the hydraulic transport aspects of the simulation problem are correctly handled. Therefore, the inadequacies in the biological portion of any total model are easily observed; this was a stated objective of this dissertation. It is interesting that Baca and Arnett (1976) had success in matching field data not achieved by other authors and they also used a well-structured vertical transport model. Although their diffusion coefficients were not verified by transporting heat and comparing their predicted temperatures to observed field temperatures, they did partially duplicate thermal stratification with an empirical exponential function for diffusion coefficients.

Discretizing the upper lake into one-meter nodes and verifying the predicted diffusion coefficients with thermal data yields a far better estimate of algal growth in the epilimnion than any of the reviewed models. Without this fine resolution, other authors were forced to use depth-averaged growth rates which are confounded by non-linear thermal, nutrient, and light intensity dependencies.

All three algal reproduction models were capable of matching both the algal increase and the phosphate depletion preceding the first algal bloom, regardless which ecosystem structure was used. The temperature dependence of zooplankton grazing rates made them ineffective predators in the early spring. This allowed all ecosystem structures, even those containing zooplankton, to behave approximately the

same until mid-May, when the average epilimnion temperature was well above 7°C. Consequently, the tuning procedure used to match each model was the same, resulting in the same values for the parameters describing algal growth.

The choice of parameter values was fixed into a narrow range when the fixed yield algal formulation was compared with field data. The analyses presented in the Cayuga Lake's Simulation section applied very well. The predicted algal peak was always defined by the choice of algal phosphorus content; algal growth and decay rates were always were always determined by the stated bloom verification criteria; and the Monod half-velocity was determined by the extent of phosphorus depletion shown in data. This meant that no freedom was available for parameter choice. The maximum specific algal growth rate, specific algal decay rate and Monod half-velocity constant were fixed at 2.0 day^{-1}, 0.5-.10 day^{-1}, and .01 g P/m^3 respectively.

The variable yield formulation used the same maximum specific growth rate and Monod half velocity, but the internal algal structure allowed a slightly faster specific growth rate ($\hat{\mu} \cdot \bar{f}(I) \cdot \frac{C}{C+K_c}$). This is reflected in the larger decay rate (.15 day^{-1}) necessary to match the field data. The maximum specific phosphate uptake rate was set from 0.3-0.5 gP/g algae/day for all variable yield and polyphosphate model comparisons. This value insured that phosphate uptake would not be growth limiting when ambient

orthophosphate levels were high.

The level of internal, nonstructural phosphorus is controlled by the choice of its maximum allowable value, C_{max} and the Monod half velocity for algal growth, K_c. Comparing Figure 14b with C_{max} = 2% (dry weight basis) and Figure 15b with C_{max} = 7%, the effect of more than tripling C_{max} is seen as only slightly increasing the rate of algal growth approaching the steady state. Even with C_{max} = 7% the value of internal, nonstructural phosphorus never exceeds 2.5%, which is well within literature values. The system solution is much more sensitive to the choice of the Monod half velocity for growth. The initial portion of the solution in Figure 16b shows retarded rates of algal increase similar to those where C_{max} was lowered from 7% to 2%, but this solution was obtained by raising K_c from 0.3% to 0.5%.

In the polyphosphate formulation, K_c ranged from 0.5% to 1.0%. Consequently the value for the specific algal decay rate had to be lowered to the rates used for the fixed yield comparisons (.05 - .10 day^{-1}), whenever the field data were acceptably matched. Simply, reduced algal growth rates require reduced algal decay rates to match the net rate of algal accumulation shown in the field data.

The parameters describing polyphosphate formation and degradation (V_{max}, r_f, K_s, r_d, K_v) were somewhat arbitrarily adjusted to yield a steady-state polyphosphate level of approximately 6%. Once all other parameters were adjusted,

the polyphosphate parameters could take on a wide range of workable values. Therefore, their actual numerical values should not be assumed correct, but their combined contribution yielded a polyphosphate component of algal structure that behaved according to literature descriptions.

The kinetic parameters necessary to maintain the polyphosphate levels at 6% during the slow growth dynamic equilibrium allowed only a very slow degradation of polyphosphates. However, batch culture data in Ketchum (1939) and Porcella et al. (1970) show that algae are not capable of high rates of growth when growing on polyphosphate stores. Thus slow polyphosphate degradation is physically realistic.

The algae-only and algae and detritus ecosystems yielded useful information for adjusting and verifying the ecosystems containing zooplankton, but without zooplankton no oscillations like those shown in the field data could be initiated. The full literature range of every kinetic parameter was tested, and while some groupings caused initial algal overshoots of the steady-state concentration, all attained a dynamic equilibrium, most asymptotically.

On the other hand, in the algae-and-zooplankton ecosystem, whenever zooplankton grazing affected the predictions (compared with similar predictions without zooplankton), oscillations were initiated for other species. These oscillations centered around a gradually increasing algal steady

state value and the oscillations grew in time after the second bloom due to the increasing euphotic zone temperature.

The gross behaviors of the algal reproduction models are the same, so that the kinetic parameters describing zooplankton growth and decay are approximately the same, no matter which algal model is used.

When zooplankton predation is adjusted to match the second algal biomass peak in both magnitude and timing, the algal minimum between blooms and the breadth of the second algal peak (duration of the bloom) are fixed also. All three algal analogs allowed zooplankton adjustment, so that both the algal minimum and second maximum were matched simultaneously. The zooplankton growth and decay rates seemed to control the timing of the second algal bloom while the Monod half velocity for grazing seemed to define the depth of the algal minimum and the height of the second algal peak. This is similar to the function of the corresponding algal rates for defining the first algal bloom and the level of orthophosphate depletion.

The addition of particulate detritus to any of the tested ecosystems tended to dampen the oscillations necessary to match field values. At no time, with any combination of parameter values, could oscillations large enough to obtain a second bloom verification be initiated in a model containing detritus, unless detrital decay rates were so high that

detritus could be neglected as it was in other verifications.

The oxygen variations in Cayuga Lake are not accounted for by any of the twelve models tested. No biological activity included in the models produce or require enough oxygen to make more than a fraction of a gram per cubic meter difference in the ambient oxygen levels.

The discussion of the second algal bloom verification attempts that began at the algal minimum are postponed until the next section, since the only bloom for which we had data in Canadarago Lake was assumed a second bloom.

Canadarago Lake Verifications

The transport analog's thermal predictions in Canadarago Lake fit their respective field temperatures even better than the Cayuga Lake predictions fit their respective field data. This was expected, since the method of introducing heat used in Canadarago Lake more closely duplicates the natural system. This method allows the lake to stratify early, while still heating the upper hypolimnion by direct absorption of solar radiation. Attempts to match the thermal profiles using the surface heating method of Edinger failed to duplicate the upper hypolimnion field data. The temperatures at the bottom nodes are not duplicated well, even by the solar radiant heating method, but they are located where only a small portion of the total lake biological activity takes place. The bottom few nodes

represent two depressions at opposite ends of the lake.

Since the predictive method was again used and the predicted thermal profiles were verified with field data for the modeled period, the best possible estimate of the turbulent diffusion coefficients was again obtained. If the heat input to the lake is structured correctly, and the predicted thermal profiles match field data, the turbulent diffusion coefficients are necessarily correct. The great care used in simulating the turbulent mass transfer within the lake again allowed observation of the biological formulations without the averaging errors that have confounded modeling attempts by other authors.

Both the second bloom comparisons for Cayuga Lake beginning in mid-July and the verification against the Canadarago Lake field data (also assumed a second bloom) begin with average epilimnion temperatures well in excess of 7°C. This means that the determination of the proper values for parameters describing algal growth and decay and zooplankton growth and decay is not as separable as it was for Cayuga Lake's first bloom. Even though the proper set of parameter values was more difficult to identify (required more model solutions), the final workable values were set by narrow limits, like in the Cayuga Lake total summer verifications.

Second bloom verification attempts in both lakes with algal growth rates of 2.0 day^{-1} required zooplankton

growth rates outside of quoted literature ranges. Also, the produced algal bloom was of short duration compared with that shown in the algal field data. The growth rate was then successively lowered and the zooplankton was retuned, to produce the bloom at the end of July in Canadarago Lake and early August in Cayuga Lake for each algal growth rate. As the algal growth rate was decreased, the required zooplankton growth rate returned to its literature range and the algal bloom duration increased (the algal peak became broader). The best fit to algal peak breadth was obtained with a maximum specific algal growth rate of 1.5 day^{-1}, and a correspondingly low specific algal decay rate of .05 day^{-1}.

During the initial prediction period, algal concentrations were so low that zooplankton only decayed; zooplankton growth was negligible compared with the zooplankton standing crop. The zooplankton decay rate was the parameter that timed this second algal bloom. Zooplankton had to decay to levels where predation on the algal community was negligible and algal growth could overcome losses to predation, decay, and sinking. The value of the specific zooplankton decay rate in Cayuga Lake that duplicated the second algal bloom development was twice as high (.18-.20 day) as it was in Canadarago Lake (.10 day), suggesting heavy upper level predation in Cayuga Lake not seen in Canadarago Lake.

Simple algal decay does not reduce algal populations at the rates calculated from field data. Therefore, the maximum specific zooplankton growth rate (μ_z) and its Monod half velocity (K_x) were chosen such that the zooplankton population would replenish itself quickly, and deplete the algal bloom as indicated by the field data.

When the fixed yield model matched the second algal bloom data in either lake, the total algal phosphorus content had a value of 1%. While the total internal phosphorus reached levels as high as 3% in the variable yield model during times of zooplankton predation, when phosphorus was not limiting, the bloom peak algal phosphorus content was approximately 1% of the algae's dry weight. The nonstructural cellular phosphorus was approximately .1% of the algae's dry weight at the peak of the algal bloom, and the structural phosphorus was again held at 1%.

The polyphosphate model allowed the algal phosphorus content to go over 6%, but again, at the peak of the algal bloom, when phosphorus is limiting, the internal soluble phosphorus and polyphosphate fractions became small, and the total algal phosphorus was approximately 1%.

While the lack of a quantitative match for hypolimnetic oxygen data might be explained by the averaging difficulties discussed earlier, the early phosphorus build-up cannot. The final magnitude of phosphorus released in the hypolimnion is approximately right but the field data

show the release actually takes place simultaneously with the development of anoxia in the lower zone, and not before as in the model predictions. It seems that the benthic formulation used in the analogs is not complete.

Again in Canadarago Lake some of the definition in the upper level oxygen profiles observed in the field data is not duplicated. Also the predictions overestimate the oxygen data just as in Cayuga Lake. Since reaeration of the upper layers of the lake's epilimnions occurs very rapidly (as evidenced by the rapid dissipation of the oxygen released during the bloom in Canadarago Lake), it is difficult to assume that the variability in oxygen concentration is due to a chemical uptake.

Conclusions

In all tested models, for all comparisons, there was only one set of kinetic parameters describing the gross behavior of the modeled species that would duplicate the algal blooms depicted by field data. Some freedom existed for the choice of the internal parameter values describing polyphosphate formation, but not in their ensemble form. During Cayuga Lake's first bloom, the polyphosphates needed to contribute 6% of the algal dry weight at the algal peak, while for both second bloom verifications polyphosphates had to be depleted to almost zero during the algal peak. These requirements placed some restraints on the combined

coefficients, but not on each individual parameter's value. The restraints resulted because algal blooms could not be terminated by zooplankton grazing in any of the tested models when phosphorus was not limiting. Therefore blooms were always controlled by a decreased algal growth rate resulting from phosphorus limitation. The total phosphorus conservation equation (Eq. 96) then set the value of the total algal phosphorus content in all tests.

The frequency of the algal oscillations is controlled by the zooplankton growth rate and Monod half velocity for zooplankton growth. Increasing zooplankton growth rates increase the frequency of algal blooms, and decreasing the Monod half velocity increases the amplitude and frequency of the oscillations.

The breadth of algal blooms is controlled by a combination of algal and zooplankton parameters. In general, for a given frequency of algal oscillation, lowering the algal growth rate and adjusting the zooplankton to obtain the desired frequency results in broadening the algal peak. This means that a larger crop of algae persists for a longer time. Consequently, slower algal systems, for a given oscillation frequency, are capable of more total primary production because of their persistence.

It is interesting to note that not only do all of the necessary parameter values fall within the range of laboratory and <u>in situ</u> values (Table 1), but they also

closely agree with those found to be necessary to match field data by other authors. For instance, Di Toro (1971), in his Mossdale verification, used an algal growth rate of 2.0 day^{-1}, an algal decay rate of .10 day^{-1}, and a zooplankton decay rate of .075 day^{-1}. Bierman (1976) used a zooplankton with a growth rate of .3 day and a decay rate of .10 day^{-1}. While portions of some models were structured in different forms by other authors, resulting in noncomparable parameters, those parameters that are comparable (and those that had their values published), agree very well with the values found to be necessary for data verification in this dissertation.

Since most temperate lakes exhibit at least two algal blooms during the summer months (Pennak, 1946; Hutchensen, 1975), any model trying to simulate summer algal populations must be capable of oscillating solutions for algae. This has been shown impossible with any model that does not include a herbivorous zooplankton. Therefore, besides the algae, oxygen, phosphorus, benthos, and dissolved organic matter mass balances, zooplankton is a necessary model component in any model of temperate lake primary productivity. Also, the dependence of any species' growth rate on its respective food source cannot be formulated as a linear, Lotka-Volterra dependence, since this method yields non-oscillating algal solutions like the models not containing zooplankton. Lotka-Volterra formulations are only

useful in dilute (very oligotrophic) non-oscillating systems.

The inclusion of detritus in any model never improved the solution even though decay rates were set as low as .05 day^{-1}. This rate implied a steady-state detrital phosphorus detention time of 20 days. In fact, in models containing zooplankton, the effect of adding detritus was to damp the needed oscillations. Therefore, particulate detritus was identified as a non-necessary component of a model for primary production.

While the resolution of the internal algal phosphorus into its various components may provide a way of modeling multispecies competition, since phosphorus storage is thought to endow a competitive advantage, it does little to help model trophic level algal growth. The behavior of the algal models was almost identical regardless which algal formulation was used. However, in Canadarago Lake, the variable yield and polyphosphate models did transport much more phosphorus to the hypolimnion. Identification of the most correct formulation would require field data taken at least on a daily basis during bloom development, including algal phosphorus contents. Then, statistical analyses of the predictions and field data may identify a "best" model.

Including zooplankton, the minimal model structure requires solution of five mass balance equations when the fixed yield algal formulation is used. The variable yield formulation requires six species and the polyphosphate formulation requires seven. Roughly, this means that if time

and depth spacings remain constant, the polyphosphate formulation requires 7/5 the computer time required to solve the fixed yield analog. Also, the maximum time step possible in the fixed yield model is 3-5 times larger than that possible in the polyphosphate model. This roughly translates into 3-5 times the required iterations and computer time needed to solve the polyphosphate model when compared with the fixed yield formulation. Since the algal models are indistinguishable at the level of prediction accuracy necessary to answer most engineering questions, the fixed yield model is the best choice available from a standpoint of model accuracy and economic model solution.

The benthic model employed in this comparison was not capable of predicting the large phosphorus release at the onset of anaerobic conditions shown in field data for Canadarago Lake and observed in other lakes. While in long-term models this will be a problem, it was not in the Canadarago Lake comparisons since severe stratification kept most of the phosphorus trapped below the euphotic zone until after anoxia. Also, the severe stratification observed in Canadarago Lake and the large amount of phosphorus unavailable for algal growth that was trapped in the hypolimnion show the necessity of accurately modeling thermal stratification. A complete mix reactor would not have allowed this phosphorus storage.

No model was capable of predicting the second algal bloom in either lake while matching the synoptic increase

in the ambient orthophosphate concentrations seen in field data. The orthophsophate build-up necessary to stimulate the second bloom was also not shown in field data. Since all current methods of simulating phosphorus uptake were tested, orthophosphate must not be directly limiting to the second bloom algae. Possibly an algal species not present in the first bloom and capable of utilizing polyphosphate byproducts of the first bloom (Lin, 1977) became dominant during the second bloom. Also, some algal species have bacteria incorporated in their gelatinous sheath that may degrade complex phosphates and make orthophosphate available for growth. Since the model was based on phosphorus and the algae could be made to match both peak algal concentrations in Cayuga Lake with the same set of parameters, phosphorus seems limiting. This may be the case, but not in the ortho form.

Summary

The minimal biological structure necessary to match the early spring bloom and consequent orthophosphate depletion in thermally stratified lakes has been identified: 1) The algae can be modelled as a fixed yield type with constant internal phosphorus levels; 2) zooplankton predation must be included to insure oscillating solutions like those in nature are acheived; 3) the dependence of one trophic level's growth rate upon its food source must be modelled as a Monod

APPENDIX A

Cayuga Lake Field Data

Table 16
Horizontally Averaged Temperature Data °C *

SAMPLING DATE	DEPTH (m) 0	2	5	10	20	50
3/28	4.5	4.5	4.5	4.5	4.5	4.5
3/31	8.0	6.4	5.2	4.6	5.1	
5/16	7.4	7.3	7.1	6.7	6.2	
6/5	12.1	11.3	9.8	7.7	6.6	
6/12	18.0	16.3	14.9	10.2	7.5	5.8
7/3	20.4	20.6	19.4	16.7	9.7	6.6
7/12	22.3	22.3	22.3	17.5	12.7	6.5
7/17	21.2	21.0	19.7	18.0	11.5	6.5
7/24	22.3	23.2	21.9	19.6	10.1	5.1
8/2	22.3	22.2	22.0	20.4	11.0	5.1
8/22	21.8	21.8	21.9	21.5	11.3	5.0
8/30	23.4	22.2	22.7	21.4	11.3	5.2

*Peterson, personal communication (1976)

Table 17

Horizontally and vertically averaged algae, orthophosphate, and oxygen data representing a zone from 1.0-7.5 meters.*

SAMPLING DATE	PHYTOPLANKTON (g dry wt./m^3)	ORTHOPHOSPHATE (mgP/m^3)	OXYGEN (g/m^3)
3/31	.024	16.4	
4/27	.089	8.7	12.5
4/29	.083	4.3	12.8
5/16	.186	4.0	12.6
6/5	.166	1.8	13.0
6/12	.213	0.4	12.4
7/3	.098	1.0	10.5
7/12	.102	0.2	9.6
7/17	.089	1.4	9.2
7/18		0.5	10.2
7/24	.120	0.3	10.7
8/2	.132	2.5	10.1
8/7	.191	2.1	10.2
8/16	.184	3.3	8.4
8/22	.144	0.0	8.6
8/30	.105	0.7	9.0

*Peterson, personal communication (1976)

APPENDIX B

Canadarago Lake Field Data

Table 18
Horizontally Averaged Temperatures Data °C*

SAMPLING DATE	DEPTH (m) 0.5	1.0	2.0	3.0	4.0	5.0	6.0	7.0	8.0	9.0	10.0	11.0	12.0
5/7	11.3	11.2	11.1	11.0	10.8	10.8	10.2	10.1	9.6	9.1	8.7	8.5	
5/22	15.4	15.1	14.9	14.7	14.5	14.0	13.6	13.1	12.6	12.2	12.0	11.2	11.1
6/5	17.9	17.8	17.7	17.5	17.3	16.9	16.4	15.7	14.1	12.8	12.2	11.9	11.5
6/19	19.8	19.6	19.6	19.4	19.0	18.7	17.9	16.8	15.3	13.5	12.8	12.4	12.1
7/2	22.2	22.1	22.0	21.8	21.7	21.3	20.4	18.2	16.6	15.3	14.2	13.2	12.7
7/17	24.7	24.5	24.2	23.8	23.3	22.3	21.5	21.1	17.6	15.3	14.0	13.1	
7/31	23.2	23.1	22.9	22.6	22.5	22.3	22.2	21.2	17.7	14.8	13.6	12.9	12.9
8/21	22.4	22.5	22.4	22.4	22.3	22.2	22.0	21.5	20.5	17.9	15.6	14.0	13.4
9/6	21.7	21.6	21.6	21.5	21.4	21.2	21.1	20.8	19.9	19.0	17.5	15.8	14.9
9/16	19.7	19.7	19.7	19.7	19.7	19.7	19.6	19.6	19.6	18.7	16.6	15.0	
10/2	16.6	16.6	16.5	16.4	16.4	16.3	16.2	16.2	16.1	16.1	16.1	15.9	15.8

*Hetling, Harr, Fuhs, and Allen (1969)

Table 19

Horizontally and vertically averaged orthophosphate and oxygen data, given in three depth zones.*

SAMPLING DATE	0-4.5 meter ORTHOPHOSPHATE (mgP/m^3)	0-4.5 meter OXYGEN (g/m^3)	4.5-THERMOCLINE ORTHOPHOSPHATE (mgP/m^3)	4.5-THERMOCLINE OXYGEN (g/m^3)	THERMOCLINE- 12.6 meter ORTHOPHOSPHATE (mgP/m^3)	THERMOCLINE- 12.6 meter OXYGEN (g/m^3)
5/7	5.0	11.6	1.6	10.2	5.8	9.6
5/22	3.1	10.0	1.1	9.2	0.7	7.2
6/5	2.3	8.8	0.9	7.0	3.7	2.5
6/19	1.0	8.0	1.2	5.3	2.1	1.4
7/2	0.5	8.7	0.5	5.5	16.4	0.8
7/17	3.1	9.9	1.2	5.9	20.0	0.2
7/31	4.1		0.5		66.6	
8/21	4.9	7.9	2.3	5.8		0.2
9/6	1.8	7.7	2.2	3.2	76.0	0
9/16	3.7	7.8	1.4	5.2	43,6	1.3
10/2	2.6	7.8	1.7	6.7	3.6	5.5

*Hetling, Harr, Fuhs, and Allen (1969)

Table 20
Total lake average phytoplankton concentration.*

SAMPLING DATE	PHYTOPLANKTON (g dry wt./m^3)
5/7	.21
5/22	.21
6/5	.03
6/19	.05
7/2	.15
7/17	1.34
7/31	1.23
8/21	.17
9/6	.41
9/16	.32
10/2	.65

*Hetling, Harr, Fuhs, and Allen (1969)

APPENDIX C

Equations

ALGAL EQUATIONS

Fixed Yield

Algae Only:

$$\frac{\partial X}{\partial t} = \frac{1}{A}\frac{\partial}{\partial z}(KA\frac{\partial X}{\partial z}) - \frac{1}{A}\frac{\partial}{\partial z}(V_x AX) + \frac{O}{O+K_o}[\hat{\mu}_x \bar{f}(I)\ \frac{N}{N+K_n} X - K_{xn}X]$$

$$- \frac{V_x}{A}\frac{\partial A}{\partial z} X$$

Algae and Detritus:

$$\frac{\partial X}{\partial t} = \frac{1}{A}\frac{\partial}{\partial z}(KA\frac{\partial X}{\partial z}) - \frac{1}{A}\frac{\partial}{\partial z}(V_x AX) + \frac{O}{O+K_o}[\hat{\mu}_x \bar{f}(I)\ \frac{N}{N+K_n} X - K_{xp}X$$

$$- \frac{V_x}{A}\frac{\partial A}{\partial z} X$$

Algae and Zooplankton:

$$\frac{\partial X}{\partial t} = \frac{1}{A}\frac{\partial}{\partial z}(KA\frac{\partial X}{\partial z}) - \frac{1}{A}\frac{\partial}{\partial z}(V_x AX) + \frac{O}{O+K_o}[\hat{\mu}_x \bar{f}(I)\ \frac{N}{N+K_n} X$$

$$- K_{xn} X - \frac{\hat{\mu} z}{Y_{zx}}\frac{X}{X+K_x} Z] - \frac{V_x}{A}\frac{\partial A}{\partial z} X$$

Algae, Detritus, and Zooplankton:

$$\frac{\partial X}{\partial t} = \frac{1}{A}\frac{\partial}{\partial z}(KA\frac{\partial X}{\partial z}) - \frac{1}{A}\frac{\partial}{\partial z}(V_x AX) + \frac{O}{O+K_o}[\hat{\mu}_x \bar{f}(I)\ \frac{N}{N+K_n} X$$

$$- K_{xp}X - \frac{\hat{\mu}_z}{Y_{zx}}\frac{X}{X+K_x} Z] - \frac{V_x}{A}\frac{\partial A}{\partial z} X$$

Variable Yield and Polyphosphate

Algae Only:

$$\frac{\partial X}{\partial t} = \frac{1}{A}\frac{\partial}{\partial z}\left(KA\frac{\partial X}{\partial z}\right) - \frac{1}{A}\frac{\partial}{\partial z}\left(V_x AX\right) + \frac{O}{O+K_o}\left[\hat{\mu}_x \bar{f}(I)\frac{C}{C+K_c}X - K_{xn}X\right] - \frac{V_x}{A}\frac{\partial A}{\partial z}X$$

Algae and Detritus:

$$\frac{\partial X}{\partial t} = \frac{1}{A}\frac{\partial}{\partial z}\left(KA\frac{\partial X}{\partial z}\right) - \frac{1}{A}\frac{\partial}{\partial z}\left(V_x AX\right) + \frac{O}{O+K_o}\left[\hat{\mu}_x \bar{f}(I)\frac{C}{C+K_c}X - K_{xp}X\right] - \frac{V_x}{A}\frac{\partial A}{\partial z}X$$

Algae and Zooplankton:

$$\frac{\partial X}{\partial t} = \frac{1}{A}\frac{\partial}{\partial z}\left(KA\frac{\partial X}{\partial z}\right) - \frac{1}{A}\frac{\partial}{\partial z}\left(V_x AX\right) + \frac{O}{O+K_o}\left[\hat{\mu}_x \bar{f}(I)\frac{C}{C+K_c}X - K_{xn}X - \frac{\hat{\mu}_z}{Y_{zx}}\frac{X}{X+K_x}Z\right] - \frac{V_x}{A}\frac{\partial A}{\partial z}X$$

Algae, Detritus, and Zooplankton:

$$\frac{\partial X}{\partial t} = \frac{1}{A}\frac{\partial}{\partial z}\left(KA\frac{\partial X}{\partial z}\right) - \frac{1}{A}\frac{\partial}{\partial z}\left(V_x AX\right) + \frac{O}{O+K_o}\left[\hat{\mu}_x \bar{f}(I)\frac{C}{C+K_c}X - K_{xp}X - \frac{\hat{\mu}_z}{Y_{zx}}\frac{X}{X+K_x}Z\right] - \frac{V_x}{A}\frac{\partial A}{\partial z}X$$

ZOOPLANKTON EQUATIONS

Fixed Yield, Variable Yield, and Polyphosphates

Algae and Zooplankton:

$$\frac{\partial Z}{\partial t} = \frac{1}{A}\frac{\partial}{\partial z}\left(KA\frac{\partial Z}{\partial z}\right) - \frac{1}{A}\frac{\partial}{\partial z}\left(V_z AX\right) + \frac{O}{O+K_o}\left[\hat{\mu}_z \frac{X}{X+K_x} Z - K_{zn} Z\right] - \frac{V_z}{A}\frac{\partial A}{\partial z} Z$$

Algae, Detritus, and Zooplankton:

$$\frac{\partial Z}{\partial t} = \frac{1}{A}\frac{\partial}{\partial z}\left(KA\frac{\partial Z}{\partial z}\right) - \frac{1}{A}\frac{\partial}{\partial z}\left(V_z AX\right) + \frac{O}{O+K_o}\left[\hat{\mu}_z \frac{X}{X+K_x} Z - K_{zp} Z\right] - \frac{V_z}{A}\frac{\partial A}{\partial z} Z$$

ORTHOPHOSPHATE EQUATIONS

Field Yield

Algae Only:

$$\frac{\partial N}{\partial t} = \frac{1}{A}\frac{\partial}{\partial z}\left(KA\frac{\partial N}{\partial z}\right) + \frac{O}{O+K_o}\left[-Y_{nx}\hat{\mu}_x \bar{f}(I) \frac{N}{N+K_n} X + Y_{nx} K_{xn} X + Y_{nb} K_{bn} B\right] + \left(Y_{nx}-Y_{nb}\right)\frac{V_x}{A}\frac{\partial A}{\partial z} X + \frac{K_o}{K_o+O} Y_{nb} K_{bd} B$$

Algae and Detritus:

$$\frac{\partial N}{\partial t} = \frac{1}{A}\frac{\partial}{\partial z}\left(KA\frac{\partial N}{\partial z}\right) + \frac{O}{O+K_o}\left[-Y_{nx}\hat{\mu}_x\bar{f}(I)\frac{N}{N+K_n}X + Y_{np}K_{pn}\cdot P\right.$$

$$\left. + Y_{nb}K_{bn}B + (Y_{nx}-Y_{np})K_{xp}X\right] + (Y_{nx}-Y_{nb})\frac{V_x}{A}\frac{\partial A}{\partial z}X$$

$$+ (Y_{np}-Y_{nb})\frac{V_p}{A}\frac{\partial A}{\partial z}P + \frac{K_o}{O+K_o}Y_{nb}\cdot K_{bd}\cdot B$$

Algae and Zooplankton:

$$\frac{\partial N}{\partial t} = \frac{1}{A}\frac{\partial}{\partial z}\left(KA\frac{\partial N}{\partial z}\right) + \frac{O}{O+K_o}\left[-Y_{nx}\hat{\mu}_x\bar{f}(I)\frac{N}{N+K_n}X + Y_{nx}K_{xn}X\right.$$

$$\left. + Y_{nb}K_{bn}B + Y_{nz}K_{zn}Z + Y_{nx}\left(\frac{1}{Y_{zx}} - 1\right)\hat{\mu}_z\frac{X}{X+K_x}Z\right.$$

$$\left. + (Y_{nx}-Y_{nz})\hat{\mu}_z\frac{X}{X+K_x}Z\right] + (Y_{nx}-Y_{nb})\frac{V_x}{A}\frac{\partial A}{\partial z}X$$

$$+ (Y_{nz}-Y_{nb})\frac{V_z}{A}\frac{\partial A}{\partial z}Z + \frac{K_o}{K_o+O}Y_{nb}K_{bd}B$$

Algae, Detritus, and Zooplankton:

$$\frac{\partial N}{\partial t} = \frac{1}{A}\frac{\partial}{\partial z}\left(KA\frac{\partial N}{\partial z}\right) + \frac{O}{O+K_o}\left[-Y_{nx}\hat{\mu}_x\bar{f}(I)\frac{N}{N+K_n}X + Y_{np}K_{pn}P\right.$$

$$\left. + Y_{nb}K_{bn}B + (Y_{nx}-Y_{np})K_{xp}X + (Y_{nz}-Y_{np})K_{zp}Z\right.$$

$$\left. + Y_{nx}\left(\frac{1}{Y_{zx}} - 1\right)\hat{\mu}_z\frac{X}{X+K_x}Z + (Y_{nx}-Y_{nz})\hat{\mu}_z\frac{X}{X+K_x}Z\right]$$

$$+ (Y_{nx}-Y_{nb})\frac{V_x}{A}\frac{\partial A}{\partial z}X + (Y_{nz}-Y_{nb})\frac{V_z}{A}\frac{\partial A}{\partial z}Z$$

$$+ (Y_{np}-Y_{nb})\frac{V_p}{A}\frac{\partial A}{\partial z}P + \frac{K_o}{K_o+O}Y_{nb}\cdot K_{bd}\cdot B$$

Variable Yield

Algae Only:

$$\frac{\partial N}{\partial t} = \frac{1}{A}\frac{\partial}{\partial z}\left(KA\frac{\partial N}{\partial z}\right) + \frac{O}{O+K_o}\left[-\hat{q}\bar{f}(I)\frac{N}{N+K_n}\frac{C_{max}-C}{C_{max}}X + (Y_{nx}+C)K_{xn}X\right.$$

$$\left. + Y_{nb}\cdot K_{bn}\cdot B\right] + (Y_{nx}+C-Y_{nb})\frac{V_x}{A}\frac{\partial A}{\partial z}X + \frac{K_o}{K_o+O}Y_{nb}K_{bd}B$$

Algae and Detritus:

$$\frac{\partial N}{\partial t} = \frac{1}{A}\frac{\partial}{\partial z}\left(KA\frac{\partial N}{\partial z}\right) + \frac{O}{O+K_o}\left[-\hat{q}\bar{f}(I)\frac{N}{N+K_n}\frac{C_{max}-C}{C_{max}}X + Y_{np}K_{pn}P\right.$$

$$\left. + Y_{nb}K_{bn}B + (Y_{nx}+C-Y_{np})K_{xp}X\right] + (Y_{nx}+C-Y_{nb})\frac{V_x}{A}\frac{\partial A}{\partial z}X$$

$$+ (Y_{np}-Y_{nb})\frac{V_p}{A}\frac{\partial A}{\partial z}P + \frac{K_o}{K_o+O}Y_{nb}\cdot K_{bd}\cdot B$$

Algae and Zooplankton:

$$\frac{\partial N}{\partial t} = \frac{1}{A}\frac{\partial}{\partial z}\left(KA\frac{\partial N}{\partial z}\right) + \frac{O}{O+K_o}\left[-\hat{q}\bar{f}(I)\frac{N}{N+K_n}\frac{C_{max}-C}{C_{max}}X + (Y_{nx}+C)K_{xn}X\right.$$

$$\left. + Y_{nb}K_{bn}B + Y_{nz}K_{zn}Z + (Y_{nx}+C)\left(\frac{1}{Y_{zx}} - 1\right)\hat{\mu}_z\frac{X}{X+K_x}Z\right.$$

$$\left. + (Y_{nx}+C-Y_{nz})\hat{\mu}_z\frac{X}{X+K_x}Z\right] + (Y_{nx}+C-Y_{nb})\frac{V_x}{A}\frac{\partial A}{\partial z}X$$

$$+ (Y_{nz}-Y_{nb})\frac{V_z}{A}\frac{\partial A}{\partial z}Z + \frac{K_o}{K_o+O}Y_{nb}K_{bd}B$$

Algae, Zooplankton, and Detritus:

$$\frac{\partial N}{\partial t} = \frac{1}{A}\frac{\partial}{\partial z}\left(KA\frac{\partial N}{\partial z}\right) + \frac{O}{O+K_o}\left[-\hat{q}\bar{f}(I)\frac{N}{N+K_n}\frac{C_{max}-C}{C_{max}}X + Y_{np}K_{pn}P\right.$$

$$+ Y_{nb}K_{bn}B + (Y_{nx}+C-Y_{np})K_{xp}X + (Y_{nz}-Y_{np})K_{zp}Z$$

$$\left. + (Y_{nx}+C)\left(\frac{1}{Y_{zx}} - 1\right)\hat{\mu}_z\frac{X}{X+K_x}Z + (Y_{nx}+C-Y_{nz})\hat{\mu}_z\frac{X}{X+K_x}Z\right]$$

$$(Y_{nx}+C-Y_{nb})\frac{V_x}{A}\frac{\partial A}{\partial z}X + (Y_{nz}-Y_{nb})\frac{V_z}{A}\frac{\partial A}{\partial z}Z$$

$$+ (Y_{np}-Y_{nb})\frac{V_p}{A}\frac{\partial A}{\partial z}P + \frac{K_o}{O+K_o}Y_{nb}K_{bd}B$$

Polyphosphates

Algae Only:

$$\frac{\partial N}{\partial t} = \frac{1}{A}\frac{\partial}{\partial z}\left(KA\frac{\partial N}{\partial z}\right) + \frac{O}{O+K_o}\left[-\hat{q}\frac{N}{N+K_n}\frac{C_{max}-C}{C_{max}}X + (Y_{nx}+C+V)K_{xn}X\right.$$

$$\left. + Y_{nb}K_{bn}B\right] + (Y_{nx}+C+V-Y_{nb})\frac{V_x}{A}\frac{\partial A}{\partial z}X + \frac{K_o}{O+K_o}Y_{nb}K_{bd}B$$

Algae and Detritus:

$$\frac{\partial N}{\partial t} = \frac{1}{A}\frac{\partial}{\partial z}\left(KA\frac{\partial N}{\partial z}\right) + \frac{O}{O+K_o}\left[-\hat{q}\frac{N}{N+K_n}\frac{C_{max}-C}{C_{max}}X + Y_{np}K_{pn} + Y_{nb}K_{bn}B\right.$$

$$\left. + (Y_{nx}+C+V-Y_{np})K_{xp}X\right] + (Y_{nx}+C+V-Y_{nb})\frac{V_x}{A}\frac{\partial A}{\partial z}X$$

$$+ (Y_{np}-Y_{nb})\frac{V_p}{A}\frac{\partial A}{\partial z}P + \frac{K_o}{K_o+O}Y_{nb}K_{bd}B$$

Algae and Zooplankton:

$$\frac{\partial N}{\partial t} = \frac{1}{A}\frac{\partial}{\partial z}\left(KA\frac{\partial N}{\partial z}\right) + \frac{O}{O+K_o}\left[-\hat{q}\frac{N}{N+K_n}\frac{C_{max}-C}{C_{max}}X + (Y_{nx}+C+V)K_{xn}X\right.$$

$$+ Y_{nb}K_{bn}B + Y_{nz}K_{zn}Z + (Y_{nx}+C+V)\left(\frac{1}{Y_{zx}} - 1\right)\hat{\mu}_z\frac{X}{X+K_x}Z$$

$$\left. + (Y_{nx}+C+V-Y_{nz})\hat{\mu}_z\frac{X}{X+K_x}Z\right] + (Y_{nx}+C+V-Y_{nb})\frac{V_x}{A}\frac{\partial A}{\partial z}X$$

$$+ (Y_{nz}-Y_{nb})\frac{V_z}{A}\frac{\partial A}{\partial z}Z + \frac{K_o}{K_o+O}Y_{nb}K_{bd}B$$

Algae, Zooplankton, and Detritus:

$$\frac{\partial N}{\partial t} = \frac{1}{A}\frac{\partial}{\partial z}\left(KA\frac{\partial N}{\partial z}\right) + \frac{O}{O+K_o}\left[-\hat{q}\frac{N}{N+K_n}\frac{C_{max}-C}{C_{max}}X + Y_{np}K_{pn}P\right.$$

$$+ Y_{nb}K_{bn}B + (Y_{nx}+C+V-Y_{np})K_{xp}X + (Y_{nz}-Y_{np})K_{zp}Z$$

$$+ (Y_{nx}+C+V)\left(\frac{1}{Y_{zx}} - 1\right)\hat{\mu}_z\frac{X}{X+K_x}Z + (Y_{nx}+C+V-Y_{nz})\hat{\mu}_z\frac{X}{X+K_x}Z]$$

$$(Y_{nx}+C+V-Y_{nb})\frac{V_x}{A}\frac{\partial A}{\partial z}X + (Y_{nz}-Y_{nb})\frac{V_z}{A}\frac{\partial A}{\partial z}Z$$

$$+ (Y_{np}-Y_{nb})\frac{V_p}{A}\frac{\partial A}{\partial z}P + \frac{K_o}{K_o+O}Y_{nb}K_{bd}B$$

OXYGEN EQUATIONS

Fixed Yield

Algae Only:

$$\frac{\partial O}{\partial t} = \frac{1}{A}\frac{\partial}{\partial z}\left(KA\frac{\partial O}{\partial z}\right) + \frac{O}{O+K_o}\left[Y_{ox}\hat{\mu}_x f(I)\frac{N}{N+K_n}X - Y_{ox}K_{xn}X\right.$$

$$\left. - Y_{ob}K_{bn}B - Y_{od}K_{dn}D\right]$$

Algae and Detritus:

$$\frac{\partial O}{\partial t} = \frac{1}{A}\frac{\partial}{\partial z}\left(KA\frac{\partial O}{\partial z}\right) + \frac{O}{O+K_o}\left[Y_{ox}\hat{\mu}_x f(I)\frac{N}{N+K_n}X - Y_{op}K_{pn}X\right.$$

$$\left. - Y_{ob}K_{bn}B - Y_{od}K_{dn}D\right]$$

Algae and Zooplankton:

$$\frac{\partial O}{\partial t} = \frac{1}{A}\frac{\partial}{\partial z}\left(KA\frac{\partial O}{\partial z}\right) + \frac{O}{O+K_o}\left[Y_{ox}\hat{\mu}_x \bar{f}(I)\frac{N}{N+K_n}X - Y_{ox}K_{xn}X\right.$$

$$\left. - Y_{ob}K_{bn}B - Y_{od}K_{dn}D - Y_{ox}\left(\frac{1}{Y_{zx}} - 1\right)\hat{\mu}_z\frac{X}{X+K_x}Z - Y_{oz}K_{zn}Z\right]$$

Algae, Detritus, and Zooplankton:

$$\frac{\partial O}{\partial t} = \frac{1}{A}\frac{\partial}{\partial z}\left(KA\frac{\partial O}{\partial z}\right) + \frac{O}{O+K_o}\left[Y_{ox}\hat{\mu}_x \bar{f}(I)\frac{N}{N+K_n}X - Y_{op}K_{pn}P\right.$$

$$\left. - Y_{ob}K_{bn}B - Y_{od}K_{dn}D - Y_{ox}\left(\frac{1}{Y_{zx}} - 1\right)\hat{\mu}_z\frac{X}{X+K_x}Z\right]$$

Variable Yield and Polyphosphate

Algae Only:

$$\frac{\partial O}{\partial t} = \frac{1}{A}\frac{\partial}{\partial z}\left(KA\frac{\partial O}{\partial z}\right) + \frac{O}{O+K_o}\left[Y_{ox}\hat{\mu}_x\bar{f}(I)\frac{C}{C+K_c}X - Y_{ox}K_{xn}X\right.$$

$$\left. - Y_{ob}K_{bn}B - Y_{od}K_{dn}D\right]$$

Algae and Detritus:

$$\frac{\partial O}{\partial t} = \frac{1}{A}\frac{\partial}{\partial z}\left(KA\frac{\partial O}{\partial z}\right) + \frac{O}{O+K_o}\left[Y_{ox}\hat{\mu}_x\bar{f}(I)\frac{C}{C+K_c}X - Y_{op}K_{pn}P\right.$$

$$\left. - Y_{ob}K_{bn}B - Y_{od}K_{dn}D\right]$$

Algae and Zooplankton:

$$\frac{\partial O}{\partial t} = \frac{1}{A}\frac{\partial}{\partial z}\left(KA\frac{\partial O}{\partial z}\right) + \frac{O}{O+K_o}\left[Y_{oz}\hat{\mu}_z\bar{f}(I)\frac{C}{C+K_x}X - Y_{ox}K_{xn}X\right.$$

$$\left. - Y_{ob}K_{bn}B - Y_{od}K_{dn}D - Y_{ox}\left(\frac{1}{Y_{zx}} - 1\right)\hat{\mu}_z\frac{X}{X+K_x}Z - Y_{oz}K_{zn}Z\right]$$

Algae, Detritus, and Zooplankton:

$$\frac{\partial O}{\partial t} = \frac{1}{A}\frac{\partial}{\partial z}\left(KA\frac{\partial O}{\partial z}\right) + \frac{O}{O+K_o}\left[Y_{ox}\hat{\mu}_x\bar{f}(I)\frac{C}{C+K_c}X - Y_{op}K_{pn}P\right.$$

$$\left. - Y_{ob}K_{bn}B - Y_{od}K_{dn}D - Y_{ox}\left(\frac{1}{Y_{zx}} - 1\right)\hat{\mu}_z\frac{X}{X+K_x}Z\right]$$

DETRITUS EQUATIONS

Fixed Yield, Variable Yield, and Polyphosphates

Algae and Detritus:

$$\frac{\partial P}{\partial t} = \frac{1}{A}\frac{\partial}{\partial z}\left(KA\frac{\partial P}{\partial z}\right) - \frac{1}{A}\frac{\partial}{\partial z}(V_p AP) + \frac{O}{O+K_o}\left[K_{xp}X - K_{pn}P\right] - \frac{V_p}{A}\frac{\partial A}{\partial z}P$$

Algae, Detritus, and Zooplankton:

$$\frac{\partial P}{\partial t} = \frac{1}{A}\frac{\partial}{\partial z}\left(KA\frac{\partial P}{\partial z}\right) - \frac{1}{A}\frac{\partial}{\partial z}(V_p AP) + \frac{O}{O+K_o}\left[K_{xp}X + K_{zn}Z - K_{pn}P\right] - \frac{V_p}{A}\frac{\partial A}{\partial z}P$$

BENTHOS EQUATIONS

Fixed Yield, Variable Yield, and Polyphosphates

Algae Only:

$$\frac{\partial B}{\partial t} = \frac{V_x}{A}\frac{\partial A}{\partial z}X - \frac{O}{K_o+O}K_{bn}B - \frac{K_o}{K_o+O}K_{bd}B$$

Algae and Detritus:

$$\frac{\partial B}{\partial t} = \frac{V_x}{A}\frac{\partial A}{\partial z}X + \frac{V_p}{A}\frac{\partial A}{\partial z}P - \frac{O}{O+K_o}K_{bn}B - \frac{K_o}{K_o+O}K_{bd}B$$

Algae and Zooplankton:

$$\frac{\partial B}{\partial t} = \frac{V_x}{A}\frac{\partial A}{\partial z}X + \frac{V_z}{A}\frac{\partial A}{\partial z}P - \frac{O}{O+K_o}K_{bn}B - \frac{K_o}{K_o+O}K_{bd}B$$

Algae, Detritus, and Zooplankton:

$$\frac{\partial B}{\partial t} = \frac{V_x}{A}\frac{\partial A}{\partial z}X + \frac{V_p}{A}\frac{\partial A}{\partial z}P + \frac{V_z}{A}\frac{\partial A}{\partial z}Z - \frac{O}{O+K_o}K_{bn}B - \frac{K_o}{K_o+O}K_{bd}B$$

INTERNAL NON-STRUCTURAL OR
SOLUBLE PHOSPHORUS

Variable Yield

$$\frac{\partial C}{\partial t} = \frac{K}{X}\frac{\partial X}{\partial z}\frac{\partial C}{\partial z} + \frac{\partial K}{\partial z}\frac{\partial C}{\partial z} + \frac{K}{A}\frac{\partial A}{\partial z}\frac{\partial C}{\partial z} + K\frac{\partial^2 C}{\partial z^2} + \frac{K}{X}\frac{\partial X}{\partial z}\frac{\partial C}{\partial z} - V_x\frac{\partial C}{\partial z}$$

$$+\frac{O}{O+K_o}\left[\hat{q}\bar{f}(I)\frac{N}{N+K_n}\frac{C_{max}-C}{C_{max}} - Y_{nx}\hat{\mu}_x\bar{f}(I)\frac{C}{C+K_c} - C\hat{\mu}_x\bar{f}(I)\frac{C}{C+K_c}\right]$$

Polyphosphates

$$\frac{\partial C}{\partial t} = \frac{K}{X}\frac{\partial X}{\partial z}\frac{\partial C}{\partial z} + \frac{\partial K}{\partial z}\frac{\partial C}{\partial z} + \frac{K}{A}\frac{\partial A}{\partial z}\frac{\partial C}{\partial z} + K\frac{\partial^2 C}{\partial z^2} + \frac{K}{X}\frac{\partial X}{\partial z}\frac{\partial C}{\partial z} - V_x\frac{\partial C}{\partial z}$$

$$+\frac{O}{O+K_o}\left[\hat{q}\frac{N}{N+K_n}\frac{C_{max}-C}{C_{max}} - Y_{nx}\hat{\mu}_x\bar{f}(I)\frac{C}{C+K_c} - C\hat{\mu}_x\bar{f}(I)\frac{C}{C+K_c}\right.$$

$$\left. - r_f\bar{f}(I)\frac{C}{C+K_c}\frac{V_{max}-V}{V_{max}} + r_d\frac{V}{V+K_v}\right]$$

POLYPHOSPHATE

$$\frac{\partial V}{\partial t} = \frac{K}{X}\frac{\partial X}{\partial z}\frac{\partial V}{\partial z} + \frac{K}{A}\frac{\partial A}{\partial z}\frac{\partial V}{\partial z} + K\frac{\partial^2 V}{\partial z^2} + \frac{K}{X}\frac{\partial X}{\partial z}\frac{\partial V}{\partial z} - V_x\frac{\partial V}{\partial z}$$

$$+\frac{O}{O+K_o}\left[r_f\bar{f}(I)\frac{C}{C+K_c}\frac{V_{max}-V}{V_{max}} - r_d\frac{V}{V+K_v} - V\hat{\mu}_x\bar{f}(I)\frac{C}{C+K_c}\right]$$

DISSOLVED ORGANIC MATTER

$$\frac{\partial D}{\partial t} = \frac{1}{A}\frac{\partial}{\partial z}\left(KA\frac{\partial D}{\partial z}\right) - \frac{O}{O+K_o}K_{dn}D + \frac{K_o}{K_o+O}K_{bd}B$$

APPENDIX D

Computer Programs

The computer pograms used in this research were initiated for analytical purposes and in themselves are not the end products of this research. Therefore, the program listings and brief operating notes are available to the serious reader upon written request and at a cost necessary to cover only reproduction and mailing charges. Address inquiries to:

Dr. K. W. Bedford
Department of Civil Engineering
The Ohio State University
2070 Neil Avenue
Columbus, Ohio 43210

REFERENCES

Allen, K. K. "Relation between production and biomass." J. Fisheries Res. Board of Canada 28, 1573 (1971).

Aronoff, S., and M. Calvin. "Phosphorus turnover and photosynthesis." Plant Physiology 23, 351 (1948).

Babajimopoulos, C. "Application of weighted least squares method in simulating one-dimensional water flow in soil." Master's Thesis, Ohio State University (1975).

Baca, R. G., and R. C. Arnett. "A limnological model for lakes and impoundments." Paper presented at USEPA Conference on Environmental Modeling and Simulation, Cincinnati, 1976.

Bannister, T. T. "Production equations in terms of chlorophyll concentration, quantum yield, and upper limit to production." Limnology and Oceanography 19, 1 (1974).

Bannister, T. T. "A general theory of steady state phytoplankton growth in a nutrient saturated mixed layer." Limnology and Oceanography 19, 13 (1974).

Barlow, J. P., and J. W. Bishop. "Phosphate regeneration by zooplankton in Cayuga Lake." Limnnology and Oceanography, Redfield Supl., R15 (1965).

Bedford, K. W., and C. Babajimopoulos. "Vertical diffusivities in aereally averaged models." J. Environmental Engineering Division of ASCE 103, 113 (1977).

Beers, J. R. "Studies on the chemical composition of the major zooplankton groups in the Sargasso Sea off Bermuda." Limnology and Oceanography 11, 520 (1966).

Bella, D. A. "Simulating the effect of sinking and vertical mixing on algal population dynamics." J. Water Pollution Control Fed. 42, R140 (1970).

Berman, M. S., and S. Richman. "The feeding behavior of Daphnia pulex from Lake Winnebago, Wisconsin." Limnology and Oceanography 19, 105 (1974).

Bierman, V. J. "Mathematical model of the selective enhancement of blue-green algae by nutrient enrichment." A paper

in Modeling Biochemical Processes in Aquatic Ecosystems, R. P. Canale (Ed.), Ann Arbor Science, 1976.

Bierman, V. J., and D. M. Dolan. "Mathematical modeling of phytoplankton dynamics in Saginaw Bay, Lake Huron." Paper presented at USEPA Conference on Environmental Modeling and Simulation, Cincinnati, 1976.

Blackman, F. F. "Optima and limiting factors." Annals of Botany 19, 281 (1905).

Brown, T. E., and F. L. Richardson. "The effect of growth environment on the physiology of algae: Light intensity." J. Phycology 4, 38 (1968).

Canale, R. P. "Predator-prey relationships in a model for the activated sludge process." Biotechnology and Bioengineering 9, 887 (1969).

Canale, R. P., D. J. Hineman, and H. E. Allen. "A dynamic model for phytoplankton production in Grand Traverse Bay." Proceedings 16th Conf. Great Lakes Res., Ann Arbor, 1973.

Canale, R. P., and A. H. Vogel. "Effects of temperature on phytoplankton growth." J. Environmental Engineering Division ASCE 100, 231 (1974).

Caperon, J. "Population growth in micro-organisms limited by food supply." Ecology 48, 715 (1967).

Caperon, J., and J. Meyer. "Nitrogen-limited growth of marine phytoplankton--II. Uptake kinetics and their role in nutrient limited growth of phytoplankton." Deep Sea Res. 19, 619 (1972).

Carnahan, B., H. A. Luther, and O. Wilkes. Applied Numerical Methods. Wiley and Sons, New York, 1969.

Carpenter, E. J. "Phosphorus requirements of two planktonic diatoms in steady-state culture." J. Phycology 6, 28 (1970).

Chen, C. W. "Concepts and utilities of ecological model." J. Sanitary Engineering Division ASCE 96, 1085 (1970).

Chen, C. W., and G. T. Orlob. "Ecological simulation for aquatic environments." Office of Water Resources, Dept. of Interior, OWRR C-2044, 1972.

Chen, C. W., M. Lorenzen, and D. J. Smith. "A comprehensive

model for Lake Ontario." Great Lakes Environmental Research Laboratory, Ann Arbor, 1975.

Chen, C. W., and D. J. Smith. "The ecological model as applied to Lake Washington." Paper presented at USEPA Conference on Environmental Modeling and Simulation, Cincinnati, 1976.

Corner, E. D. S. "Phosphorus in marine zooplankton." Water Res. 7, 93 (1973).

Culver, D. A. Personal communication, Professor of Zoology, The Ohio State University, 1977.

Curnutt, S. G., and R. K. Schmidt. "Possible mechanisms controlling the intracellular level of inorganic polyphosphate during synchronous growth of Chlorella pyrenoidosa." Experimental Cell Research 36, 102 (1964).

Cushing, D. H. Marine Ecology of Fisheries. Cambridge Press, New York, 1975.

De Pinto, J. V., V. J. Bierman, and F. H. Verhoff. "Seasonal phytoplankton succession as a function of species competition for phosphorus and nitrogen." In Modeling Biochemical Processes in Aquatic Ecosystems, R. P. Canale (Ed.), Ann Arbor Science, Ann Arbor, Mich., 1976.

Di Toro, D. M., D. J. O'Connor and R. V. Thomann. "A dynamic model of the phytoplankton population in the Sacramento-San Joaquin Delta." Nonequilibrium Systems in Natural Waters, Adv. Chemical Ser. 106, Am. Chemical Soc., Washington, 1971.

Di Toro, D. M., and W. F. Matystik, Jr. "Phytoplankton biomass model of Lake Huron and Saginaw Bay." USEPA Conference on Environmental Modeling and Simulation, Cincinnati, Ohio, 1976.

Droop, D. M. "Some thoughts on nutrient limitation of algae." J. Phycology 9, 264 (1973).

Echelberger, W. F., and M. W. Tenney. "Engineering aspects of polluted lake reclamation." Proceedings 2nd Annual Environmental Engineering and Science Conference, Univ. of Louisville, Louisville, Kentucky, 1972.

Edinger, J. E., D. W. Duttweiler, and J. C. Geyer. "The response of water temperature to meteorological conditions." Water Resources Research 4, 1137 (1968).

Edmondson, W. T., G. W. Comita , and G. C. Anderson. "Reproductive rate of copepods in nature and its relation to phytoplankton population." Ecology 43, 625 (1962).

Emerson, R. L., J. F. Stauffer, and W. W. Umbreit. "Relationship between phosphorylation and photosynthesis in Chlorella." Am J. Botany 31, 107 (1944).

Faust, M. A., and E. Gantt. "Effect of light intensity and glycerol on the growth, pigment composition, and ultrastructure of chroomonas sp." J. Phycology 9, 489 (1973).

Fillos, J., and H. Biswas. "Phosphate release and sorption by Lake Mohegan sediments." J. Environmental Engineering Division ASCE 102, 239 (1976).

Fitzgerald, G. P. "Evaluations of available sources of nitrogen and phosphorus for algae." J. Phycology 6, 239 (1970).

Fogg, G. E. Algal Cultures and Phytoplankton Ecology. Univ. Wisconsin Press, Madison, Wisc.,1965 .

Force, E. G. "The decomposition of algae in anaerobic waters." Fed. Water Pollution Control Assoc., Technical Report #95, 1968.

Freedman, P. L., and R. P. Canale. "Nutrient release from anaerobic sediments." J. Environmental Engineering Division ASCE 103, 233 (1977).

Fritz, S. "Solar energy on clear and cloudy days." Scientific Monthly, February 1957.

Fuhs, G. W. "Nutrients and aquatic vegetation effects." J. Environmental Engineering Div. ASCE 100, 269 (1974).

Fuhs, G. W. "Phosphorus content and the rate of growth in the diatoms Cyclotella nana and Thalassira fluviatilis." J. Phycology 5, 312 (1969).

Fuhs, G. W., S. D. Deminerle, E. Canelli, and M. Chen. "Characterization of phosphorus limited plankton algae." New York Dept. Environmental Conservation, Technical Paper #6, 1971.

Fuller, J. L. "Feeding rate of Calanus finmarchicus in relation to environmental conditions." Biological Bulletin 72, 233 (1937).

Gerloff, G. C., and F. Skoog. "Cell contents of nitrogen and phosphorus as a measure of their availability for

growth of Microcystis aeruginosa." Ecology 35, 348 (1954).

Gest, H., and M. D. Kamen. "Studies on the phosphorus metabolism of green algae and purple bacteria in relation to photosynthesis." J. Biological Chemistry 176, 299 (1948).

Glover, H., J. Beardall, and I. Morris. "Effects of environmental factors on photosynthesis patterns in Phaeodactylum tricornutum (Bacillariophyceae). I. Effect of nitrogen deficiency and light intensity." J. Phycology 11, 424 (1975).

Goldman, J. C., and E. J. Carpenter. "A kinetic approach to the effect of temperature on algal growth." Limnology and Oceanography 19, 756 (1974).

Grenney, W. J., D. A. Bella, and H. C. Curl, Jr. "A theoretical approach to interspecific competition in phytoplankton communities." Am. Naturalist 107, 405 (1973).

Hall, D. J. "An experimental approach to the dynamics of a natural population of Daphnia galeata mendotae." Ecology 45, 94 (1964).

Harold, F. M. "Inorganic polyphosphates in biology: Structure, metabolism, and function." Bacteriological Reviews 30, 772 (1966).

Henderson-Sellers, B. "Role of eddy diffusivity in thermocline formation." J. Environmental Engineering Division ASCE 102, 517 (1976).

Herbert, D. "A theoretical analysis of continuous culture systems." Soc. Chemical Industry, Monograph #12, 1960.

Herbert, D. "Some principles of continuous culture." A paper in Recent Progress in Microbiology," G. Tunesall (Ed.), Blackwell Sci. Pub., Oxford, 1958.

Herbert, D. E., R. Elsworth, and R. C. Telling. "The continuous culture of bacteria: A theoretical and experimental study." J. General Microbiology 14, 601 (1956).

Hetling, L. J., and R. M. Sykes. "Sources of nutrients in Canadarago Lake." New York Dept. of Environmental Conservation, Technical Paper #3, 1971.

Hetling, L. J., T. E. Harr, G. W. Fuhs, and S. P. Allen. "North America project, Canadarago Lake, Otsego County, State of New York: Phase I." National Environmental Research Center, Pacific Northwest, USEPA, 1974.

Hill, M. N. (Ed.) The Sea. Vol. 2: The Composition of Sea-Water Comparative and Descriptive Oceanology. Interscience, London, 1963.

Hutchensen, G. E. A Treatise on Limnology. Wiley and Sons, New York, 1975.

Hynes, H. B. N. The Ecology of Running Waters. Toronto Press, Toronto, 1970.

Jassby, A. D., and T. Platt. "Mathematical formulation of the relationship between photosynthesis and light for phytoplankton." Limnology and Oceanography 21, 540 (1976).

Jenkin, R. M. "Oxygen production by the diatom Coscinodiscus excentricus EHK in relation to submarine illumination in the English Channel." Marine Biological Assoc. United Kingdom 22, 301 (1937).

Jewell, W. J., and P. J. McCarty. "Aerobic decomposition of algae and nutrient regeneration." Fed. Water Pollution Control Assoc., Technical Report #91, 1968.

Johannes, R. E., and M. Satomi. "Composition and nutritive value of fecal pellets of a marine crustacean." Limnology and Oceanography 11, 191 (1966).

Johnson, F. H. "The action of pressure and temperature." Microbial Ecology, 7th Symp. Soc. General Microbiology, Cambridge Univ. Press, 1957.

Johnson, M. G., and R. O. Brinkhurst. "Benthic community metabolism in Bay of Quinte and Lake Ontario." J. Fisheries Research Board of Canada 28, 1715 (1971).

Jorgensen, S. E. "A eutrophication model for a lake." Ecological Modeling 2, 147 (1976).

Keenan, J. D. "Response of anabaena to pH, carbon, and phosphorus." J. Environmental Engineering Division ASCE 99, 607 (1973).

Kelly, R. A. "Conceptual ecological model of the Delaware Estuary." Unpublished manuscript, 1973.

Ketchum, B. H. "The absorption of phosphate and nitrate by illuminated cultures of Nitzschia closterium." Am. J. Botany 26, 399 (1939).

Ketchum, B. H. "The development and restoration of deficiencies in the phosphorus and nitrogen composition of unicellular plants." J. Cellular Composition 13, 373 (1939).

Kholy, A. A. A. "On the assimilation of phosphorus in Chlorella pyrenoidosa." Physiologia Plantarum 9, 137 (1956).

Kiefer, D. A., and R. W. Austin. "The effect of varying phytoplankton concentration on submarine light transmission in the Gulf of California." Limnology and Oceanography 19, 55 (1974).

Knaus, H. J., and J. W. Porter. "The absorption of inorganic ions by Chlorella pyrenoidosa." Plant Physiology 29, 229 (1954).

Koberg, G. E. "Methods to compute long-wave radiation from the atmosphere and reflected solar radiation from a water surface." Geological Survey Paper 272-F, U.S. Government Printing Office, Washington, D.C., 1964.

Kuenzler, E. J. "Glucose-6-phosphate utilization by marine algae." J. Phycology 1, 156 (1965).

Kuenzler, E. J. "Dissolved organic phosphorus excretion by marine phytoplankton." J. Phycology 6, 7 (1970).

Lam, R. K., and B. W. Frost. "Model of copepod filtering response to changes in size and food concentration." Limnology and Oceanography 21, 490 (1976).

Lehman, J. T., D. B. Botkin, and G. E. Likens. "The assumptions and rationales of a computer model of phytoplankton population dynamics." Limnology and Oceanography 20, 343 (1975).

Lehman, J. T. "The filter-feeder as an optimal forager and the predicted shapes of feeding curves." Limnology and Oceanography 21, 501 (1976).

Lewin, R. A. Physiology and Biochemistry of Algae. Academic Press, 1962.

Lin, C. K. "Accumulation of water soluble phosphorus and hydrolysis of polyphosphates by Cladophora glomeratu (Chlorophyceae)." J. Phycology 13, 46 (1977).

Lund, J. W. G. "Studies on Asterionella formosa Hass." J. Ecology 38, 15 (1950).

Mann, J. E., and J. Meyers. "On pigments growth and photosymthesis of Phaeodactylum tricornutum." J. Phycology 4, 349 (1968).

Marshall, S. M., and A. P. Orr. "The photosynthesis of diatom cultures in the sea." Marine Biological Association of the United Kingdom 15, 321 (1928).

Mateles, R. I., and S. K. Chian. "Kinetics of substrate uptake in pure and mixed culture." Environmental Science and Technology 3, 569 (1969).

McMahon, J. W., and F. H. Rigler. "Feeding rates of Daphnia magna straus in different foods labeled with radioactive phosphorus." Limnology and Oceanography 10, 105 (1965).

Mitchell, P. "Transport of phosphate across the surface of Micrococcus pyogenes: Nature of the cell inorganic phosphorus." J. General Microbiology 9, 273 (1953).

Mitchell, P. "Transport of phosphate across the surface of Micrococcus pyogenes: Specificity and kinetics." J. General Microbiology 11, 73 (1954).

M'Kendrick, A. G., and M. K. Pai. "The rate of multiplication of micro-organisms: A mathematical study." Proc. Royal Soc. Edinburough 31, 649 (1910).

Monod, J. "The growth of bacterial cultures." Annual Review Microbiology 3, 371 (1949).

Muck, R. E., and C. P. L. Grady. "Temperature effects on microbial growth in CSTR's." J. Environmental Engineering Division ASCE 100, 1147 (1974).

Nalewajko, C., and D. R. S. Lean. "Growth and excretion in planktonic algae and bacteria." J. Phycology 8, 361 (1972).

Neuman, S. P., and T. N. Narasimhan. "Mixed explicit-implicit iterative finite element scheme for diffusion-type problems: I. Theory." Int. J. Numerical Methods in Engineering 11, 309 (1977).

Newbold, J. D., and J. A. Liggett. "Oxygen depletion model for Cayuga Lake." J. Environmental Engineering Division ASCE 100, 41 (1974).

O'Connor, D. J., and D. M. Ditorro. "Photosynthesis and oxygen balance in streams." J. Sanitary Engineering Division 96, 547 (1970).

Oglesby, R. T., and D. J. Alee (Eds.) "Ecology of Cayuga Lake and the proposed Bell Station." Water Resources and Marine Sciences Center, Cornell Univ., Publication #27, 1969.

Omori, M. "Weight and chemical composition of some important oceanic zooplankton in the North Pacific Ocean." Marine Biology 3, 4 (1969).

Park, R. A. "A generalized model for simulating lake ecosystems." Simulation, August 1974.

Pusciak, J. W., and J. Gavis. "Transport limitation of nutrient uptake in phytoplankton." Limnology and Oceanography 19, 881 (1974).

Pennak, R. W. Fresh-Water Invertebrates of the United States. Ronald Press, New York, 1953.

Pennak, R. W. "The dynamics of fresh-water plankton populations." Ecological Monographs 16, 340 (1946).

Pirt, S. J. "The maintenance energy of bacteria in growing cultures." Proc. Royal Soc. London 163, 224 (1965).

Peters, R. H. "Phosphorus excretion and the measurement of feeding and assimilation by zooplankton." Limnology and Oceanography 20, 858 (1975).

Porcella, D. B., P. Grau, C. H. Huang, J. Radimsky, D. F. Toerien, and E. A. Pearson. "Provisional algal assay procedures: First annual report." Sanitary Engineering Research Laboratory, Berkeley, 1970.

Porcella, D. B., J. S. Kumagai, and E. J. Middlebrooks. "Biological effects of sediment-water nutrient interchange." J. Sanitary Engineering Division ASCE 96, 911 (1970).

Prescott, G. W. The Algae: A Review. Houghton-Mifflin, New York, 1968.

Rhee, G. "A continuous culture study of phosphate uptake, growth rate, and polyphosphate in scenedesmus sp." J. Phycology 9, 1973.

Rhee, G. "Phosphate uptake under nitrate limitation by scenedesmus sp. and its ecological implications." J. Phycology 10, 470 (1974).

Rigler, F. H. "The relation between concentration of food and feeding rate of Daphnia magna Straus ." Canadian J. Zoology 39, 857 (1961).

Rigler, F. H. "The uptake and release of inorganic phosphorus by Daphnia magna Straus ." Limnology and Oceanography 6, 165 (1961).

Roache, P. V. Computational Fluid Dynamics. Hermosa, Albuquerque, N.M., 1976.

Roberts, D. V. Enzyme Kinetics. Cambridge Press, New York, 1977.

Ruttner, F. Fundamentals of Limnology. Univ. of Toronto, Toronto, Canada, 1974.

Ryther, J. H. "Inhibitory effects of phytoplankton upon feeding of Daphnia magna with reference to growth reproduction and survival." Ecology 35, 522 (1954).

Ryther, J. H. "Photosynthesis in the ocean as a function of light intensity." Limnology and Oceanography 1, 61 (1956).

Ryther, J. H. "Geographic variations in productivity." In The Sea. Vol. 2: The Composition of Sea-Water--Comparative and Descriptive Oceanology. Interscience, London, 1963.

Scavia, D., B. J. Eadie, and C. A. Robertson. "An ecological model for the Great Lakes." USEPA Conf. Environmental Modeling and Simulation, Cincinnati, Ohio, 1976.

Schindler, D. W. "Feeding, assimilation and respiration rates of Daphnia magna under various environmental conditions and their relation to production estimates." J. Animal Ecology 37, 369 (1968).

Schindler, D. W. "Carbon, nitrogen, phosphorus, and the eutrophication of fresh-water lakes." J. Phycology 7, 321 (1971).

Schumacher, G. J., and L. A. Whitford. "Respiration and P^{32} uptake in various species of fresh-water algae as affected by current." J. Phycology 1, 78 (1965).

Scott, G. T. "The mineral composition of phosphate deficient cells of Chlorella pyrenoidosa during the restoration of phosphate." J. Cellular and Comparative Physiology 25, 35 (1944).

Serruya, C., and T. Berman. "Phosphorus, nitrogen, and the growth of algae in Lake Kinneret." J. Phycology 11, 155 (1975).

Smayda, T. J. "Experimental observations on the influence of temperature light and salinity on cell division of

the marine diatom, Deutonula confervacea (cleve) gran." J. Phycology 5, 150 (1969).

Smayda, G. J. "Some experiments on the sinking characteristics of two freshwater diatoms." Limnology and Oceanography 19, 628 (1974),

Smith, E. L. "Photosynthesis in relation to light and carbon dioxide." Proc. Nat. Academy of Sciences 22, 504 (1936).

Sorokin, C. "Growth rate measurements on phytoplanktonic organisms." Chesapeake Science 10, 393 (1969).

Sonnichsen, J. C., and C. A. Ostek, "Examination of the thermocline." J. Sanitary Engineering Division ASCE 96, 353 (1970).

Stross, R. G., and S. M. Pemrick. "Nutrient uptake kinetics in phytoplankton: A basis for niche separation." J. Phycology 10, 164 (1974).

Stumm, W., and J. T. Morgan. Aquatic Chemistry. Wiley, New York, 1970.

Sundaram, T. R., and R. G. Rehm. "Formation and maintenance of thermoclines in temperate lakes." J. AIAA 9, 1322 (1971).

Sykes, R. M. "The Canadarago Lake eutrophication study: Nutrient inputs." New York State Dept. Environmental Conservation, 1971.

Sykes, R. M. "The trophic-dynamic aspects of ecosystem models." Proc. 16th Conf. Great Lakes Research, 1973, 977-988.

Thomann, R. W., K. P. Winfield, D. M. Ditorro, and D. J. O'Connor. "Mathematical modeling and phytoplankton in Lake Ontario." USEPA Office of Research and Development, EPA-6001/3-76-065 (1976).

Thomas, W. H. "Effects of temperature and illuminance on cell division rate of three species of tropical oceanic phytoplankton," J. Phycology 2, 17 (1966).

Toerien, D. F., C. H. Huang, J. Radimsky, E. A. Pearson, and J. Scherfig. "Provisional algal assay procedures: Final report." Sanitary Engineering Research Laboratory, Berkeley, 1971.

van Uden, N. "Kinetics of nutrient-limited growth." Ann. Review Microbiology 23, 473 (1969).

Varga, L. P., and C. P. Falls. "Continuous system models of oxygen depletion in a eutrophic reservoir." Current Research 6, 135 (1972).

Verhoff, F. H., J. B. Carberry, V. J. Bierman, Jr., and M. W. Tenney. "Mass transport of metabolites, especially phosphorus in cells." Paper presented at 71st National Meeting Am. Inst. Chemical Engineers, Dallas, Texas (1972).

Welch, H. E., and J. Kalff. "Benthic photosynthesis and respiration in Char Lake." J. Fisheries Research Board of Canada 31, 609 (1974).

Wetzel, R. G. Limnology. W. B. Saunders, London, 1975.

Zaika, V. E. Specific Production of Aquatic Invertebrates. Wiley and Sons, New York, 1973.